MATHEMATICAL MODEL OF HIGH PURITY C-PHYCOCYANIN EXTRACTION FROM *SPIRULINA PLATENSIS*

SAKAWDUAN KAEWDAM

DOCTOR OF ENGINEERING IN FOOD ENGINEERING

MAEJO UNIVERSITY

2020

MATHEMATICAL MODEL OF HIGH PURITY C-PHYCOCYANIN EXTRACTION FROM *SPIRULINA PLATENSIS*

SAKAWDUAN KAEWDAM

A DISSERTATION SUBMITTED IN PARTIAL FULFILLMENT
OF THE REQUIREMENTS FOR THE DEGREE OF DOCTOR OF ENGINEERING
IN FOOD ENGINEERING
ACADEMIC ADMINISTRATION AND DEVELOPMENT MAEJO UNIVERSITY
2020

Copyright of Maejo University

MATHEMATICAL MODEL OF HIGH PURITY C-PHYCOCYANIN EXTRACTION FROM *SPIRULINA PLATENSIS*

SAKAWDUAN KAEWDAM

THIS DISSERTATION HAS BEEN APPROVED IN PARTIAL FULFLLMENT
OF THE REQUIREMENTS FOR THE DEGREE OF DOCTOR OF ENGINEERING
IN FOOD ENGINEERING

APPROVED BY **Advisory Committee**

Chair .....
(Associate Professor Dr. Somkiat Jaturonglumlert)
...../...../ .....

Committee .....
(Associate Professor Dr. Jaturapatr Varith)
...../...../ .....

Committee .....
(Assistant Professor Dr. Kanjana Narkprasom)
...../...../ .....

Program Chair, Doctor of Engineering .....
in Food Engineering(Assistant Professor Dr. Chanawat Nitatwichit)
...../...../ .....

CERTIFIED BY ACADEMIC .....
ADMINISTRATION AND DEVELOPMENT

(Associate Professor Dr. Yanin Opatpatanakit)
Vice President for the Acting President of Maejo University
...../...../ .....

ชื่อเรื่อง แบบจำลองทางคณิตศาสตร์ของการสกัดสารไฟโคไซยานินความบริสุทธิ์สูงจากสาหร่ายสไปรูลินา
ชื่อผู้เขียน นางสาวสกาวเดือน แก้วดำ
ชื่อปริญญา วิศวกรรมศาสตรดุษฎีบัณฑิต สาขาวิชาวิศวกรรมอาหาร
อาจารย์ที่ปรึกษาหลัก รองศาสตราจารย์ ดร.สมเกียรติ จตุรงค์ล้ำเลิศ

บทคัดย่อ

ซี-ไฟโคไซยานิน (CPC) เป็นสารสีธรรมชาติที่สามารถสร้างได้จากสาหร่ายสไปรูลินา ถูกนำมาใช้อย่างแพร่หลายทั้งในอุตสาหกรรมอาหาร ยา และเครื่องสำอาง ในการศึกษานี้จึงมุ่งเน้นที่จะศึกษาและพัฒนากระบวนการผลิตสารสกัดซี-ไฟโคไซยานินที่มีความบริสุทธิ์สูงตั้งแต่ต้นน้ำ (การเลี้ยง) ไปจนถึงกลางน้ำ (กระบวนการผลิต) ของห่วงโซ่การผลิตสาหร่ายสไปรูลินา เพื่อให้ได้สารสกัดซี-ไฟโคไซยานินความบริสุทธิ์สูงที่จะสามารถนำไปพัฒนาต่อยอดเป็นผลิตภัณฑ์ต่อไปได้

การเพาะเลี้ยงแบบเป็นรอบที่มีการเติมสารอาหาร (Fed-batch cultivation) คือการเพาะเลี้ยงที่มีการเติมสารอาหารเพิ่มระหว่างการเลี้ยงซึ่งเป็นกลยุทธ์ที่ถูกใช้เพื่อช่วยเพิ่มอัตราการเจริญเติบโตและการสะสมสารซี-ไฟโคไซยานินภายในเซลล์ของสาหร่าย โดยในการศึกษานี้ได้ศึกษาการเลี้ยงแบบเป็นรอบ (Batch cultivation) เทียบกับการเลี้ยงแบบเป็นรอบที่มีการเติมสารอาหาร พบว่า ในการเลี้ยงแบบเป็นรอบเมื่อเพิ่มปริมาณไนโตรเจน สามารถช่วยเพิ่มการสะสมสารซี-ไฟโคไซยานินได้และค่าสูงสุดคือ 2.258 g/L เมื่อเลี้ยงด้วยโซเดียมไนเตรตความเข้มข้น 3.5 g/L สำหรับการเลี้ยงแบบเป็นรอบที่มีการเติมสารอาหาร จะได้ปริมาณสารซี-ไฟโคไซยานินสูงสุดและค่าผลิตภาพ (Productivity) คือ 4.354 g/L และ 97.53 mg/L.d ตามลำดับ เมื่อเติมด้วยแอมโมเนียมไบคาร์บอเนตความเข้มข้น 3.0 mM โดยแบบจำลองจลนศาสตร์สามารถอธิบายอัตราการเจริญเติบโตและการสะสมสารซี-ไฟโคไซยานินที่สัมพันธ์กับปริมาณไนโตรเจนที่เหลืออยู่ได้อย่างมีประสิทธิภาพ

การสกัดด้วยสารละลายน้ำสองสถานะ (Aqueous Two Phase Extraction: ATPE) เป็นกระบวนการทำบริสุทธิ์ที่มีประสิทธิภาพสูง เมื่อใช้สารละลายโพลีเอทิลีนไกลคอลร่วมกับสารละลายโพแทสเซียมฟอตเฟส นอกจากนี้ยังมีการประยุกต์ใช้วิธี ATPE ร่วมกับการลาดชันของอุณหภูมิ (Temperature gradient: TG) เพื่อช่วยเพิ่มประสิทธิภาพการสกัดให้มากยิ่งขึ้น โดยศึกษาผลของการลาดชันของอุณหภูมิ (TG) ที่มีต่อค่าความบริสุทธิ์ (Extract purity: EP) การแยกเฟส และสัมประสิทธิ์การแพร่มวลสาร ซึ่งพบว่า สภาวะที่ดีที่สุดของการทำบริสุทธิ์คือการใช้ TG25 โดยค่า

ความบริสุทธิ์ของสารสกัดซี-ไฟโคไซยานินเพิ่มขึ้นจาก 1.106 เป็น 2.337 ความเข้มข้นและผลผลิต (Recovery yield) เป็น 13.932 g/L และ 91.18% ตามลำดับ ซึ่งมากกว่าวิธีการแบบทั่วไป (ไม่มีผลของ TG) อย่างมีนัยสำคัญทางสถิติ เนื่องจาก TG ส่งผลต่อค่าความหนืดของระบบ โดยเมื่อค่าความหนืดของสารค่าลดลงจะทำให้ความสามารถในการละลายเพิ่มมากขึ้นและนอกจากนั้นยังช่วยเพิ่มประสิทธิภาพในการแพร่ของสารมากขึ้นอีกด้วย โดยงานวิจัยนี้ยังได้ศึกษาการเปลี่ยนแปลงสัมประสิทธิ์การแพร่ (Diffusion coefficient) เมื่อ TG เปลี่ยนแปลงไป โดยพบว่า ค่าสัมประสิทธิ์การแพร่ที่อุณหภูมิคงที่ (Isothermal diffusion coefficient: D_i) ค่า Soret effect (S_T) และค่าสัมประสิทธิ์การแพร่ความร้อน (Thermal diffusion coefficient: D_T) มีค่าเพิ่มขึ้นเมื่อค่า TG สูงขึ้นแต่ไม่ควรเกิน 25 นั้นแสดงให้เห็นว่าทำไมการใช้การลาดชันของอุณหภูมิจึงสามารถช่วยเพิ่มประสิทธิภาพกระบวนการทำบริสุทธิ์ได้

แบบจำลองการทางคณิตศาสตร์ของการทำบริสุทธิ์สารสกัดซี-ไฟโคไซยานินด้วยการใช้วิธี ATPE ที่สภาวะอุณหภูมิคงที่ (วิธีการแบบดั้งเดิม) และวิธีการ ATPE ร่วมกับ TG สามารถอธิบายได้โดยพฤติกรรมของการแยกเฟสของสารผสมเมื่อกระบวนการเข้าสู่สมดุลทางเคมี โดยศักย์ทางเคมีเป็นตัวบ่งชี้ที่ทำให้เกิดการเปลี่ยนแปลงในระบบ ระบบจะเข้าสู่สมดุลก็ต่อเมื่อทั้งเฟสบนและเฟสล่างมีศักย์ทางเคมีที่เท่ากัน และสามารถทำนายสัมประสิทธิ์ของการแยกและความบริสุทธิ์ของสารสกัดได้อย่างแม่นยำโดยมีค่าความคลาดเคลื่อนน้อยกว่า 10%

ท้ายที่สุด การออกแบบเชิงแนวคิดของต้นแบบเครื่องทำบริสุทธิ์สารสกัดไฟโคไซยานินด้วยวิธีการ ATPE ร่วมกับ TG โดยสามารถวิเคราะห์ต้นทุนของเครื่องต้นแบบราคาประมาณ 1,200,000 บาท และการวิเคราะห์เศรษฐศาสตร์วิศวกรรมสำหรับผลิตภัณฑ์สารสกัดซี-ไฟโคไซยานินผงบริสุทธิ์ที่กำลังการผลิต 1,200 กรัมต่อวัน จะได้ระยะเวลาคืนทุนอยู่ที่ประมาณ 2 ปี ซึ่งสามารถนำไปใช้ประกอบการตัดสินใจลงทุนของผู้ประกอบการได้

คำสำคัญ : สาหร่ายสไปรูลินา, ซี-ไฟโคไซยานิน, การทำบริสุทธิ์, การสกัดด้วยสารละลายน้ำสองสถานะ, แบบจำลองทางคณิตศาสตร์

Title	MATHEMATICAL MODEL OF HIGH PURITY C-PHYCOCYANIN EXTRACTION FROM *SPIRULINA PLATENSIS*
Author	Miss Sakawduan Kaewdam
Degree	Doctor of Engineering in Food Engineering
Advisory Committee Chairperson	Associate Professor Dr. Somkiat Jaturonglumlert

ABSTRACT

C-Phycocyanin (CPC) is a high-value bioproduct created by blue-green algae *Spirulina platensis*. It is widely used in various industries, such as, in food pharmaceutical and cosmetics industries. This study aimed to develop a high purity C-phycocyanin extraction process from the upstream (farming) to the middle stream (processing), of spirulina chain production to produce high purity CPC extracts to develop into further products.

The fed-batch cultivation was applied as a strategy to enhance growth and CPC accumulation. In this study, *Spirulina platensis* was cultured in the batch and fed-batch to investigate CPC production. On batch cultivation, it was found that increasing nitrogen source concentration led to an increase in CPC accumulation. The maximum CPC concentration (2.258 g/L) occurred when $NaNO_3$ was 3.5 g/L. The results indicate that the maximum CPC production (4.354 g/L) and productivity (97.53 mg/L·d) were obtained when using fed-batch with the NH_4HCO_3 2.0 mM. Kinetic model to describe the *Spirulina platensis* culture system, including cell growth, CPC formation, as well as nitrogen consumption, was proposed and found in good agreement with the experimental results. It can be employed to predict the production of biomass, CPC, and the consumption of nitrogen in culture.

For extraction, The Aqueous Two-Phase Extraction (ATPE) is to purify of CPC extract was studied. The polyethylene glycol and potassium phosphate were

used to purify CPC. Also, the effect of temperature differences with the ATPE process was applied to improve the efficiency of purification. The influence of various temperature gradient (TG) of process on purity (EP) partitioning and diffusion coefficient were evaluated. The optimal conditions for CPC purification was found at TG25. The CPC purity increased to 2.337 from an initial purity of 1.106. The concentration and recovery yield reached highest value with TG25 (13.932 g/L and 91.18, respectively), which were significantly higher than those of the conventional process. The TG necessarily affected the fluid viscosity variable, possibly due to a decrease in viscosity of the mixture, and increases in the solvent solubility and diffusion capacity. The isothermal diffusion coefficient (D_i) significantly increases with TG. The Soret effect (S_T) and thermal diffusion coefficient (D_T) was obtained at the high TG, but it should be less than 25.

A mathematical model of CPC purification using ATPE method at constant temperature conditions. (Conventional method) and ATPE on the temperature gradient process was studied to explain the behavior of the phase separation of the process. The chemical potential was an indicator of a system, when the system reaches equilibrium. The chemical potential in both the upper and lower phases have the same. The mathematical model can predict the partition coefficient and purity of the extract with the error less than 10%.

Finally, ATPE on the temperature gradient prototype concept design was proposed The investment of ATPE extractor was approximately 1,200,000 Bahts. To produce the pure CPC as powder with capacity of 1,200 g/days. The result found that the simple payback period for the extractor was about 2 year.

Keywords : Spirulina platensis, C-phycocyanin, Purification, Aqueous Two Phase Extraction, Mathematical model

ACKNOWLEDGEMENTS

Firstly, I would like to acknowledge this project funded by The Thailand Research Fund (TRF) under the program Research and Researchers for Industries of doctor's degree (RRi). The opinion in the research report is those of the researcher. The Thailand Research Fund and Teerawut commerce not necessarily always agree.

I would like to express my sincere gratitude to my advisor Assoc. Prof. Dr. Somkiat Jaturonglumlert for the continuous support of my study and related research, for his patience, motivation, and immense knowledge. His guidance helped me in all the time of research and writing of this thesis. I could not have imagined having a better advisor and mentor for my study.

Besides my advisor, I would like to thank the rest of my thesis committee: Assoc. Prof. Dr. Jaturapatr Varith, and Asst. Prof. Dr. Kanjana Narkprasom, for their insightful comments and encouragement, but also for the hard question which incented me to widen my research from various perspectives.

My sincere thanks also go to Asst. Prof. Dr. Chanawat Nitatwichit, and Asst. Prof. Dr. Yardfon Tanongkankit, who gave access to the laboratory and research facilities. Without their precious support, it would not be possible to conduct this research.

Last, I would like to thank my family: my parents and to my brothers and sister for supporting me spiritually throughout writing this thesis and my life in general.

Sakawduan Kaewdam

TABLE OF CONTENTS

Page

ABSTRACT (THAI) C

ABSTRACT (ENGLISH) ..... E

ACKNOWLEDGEMENTS ..... G

TABLE OF CONTENTS ..... H

LIST OF TABLE ..... M

LIST OF FIGURE ..... N

LIST OF SYMBOLS ..... P

CHAPTER 1 INTRODUCTION 1

1.1 Background and significance of research 1

1.2 Objectives of research 3

1.3 Scope of the study 3

1.4 Keywords 3

CHAPTER 2 LITERATURE REVIEW 4

2.1 Background of *Spirulina platensis* 4

2.1.1 *Spirulina platensis* 4

2.1.2 Spirulina cultivation 5

2.1.3 Biochemical composition 6

2.1.4 Spirulina cultivation system 10

2.1.5 Cultivation model 12

2.2 C-phycocyanin (CPC) 14

2.3 CPC Extraction 15

2.4 CPC Purification 17
2.4.1 Precipitation 18
2.4.2 Membrane filtration 19
2.4.3 Ion exchange chromatography 20
2.5 Aqueous two phase extraction (ATPE) 21
2.5.1 Phase diagram 22
2.5.2 Process of phase formation 24
2.5.3 System variables influencing partitioning 25
2.5.4 Protein properties affecting partitioning 26
2.5.5 Application of ATPE 28
2.6 Mathematical model of Aqueous Two-Phase Extraction behavior 32
2.6.1 Osmotic Virial Expansions 32
2.6.2 Integral Equation Theory 33
2.6.3 Lattice Theory 33
2.7 Mass transfer models 36
2.7.1 Disperse phase 36
2.7.2 Continuous phase 38
2.7.3 Hydrodynamic parameters and mass transfer coefficients 40
CHAPTER 3 METHODOLOGY 42
Chemical 42
Equipment 42
Analytical method 44
Statistical analysis 46
3.1 Enhancing cell growth and CPC production of *Spirulina platensis* 46

3.1.1 Operation of batch cultivation 47

3.1.2 Operation of fed-batch cultivation 47

3.1.3 Kinetic model development 48

3.2 Purification of CPC extracted from *Spirulina platensis* by Aqueous Two - Phase Extraction 49

3.2.1 Selection of type of Aqueous Two-Phase System. 51

3.2.2 Effect of dimension ratio (H/D) on Aqueous Two - Phase Extraction 51

3.3 Application of Aqueous Two-Phase Extraction on the temperature gradient process 52

3.3.1 Effect of the temperature gradient (TG) on ATPE process 52

3.3.2 Effect of temperature gradient (TG) on phase partitioning in the ATPE process 53

3.4 Mass transfer studies on Aqueous Two-Phase Extraction on the temperature gradient process 53

3.4.1 Prediction of overall mass transfer coefficients (k_La) 53

3.4.2 Prediction of diffusion coefficients 54

3.5 Simulation mathematical model of Aqueous Two-Phase Extraction process 55

3.6 Design the high CPC purity extractor and the engineering economic analysis 56

CHAPTER 4 RESULT AND DISCUSSION 59

4.1 Enhancing cell growth and CPC production of *Spirulina platensis* 59

4.1.1 Effect of Sodium nitrate on cell growth and CPC production 59

4.1.2 Improvement of CPC production of *Spirulina platensis* by using fed-batch operation 61

4.1.3 Kinetic model for CPC production 67

4.2 Purification of CPC extracted from *Spirulina platensis* by ATPE 68

4.2.1 System selection for ATPE 69

4.2.2 Effect of dimension ratio (H/D) on ATPE.....70

4.3 Application of Aqueous Two-Phase Extraction on the temperature gradient process 71

4.3.1 Effect of the temperature gradient (TG) on ATPE process.....71

4.3.2 Effect of temperature gradient (TG) on phase partitioning.....75

4.4 Mass transfer studies of Aqueous Two-Phase Extraction on the temperature gradient process.....80

4.4.1 Prediction of overall mass transfer coefficients (k_La).....80

4.4.2 Prediction of diffusion coefficients.....81

4.5 Mathematical model of Aqueous Two-Phase Extraction process 83

4.5.1 The fitting of binodal curve 83

4.5.2 The simulation of phase equilibrium behavior.....84

4.6 Design the high CPC purity extractor and the engineering economic analysis...90

4.6.1 Food machine concept design.....90

4.6.2 Engineering economic analysis.....94

CHAPTER 5 CONCLUSION.....96

5.1 General conclusion 96

5.1.1 Enhancing cell growth and CPC production of *Spirulina platensis* 96

5.1.2 Purification of CPC extracted from *Spirulina platensis* by Aqueous Two - Phase Extraction 97

5.1.3 Application of Aqueous Two-Phase Extraction on the temperature gradient process 97

5.1.4 Mass transfer studies of Aqueous Two-Phase Extraction on the temperature gradient process.....97

5.1.5 Mathematical model of Aqueous Two-Phase Extraction process.....98

5.1.6 Design the high purity CPC extractor and engineering economic analysis 98

5.2 Recommendation.....98

5.3 Novelty of this research.....99

REFERENCES..... 101

APPENDIX 117

APPENDIX A MATLAB script..... 118

APPENDIX B Research Publications I..... 128

APPENDIX C Research Publications II..... 136

CURRICULUM VITAE 144

LIST OF TABLE

Page

Table 1 Reviews of CPC extraction.....16

Table 2 Alternative applications of aqueous two-phase systems.....31

Table 3 The effect of sodium nitrate concentration on kinetic parameters 60

Table 4 The effect of ammonium concentration on kinetic parameters of fed-batch cultivation of *Spirulina platensis*. 63

Table 5 Comparison of kinetic parameters under fed-batch operation from this work with those reported in the literature. 66

Table 6 Effect of different salt and PEG on ATPE 69

Table 7 The results of effect of height and diameter column ratio (H/D).....70

Table 8 Effect of different temperature on concentration and purity in ATPE 71

Table 9 Process efficiency in terms of time.....73

Table 10 Comparison of the result from this work with those reported in the literature.....75

Table 11 The overall mass transfer coefficient.....81

Table 12 The mass diffusion times, Soret coefficient, the isothermal diffusion coefficient, and the thermal diffusion coefficient of ATPE on TG process 82

Table 13 Literatures empirical of correlation 84

Table 14 Comparison of the values obtained from experiments and simulation 90

Table 15 Calculated height using equation 91

Table 16 The assembly details and cost of extractor machine.....94

Table 17 The economic analysis of extractor full capacity 30 L.....95

LIST OF FIGURE

Page

Figure 1 Spirulina cell 4

Figure 2 A pigments in *Spirulina platensis* 8

Figure 3 Schematic diagram of the OD-based feedback cultivation system..... 11

Figure 4 Schematic diagram of phycobilisome situated on the thylakoid membrane. 15

Figure 5 Scatter plot of the price of CPC of various grades. 18

Figure 6 Schematic illustration of a phase diagram for ATPE 23

Figure 7 Differential section with axial mixing for the disperse phase. 37

Figure 8 Differential section with axial mixing for the continuous phase 38

Figure 9 Flow chart of overall research methodology 43

Figure 10 Operation of batch and fed-batch cultivation 47

Figure 11 Overview of experiment framework for ATPE 50

Figure 12 Schematic diagram of the ATPE procedure 51

Figure 13 Schematic diagram in experiment of ATPE 52

Figure 14 Extraction equipment overview 56

Figure 15 The effect of sodium nitrate concentration on cell growth 59

Figure 16 Time-course profiles of growth rate, nitrate concentration and CPC 60

Figure 17 Biomass concentration of fed-batch cultivation of *Spirulina platensis* 62

Figure 18 Time-course profiles of growth rate, N-source concentration 64

Figure 19 Time-course profiles of growth rate, N-source concentration 65

Figure 20 Time-course profiles of growth rate, N-source concentration and CPC 66

Figure 21 (A) Concentration profiles and (B) purity of CPC in top phase.....72

Figure 22 SDS-PAGE analysis of CPC.....74

Figure 23 Effect of TG on phase partitioning in the ATPE process 76

Figure 24 Effect of TG on phase partitioning in the ATPE process 76

Figure 25 Modified binodal curve of PEG4000 and potassium phosphates in ATPE ...77

Figure 26 TLL of ATPE process over time in different TG.....78

Figure 27 Determination of overall mass transfer coefficient 81

Figure 28 Nonlinear regression for binodal curve by MATLAB program 83

Figure 29 The algorithm calculation and simulation flow chart 88

Figure 30 Screen example of a MATLAB program to simulate the phase equilibrium behavior. 89

Figure 31 Assembly view of column 92

Figure 32 Conceptual prototype machine design 93

LIST OF SYMBOLS

General Notations

		Unit
A_{280} , A_{620} , A_{652}	the maximum absorbance of total protein CPC and	-
A_{φ} , b	Partanen's constant	-
a	specific interfacial area	1/cm
c_k	the coefficients regression by Partanen et al. (2003)	
d_{vs}	average drop diameter	cm
D	diameter of column	m
D_c	whirlpool axial diffusivity of the continuous phase	cm^2/s
D_d	whirlpool axial diffusivity of the disperse phase	cm^2/s
D_i	isothermal diffusion coefficient	m^2/s
D_T	thermal diffusion coefficient	$m^2/s.\ K$
D_w	biomass weight	g dw
f	fugacity	
g_{13}	empirical function of interaction parameter between	
H	height of column	m
HTU	height of transfer unit	m
I	ionic strength	
$k_L a$	overall mass transfer coefficient	min^{-1}
K	partition coefficient	
K_d	mass transfer coefficient referred to the disperse	cm
m	slope of the equilibrium curve	-
MW_i	molecular weight of component	g/mol
n_i	number of moles of component	-
N_A	mass transfer flux	mol/cm^2s
NTU	number of transfer unit	
OD_{680}	optical density at wavelength 680 nm	
P_w	biomass productivity	g/L.d
r_i	number of segment per polymer; ratio of molar	
R	universal gas constant	
R_G	radius of gyration	Å

S_T	soret coefficient	1/K
t	time	day , min
T	absolute temperature	K
TG	temperature gradient	°C
V	volume of solvent	mL
V_c	continuous phase superficial velocity	cm/s
V_d	disperse phase superficial velocity	cm/s
W	wet biomass concentration	g/L
W_i	weight of component	g
χ	continuous phase solute concentration	mol/cm^3
x_F	continuous phase solute feed concentration	mol/cm^3
x_i	mole fraction of component	
y	disperse phase solute concentration	mol/cm^3
y_o	disperse phase solute feed concentration	mol/cm^3
z_A , z_B	the valences of cation and anion for a salt	

Greek

		Unit
ϕ_i	volume fraction of component i in the mixture	-
f		
ΔG_m	Gibbs energy of mixing for a mixture	
η	dynamic viscosity of the solvent	Pa.s
τ_D	mass diffusion time	min
μ	growth rate	d^{-1}
μ_i^0	chemical potential of component i in the standard	
μ_i	chemical potential of component i	
χ_{ij}	interaction parameter between component i and j	
v_d	superficial velocity of dispersed phase	mm/s
v_i	specific volume of component i	
$\overline{v_i}$	molar volume of component i	

Subscript

CPC	value of CPC
i	component 1 = water
	2 = PEG4000
	3 = Salt
	4 = CPC
m	maximum value
P	value of PEG
S	value of salt

Superscript

t	Top phase
b	Bottom phase

มหาวิทยาลัยแม่โจ้ MAEJO UNIVERSITY

CHAPTER 1
INTRODUCTION

1.1 Background and significance of research

Spirulina platensis is a blue green algae. The shape like a spring. It grows in water, can be harvested and processed easily and has significantly high macro- and micronutrient contents. The chemical composition of *Spirulina platensis* indicates that it has high nutritional value due to its content of a wide range of essential nutrients, such as provitamins, minerals, proteins and polyunsaturated fatty acids such as gamma-linolenic acid (GLA) (Nascimento et al., 2014). In many countries of Africa, it is used as human food as an important source of protein and is collected from natural water, dried and eaten. It has gained considerable popularity in the human health food industry and in many countries of Asia it is used as protein supplement and as human health food. It known as a "super food" (Gershwin and Belay, 2007; Henrikson, 1989) because widely used in feed, food, cosmetics and pharmaceuticals. The United States Food and Drug Administration confirmed in 1981 that spirulina is a source of protein and contains various vitamins and minerals and may be legally marketed as a food supplement. Many countries have set up food quality and safety standards for spirulina (FDA, 1981).

There are many factors that influence the yields of *Spirulina platensis* cultivation, such as temperature, light intensity, pH, nutrient etc. Nitrogen is one of the most important factor for cell growth and pigment productivity. Colla et al., (2007) reported nitrogen source important for growth and accumulation of nutrients in the cells of *Spirulina platensis*. Nitrogen is involved in formation process of essential components such as amino acids, chlorophyll, nucleic acid, and amylase. Especially protein with up to 60-70% of dry weight. Protein contains mainly two phycobiliproteins, namely, C-phycocyanin (CPC) and allophycocyanin (APC) approximately at a ratio of 10:1 (Bermejo et al., 1997). The supply of nitrogen source in the medium is a fundamental requisite to cultivate *Spirulina platensis* and

ammonium salt was shown to be particularly effective not only to produce biomass, but also to exalt its CPC content.

CPC has thus been widely investigated with regard to its characteristics and commercial potential. The application of CPC has been examined in a wide range of fields. First, CPC has been developed as the natural food colorant in food industries replacing the toxic synthetic pigments due to its unique color (Leema et al., 2010). It is also used as colorant in cosmetic products like eyeliner and lipstick (Sarada et al., 1999). In the industrial process of CPC extraction. The purity level has different and the price depends on each level. From the report Soley biotechnology institute. There are 4 levels of CPC purity classified: the colorant is 0.75 to 1.50, cosmetics is 1.50 to 2.50, the drug and the food supplement 2.50 to 3.50 and analytical grad is more than 4.0. The price of analytical grad high as 37,275 $/ 10 g, and the drug and food supplements are 15,050 $/ 10 g (Soley biotechnology Institute, 2000).

Minkova et al., (2003) reported the purification of CPC from *Spirulina (Arthrospira) fusiformis* by a multistep treatment of the crude extract with rivanol in a ratio of 10:1 (v/v), and 40 % ammonium sulfate precipitation. The purity was 4.3 and yield of CPC was 43 % from its content in the crude extract (Silveira et al., 2008) present the purification of CPC using ion exchange chromatography. The highest partition coefficients were obtained in the pH range from 7.5 to 8.0 at 25°C. Under these conditions the equilibrium isotherm for CPC adsorption was well described by the Langmuir model. The best conditions for CPC purification using the ion exchange column were at pH 7.5 with an elution volume of 36 mL, obtaining 77.3% recovery and a 3.4-fold increase in purity. Chromatographic method results in dilution of CPC pigment, needing an additional step for concentrating it to the desired level. Similarly, additional step of dialysis is required for the removal of salt after salt (ammonium sulfate) precipitation. Thus, the conventional purification of CPC involves many process steps and it is known that at each step there will be a loss of product yield. (Chethana et al., 2015; Patil et al., 2008; Patil and Raghavarao, 2007; Zhang et al., 2015) These problems can be eliminated to a large extent by using Aqueous Two - Phase Extraction (ATPE).

The purpose of this research is to study and develop the cultivation of Spirulina platensis to obtain high CPC productivity and lead to the development of CPC processing to obtained higher purity than food grade.

1.2 Objectives of research

1. To study and develop for enhancing CPC production of *Spirulina platensis* for crude CPC extraction.

2. To study and develop purification process by Aqueous Two-Phase Extraction.

3. To study mathematical model for predict purification process.

4. To design a prototype of extractor and evaluation with engineering economic analysis.

1.3 Scope of the study

1. *Spirulina platensis* strain was cultured in Zarrouk's medium in 5 L flask from *Spirulina platensis* laboratory at faculty of engineering and agro-industry, Maejo University, Thailand.

2. The preparation of crude CPC following the research by Thaisamak et al. (2019).

3. The prototype designing in this research would conduct in a range capacity of 10-30 liters.

1.4 Keywords

Spirulina platensis; C-phycocyanin; Purification; Aqueous Two-Phase Extraction (ATPE); Mathematical model.

CHAPTER 2

LITERATURE REVIEW

2.1 Background of *Spirulina platensis*

2.1.1 *Spirulina platensis*

They are the very organism which were curious to know due to their photosynthetic behavior which are mostly absent in case of prokaryotes and also due to is basic composition and cell structure that are very much alike of Gram-negative bacteria which is an eukaryotes Figure 1 (Ben-Amotz et al., 1985). Under the high resolution electron microscope it shows prokaryotic organization like capsule, ribosome, thylakoid, fibrils of DNA with numerous inclusions and pluri-stratified cell wall. It has irregular capsule around the filament which has a differentiating morphological characteristic. There is a change of shape from helical to spiral when it is transferred to a solid media from liquid media due to hydration or dehydration of oligopeptides in peptidoglycan layer. The cell wall of spirulina is formed of four layers which are made up of peptidoglycan, which are the main reasons for the easy digestion of spirulina by human. The thylakoid system contains chlorophyll, carotenes and phycocyanin which is our main concern and it also has the electronically transparent protein gas vesicles which help them to float. It also contains polyglucan granules, cyanophycin granules, lipid granules, polyhedral bodies and polyphosphate granules which are highly valuable for its chemical nature and pigments.

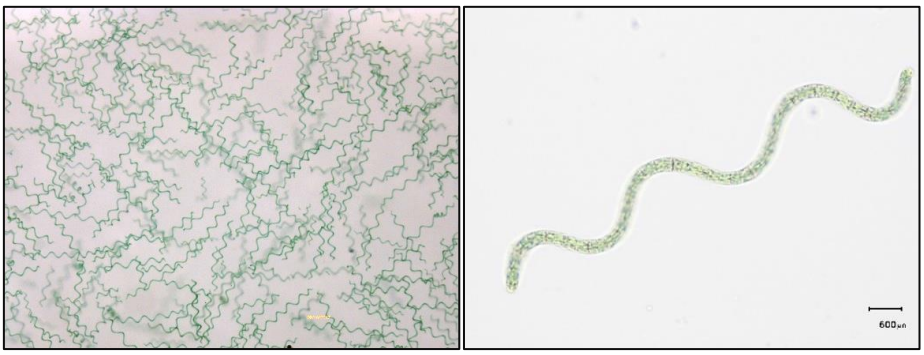

Figure 1 Spirulina cell

2.1.2 Spirulina cultivation

Environmental factors such as temperature light nutrients and pH are very essential in the microalgae cell metabolic processes.

1. Nutrients

Morphology of the spirulina can be altered due to the nutrient concentration and light intensity like in a nutrient deficit condition the degree of coiling increases as a result of which a tight trichome is formed, but in case of high nutrient concentration and high light intensity the opposite occurs that is the tight trichome losses themselves (Bai and Seshadri, 1980). For the cultivation of these algae carbon plays an essential nutrient which is being taken either in inorganic or organic form (Badger and Price, 2003). For synthesis of proteins, amino acids and other cellular components nitrogen is required (Yang et al., 2011). Costa et al., (2003) reported the influence of nutrient for biomass production and growth rate of *Spirulina platensis*, in open raceway ponds.

2. Temperature

Temperature effect on Spirulina biochemical composition of this algae can be altered by the temperature exerting different biochemical reaction (Hu, 2004). 35 to 38°C is the optimum temperature for their growth (Ciferri, 1983). Oliveira et al., (1999) examined that temperature has a great impact on production of *Spirulina maxima* and *Spirulina platensis* used for food.

3. pH

Vincent and Silvester, (1979) reported that, the pH had a direct effect on the physiological properties of algae and the availability of nutrient. pH determined the solubility of carbon source and minerals in the culture directly or indirectly. The optimal pH of the Spirulina nutrient medium was shifted from 8.4 to 9.5 during the mass cultivation, due to the consumption of bicarbonate and sodium ions. Spirulina grew well at pH values between 9 and 11, which are the limiting conditions for the cultivation of microalgae in open reactor (Volkmann et al., 2008). Pandey et al., (2010) examined the influence of pH in *Spirulina platensis* growth, protein and

chlorophyll-a content. The dry weight of *Spirulina platensis* was 0.91 g/500 mL and protein and chlorophyll-a contents were 64.3 % and 13.2 mg/g respectively at pH 9.

4. Light

Light intensity and the efficient utilization of it plays a vital role in increasing of biomass yield (Barbosa et al., 2001). Spirulina required light intensities during its growth phase. The optimal light intensity was between 20 and 30 klux. Jaturonglumlart et al., (2017) reported different effects on growth, pigment and protein synthesis caused of light quality in *Spirulina platensis*. The controlled cultivation of algae in a greenhouse yielded better growth rate than that of algae cultivated in natural system. The LED illumination with the ratio of red and blue as 3:1 with lighting period of 16 hours per day at 350 μmol/m^2.s yielded the best growth of *Spirulina platensis*. From economic analysis, the development of smart algae farming by LED electric solar cell was found to have breakeven point of 2.03 years.

5. Salinity

Imbalance of cellular ions result in osmotic stress and ion toxicity which can be caused due to salt stress which leads to growth retardation, directly or indirectly by oxidative stress, the salt stress can also alter the metabolic pathways leading to the death of the organism (Pahlich et al., 1983; Shalaby et al., 2010). The salt concentration (mostly carbonates and bicarbonates) plays a direct role in the growth of Spirulina.

2.1.3 Biochemical composition

Spirulina is very rich from a biochemical and nutritional point of view, having a significant amount of:

1. Amino acids

The most significant, in terms of number, essential amino acids present in Spirulina are isoleucine, leucine and valine and the most significant non-essential amino acids are glutamic and aspartic acids (Henrikson, 1989; Moorhead et al., 2011). Isoleucine is needed for growth, intelligence development and nitrogen balance.

Leucine helps to increase muscular energy levels and stimulate brain function. Valine assists with the co-ordination of muscular system as well as contributing to improved mental capacity. Aspartic acid helps with the transformation of carbohydrates to energy. Glutamic acid, along with glucose, fuels the brain cells. It can also reduce the craving for alcohol and stabilize mental health (Moorhead et al., 2011; Tietze, 2004).

2. Proteins

Proteins correspond to about 60-70% of the dry weight of Spirulina. These proteins are easily digested and quickly assimilated satisfying hunger very quickly because of the thin membrane. Thus, the digestibility and adsorption are higher, fact that is very important for undernourished people (Adams, 2005; Henrikson, 1989; Moorhead et al., 2011; Tietze, 2004; Vonshak et al., 1994).

Spirulina also contains enzymes, more precisely, the enzyme superoxide dismutase- SOD. This enzyme catalyses the dismutation of superoxide radicals to hydrogen peroxide, protecting cells from toxic and reactive oxygen species. Also, it may be involved in age-related degeneration (Moorhead et al., 2011)

3. Vitamins

Particularly rare is vitamin B12 and provitamin A (retinol). It is important to mention that vitamin B12 is indicated in cases of fatigue, moodiness, pernicious anaemia and nerve degeneration (Henrikson, 1989; Moorhead et al., 2011; Tietze, 2004).

4. Minerals

There are many mineral in spirulina such as iron that is used for making haemoglobin (the oxygen carrier in the blood) and potassium that is used for regulating electrolytes. A deficiency in potassium can lead to heart attack and muscular collapse.

5. Lipids

Animal protein foods are high in calories, fat and cholesterol, however Spirulina as a source of proteins is only five percent fat. The major lipids present in *Spirulina platensis* are monogalactosyldiacylglycerol (MGDG) sulfoquinovosyldiacyl-

glycerol (SQDG) and phosphatidylglycerol (PG). Apart from that, this cyanobacterium has fatty acids such as omega-3 and γ-linolenic acid (GLA). The latter is a rare polyunsaturated fatty acid (PUFA) that has been used for alleviating the symptoms of premenstrual syndrome and for the treatment of atopic eczema. It is also a skin protector against UV radiation, dehydration and activates the blood circulation in skin (Adams, 2005; Charpy et al., 2008; Moorhead et al., 2011; Tietze, 2004; Vonshak et al., 1994).

6. Polysaccharides

Polysaccharides formed by six neutral sugars such as fructose, rhamnose, mannose, glucose, galactose and xylose. These microalgae have shown the ability to excrete polysaccharides to the growth medium. Spirulina is also constituted by sulphate polysaccharides like calcium-spirulan (Ca-Sp) and sodium spirulan (Na-Sp). The Ca-Sp has the capacity to inhibit replication of several virus and because of this it can be a good candidate to fight HIV. It is also used in reducing cholesterol levels (Belay, 2002; Moorhead et al., 2011).

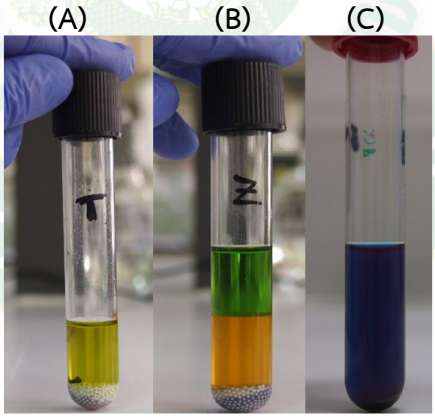

Figure 2 A pigments in *Spirulina platensis*

(A) Extraction of all pigments (B) Separation between chlorophylls (green phase) and zeaxanthin (orange phase). (C) Extraction of CPC present in *Spirulina platensis.*

Source: Veiga, (2016)

7. Pigments

This cyanobacterium is very rich in pigments too (Figure 2A). In its chloroplasts there are pigments like chlorophylls, phycobilines like phycocyanin (with blue fluorescence) and phycoerythrin (with red fluorescence), carotenoids (β -carotene and others) and xanthophylls (zeaxanthin, myxoxanthophyll, cryptoxanthin, echinenone, fucoxanthin, violaxanthin and astaxanthin) (Charpy et al., 2008; Henrikson, 1989; Moorhead et al., 2011; Vonshak et al., 1994).

Chlorophyll a (Figure 2B): this pigment is known as "green blood" because it is regarded as the haemoglobin molecule in the human body. It is a phytonutrient responsible for cleaning and detoxifying and is very beneficial for a healthy skin (avoids inflammations) (Dominguez, 2013; Henrikson, 1989; Tietze, 2004; Vonshak et al., 1994).

C-Phycocyanin (CPC) (Figure 2C): it is the major component of the phycobiliprotein family. CPC is a powerful water-soluble antioxidant blue pigment that gives *Spirulina platensis* its bluish tint. It can only be found in blue-green algae. CPC is thought to help protect against renal failure and against degenerative diseases like Parkinson and Alzheimer in rats. Recently, CPC has showed itself promising in treating cancer in animals, stimulate immune system and inhibit allergic inflammatory response (Belay, 2002). It is also used as a nutritive ingredient and natural dye in foods (dairy products, ice sherbets, jellies and chewing gums) and cosmetics (Antelo et al., 2010; Boussiba and Richmond, 1979; Charpy et al., 2008; Silveira et al., 2007).

Phycoerythrin (PE) is a large, red protein pigment complex accessory to the main chlorophyll pigments. This pigment is very useful in laboratories for labelling antibodies in techniques of immunofluorescence: fluorescent dyes for FACS analysis, for example. Carotenoids are used and stored in several parts of the body including the reproductive system, the skin (gives it elasticity) and the retina. For β -carotene, spirulina has been described as the richest food in β -carotene, an important antioxidant, having ten times more β -carotene than carrots. This pigment has therapeutic effects like reducing cancer risks and reducing cholesterol (Henrikson, 1989; Moorhead et al., 2011; Tietze, 2004). Zeaxanthin (Figure 2B) is a very important antioxidant because it can cross the blood-brain barrier and protect the eyes, brain

and central nervous system and it does not become a pro-oxidant (Moorhead et al., 2011).

2.1.4 Spirulina cultivation system

The growth characteristics and composition of microalgae significantly depend on the cultivation conditions. The major types of cultivation conditions based on the supply energy carbon sources and nitrogen sources are photoautotrophic, heterotrophic, mixotrophic and photoheterotrophic used for microalgae. Microalgae use light, (sunlight, LED) as the energy source, inorganic carbon (e.g.,carbon dioxide) as the carbon source and nitrate or ammonium as nitrogen sources to form chemical energy through photosynthesis in phototrophic cultivation and is the commonly used cultivation method. High cell density culture is desirable in order to reduce the cost for down- stream processing in commercial production. Culture methods like batch, fed batch and continuous used in the cell cultures are applied for the cultivation of microalgae.

1. Batch cultivation

In the batch culture, the nutrients and microalgae inoculate added in the beginning of the batch, and the cultivation is continued until the end of the growth period. The growth stage contains lag, log a, stationary and decline stages. During the sufficient availability of nutrient in the beginning of growth time, the cell proliferate at the exponential rate and reaches to stationary phase when the nutrients are exhausted where the cells experience stress and induce the protein accumulation. Biomass productivity is reduced as the nutrients were depleting during which the protein production is enhanced. Nutrient limitation evokes change in the physiology and the cells re-program their metabolism to cope with change in nutrient supply or to activate a survival program to outlive sustained periods of starvations.

2. Fed-batch cultivation

A batch culture of microbes fed continuously with culture medium is described as a “fed-batch” culture. The reduced biomass productivity compromises

the increased lipid productivity enhanced by the feeding of the fresh media or nutrients to increase the cell growth. In fed-batch, cultures may reach a "quasi-steady state" in which the specific growth rate (μ) virtually equals the dilution rate, that is, the ratio of medium flow rate to culture volume. In a quasi-steady state the specific growth rate gradually decreases. A unique feature of a fed-batch culture is that it allows continuous reproduction of the transient conditions between two specific growth rates, which can be chosen at will. Fed-batch culture may be used to determine the relation between specific growth rate and the growth-limiting substrate concentration and to determine the maintenance energy

Bao et al., (2012) study in the relationship between biomass production and ammonium consumption in the fed-batch culture of *Spirulina platensis* using ammonium bicarbonate as a nitrogen nutrient source, an online adaptive control strategy based on optical density (OD) measurements for controlling ammonium feeding was presented. The ammonium concentration was successfully controlled between the cell growth inhibitory and limiting concentrations using this OD-based feedback feeding method. The schematic diagram of the OD-based fed-batch cultivation control system is shown in Figure 3

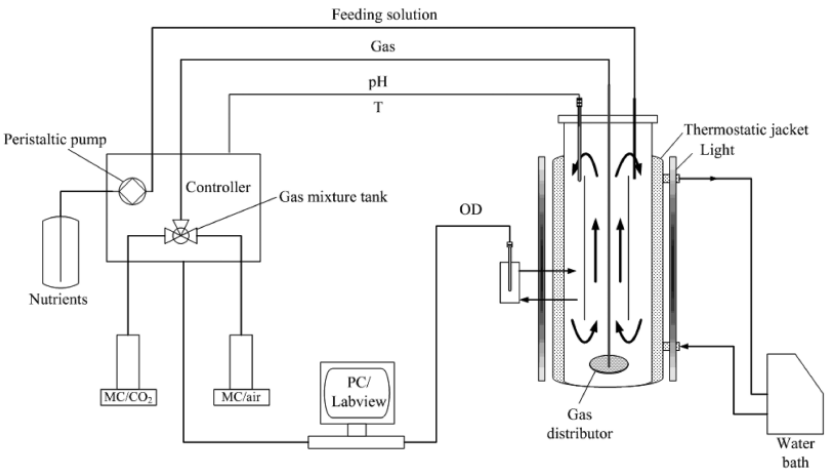

Figure 3 Schematic diagram of the OD-based feedback cultivation system

Source: Bao et al. (2012)

2.1.5 Cultivation model

1. Cell growth model

The most widely used unstructured model for the specific growth rate, μ , is the Monod equation, which increases monotonically as a function of the substrate concentration and substrate inhibition of growth at higher substrate concentrations (Monod, 1949):

$$\mu = \frac{\mu_m C_S}{K_S + C_S + \frac{C_S^2}{K_i}} \qquad \text{Eq. (1)}$$

Practically, the most important environmental factor for the algal culture is light, which primarily concerns photosynthesis. In a manner similar to that of the expression $(1 - C_P / C_{P_m})$. (Zeng et al., 1994) Thus the model may be extended as follows:

$$\mu = \mu_m \frac{\mu_m C_S}{K_S + C_S + \frac{C_S^2}{K_{Xi}}} \left(1 - \frac{C_P}{C_{P_m}}\right) \qquad \text{Eq. (2)}$$

Where μ is the specific growth rate (1/day),

μ_m is the maximum specific growth rate (1/day),

C_X, C_P, C_S are the cell product and substrate concentration (g/L)

C_{X_m}, C_{P_m} are the maximum cell and product concentration (g/L)

K_S, K_{X_i} are the substrate saturation constant and the substrate inhibition constant of cell growth (g/L) respectively.

2. Product formation model

The much-discussed kinetic model for product formation is the following equation (Luedeking and Piret, 1959):

$$\frac{dC_P}{dt} = Y_{PX} \frac{dC_X}{dt} + \mu_{PX} C_X \qquad \text{Eq. (3)}$$

The model states that the product formation rate of cells can be attributed to a growth-associated part and a non-growth-associated part. Apparently, the model does not take into account the inhibition effects of glucose, product itself and light intensity. (Moraine and Rogovin, 1971) Similarly, the logistic expression $(C_P(1-C_P/C_{P_m}))$ were formulated accordingly to describe light influence and product inhibition, respectively. Therefore, the Luedeking-Piret equation for product formation is extended as follows:

$$\frac{dC_P}{dt}=\left(Y_{PX}\frac{dC_X}{dt}+\mu_{PX}C_X\right)\left(\frac{C_SC_P}{K_{PS}+C_S+\frac{C_S^2}{K_{Pi}}}\right)\left(1-\frac{C_P}{C_{X_m}}\right)\left(1-\frac{C_X}{C_{X_m}}\right) \qquad \text{Eq. (4)}$$

Where K_{PS} is the substrate saturation constant.

K_{Pi} is the substrate inhibition constant.

Y_{PX} is the instantaneous yield coefficient of product formation (g/g)

μ_{PX} is the specific formation rate of product (1/day).

3. Substrate consumption model

The most widely used substrate consumption model can be expressed as:

$$-\frac{dC_S}{dt}=\frac{1}{Y_{PX}}\frac{dC_X}{dt}+\frac{1}{Y_{PS}}\frac{dC_P}{dt}+\mu_{SX}C_X \qquad \text{Eq. (5)}$$

In this study, a Monod-type expression $C_S/K_{SA}+C_S$ was employed to describe the autoinhibition of substrate itself. Eq (5) can be written as

$$-\frac{dC_S}{dt}=\frac{C_S}{K_{SA}+C_S}\left(\frac{1}{Y_{XS}}\frac{dC_X}{dt}+\frac{1}{Y_{PS}}\frac{dC_P}{dt}+\mu_{SX}C_X\right) \qquad \text{Eq. (6)}$$

K_{SA} is the autoinhibition constant of substrate.

Y_{XS} is the instantaneous yield coefficient of cells on substrate (g/g)

μ_{SX} is the specific consumption rate of substrate (1/day).

Y_{PS} is the instantaneous yield coefficient of product on substrate (g/g)

2.2 C-phycocyanin (CPC)

Cyanobacterium *Spirulina* has been commercialized in several countries for its use in health foods and for therapeutic purposes due to its valuable constituents particularly proteins and vitamins (Benneman, 1988). The growing awareness of importance of natural colors especially food and cosmetic colorants has placed great demand on biological sources of natural colors. Cyanobacteria and algae possess a wide range of color components including carotenoids, chlorophyll and phycobiliprotieins (Henrikson, 1989). Although the algae contain many colors, the explanation here is restricted only to phycobiliproteins as in the present study more emphasis is given for its purification. Phycobiliproteins are water soluble, highly fluorescent proteins generally found in Cyanobacteria (blue-green algae) and red algae (Glazer, 1994). The biliproteins are broadly classified into three groups based on the spectroscopic properties, namely (1) phycoerythrin (PE), $A_{540-570}$ nm, which has the red chromophore phycoerythrobilin; (2) C-phycocyanin (CPC), $A_{610-620}$ nm, which contains either a mixture of the phycocyanobilin and phycoerythrobilin chromophores or just phycocyanobilin, depending on the species of origin and (3) allophycocyanin (APC), $A_{650-655}$ nm, with phycocyanobilin as prosthetic group (Gantt, 1981).

Phycobiliproteins are assembled into particles named phycobilisomes which are attached in regular arrays to the external surface of the thylakoid membrane and act as major light harvesting pigments in Cyanobacteria and red algae. Phycobilisomes consist of allophycocyanin cores surrounded by rods contain phycocyanins and phycoerythrins on the periphery as shown in the Figure 4.

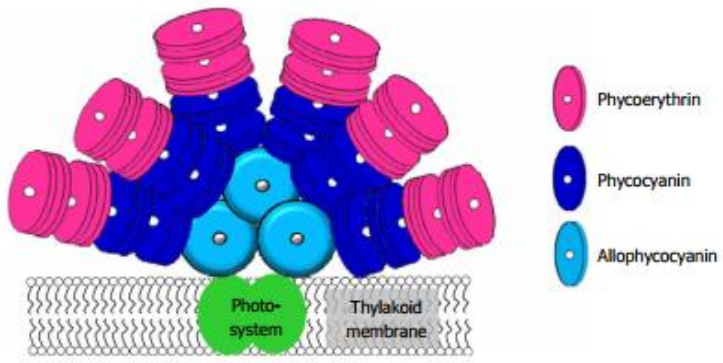

Figure 4 Schematic diagram of phycobilisome situated on the thylakoid membrane.
Source: Sonani et al., (2016).

CPC is the major component of the phycobiliprotein family. CPC exhibits a strong red fluorescence when it is present in native and concentrated form. The purity of CPC is generally evaluated based on the absorbance ratio of A_{620}/A_{280}. CPC of purity 1.7 is considered as food grade, 3.9 as reactive grade and greater than 4.0 as analytical grade (Rito-Palomares et al., 2001). Based on purity, the phycocyanin has got wide range of applications starting from nutritional field to that of research and industry.

2.3 CPC Extraction

The extraction methods are the factor for the maximum recovery of phycobiliproteins in the natural state from the algae. The phycobiliprotein extraction involves rupture the cell biomass for the extraction of protein from the cell, (Hemlata et al., 2011). Cyanobacteria are extremely resistant to the disruption of their cell walls.

Table 1 Reviews of CPC extraction

Reviews	Type of biomass	Extraction method	Type of solvent	Ratio (w/v)	CPC (mg/ml)	Yield (mg/g)	Purity
Minkova et al., 2003	Wet	RFT + stirring	Potassium phosphate	1:10	1.28	12.8	0.95
Moraes et al., 2011	Wet	RFT	Sodium phosphate	1:5	0.21	13.7	-
Niyamat, 2013	Wet	Homogenization	Sodium phosphate	1:10	1.44	14.5	-
Kumar et al., 2014	Wet	Homogenization and RFT	Acetate buffer	1:20	0.67	13.4	0.75
Ruangyot et al., 2016	Wet	UA + RFT	Sodium phosphate	1:0.6	3.72	1.15	1.54
Manirafasha et al., 2018	Wet	RFT	NH_4Cl solution	1:10	0.21	6.14	1.5
Chaiklahan et al., 2011	Dried	Continuous mixing	Phosphate	1:100	1.09	109	1.04
Pan-utai et al., 2018	Dried	Freeze-Thaw	Sodium phosphate	1:15	2.26	104.78	3.29
Su et al., 2014	Dried	Stirring	Sodium phosphate	1:25	2.1	52.5	
Avila and Prabu, 2015	Dried	Shaker	Sodium phosphate	1:100	0.11	10.8	0.91
Hadiyanto and Suttrisnorhadi, 2016	Dried	UAE	Ethanol	1:16	9.56	152.96	
Tavanandi et al., 2018	Dried	UA+RFT	Potassium phosphate	1:6	18.26	109.57	0.8
Nagar et al., 2018	Dried	UAE	Distilled water	1:25	0.25	62.5	-

Note: RFT is mean Repeat Freeze Thaw; UAE is mean Ultrasonic Assisted Extraction

Source: Thaisamak (2020)

Hence the use of variations in the osmotic pressure, abrasive conditions, chemical treatment, freezing and thawing, sodium phosphate buffer and sonication, (Duangsee et al., 2009) apart from the usage of these methods mechanical disintegration methods are currently preferred for large scale operations. The review of CPC extraction method as shown in Table 1.

The report from Thaisamak et al., (2019) demonstrate the potential of the ultrasonic-assisted extraction with controlled temperature (UAET). The UAET was used to improve the extraction efficiency, in terms of time, concentration and yield of the CPC. The operating parameters were investigated that are ultrasonic frequencies (28, 45 and 100 kHz) and controlled extraction temperatures (40, 45 and 50 °C), and the best parameter values were identified. The highest values of the

concentration and yield were recorded by the UAET method that is 2.55 mg/ml and 127.70 mg/g, respectively. The optimal extraction conditions were achieved at 30 min and 45°C of controlled temperature, with 100 kHz of ultrasonic frequency, and the solid-liquid ratio of 1:5 w/v.

2.4 CPC Purification

CPC purity is recognized as a good indicator of preparation purity, especially where other protein contaminants may be involved in the preparation processes. The sale price of CPC is dependent on purity, where purity is typically graded in three bandings based on the pigment: protein ratio measured at an absorbance of A620/A280. Below 1.5 CPC purity ratio is classified as food grade, up to 3.9 is reactive grade and above 4 is analytical grade (Rito-Palomares, 2001). The lower end of the reactive grade banding (1.5- 2.4 purity) is usually graded as suitable for cosmetics. Food and cosmetic grade CPC is used mainly for its color, reactive grade CPC is of a quality to be used as biomarkers and in gel electrophoreses and analytical grade CPC can be used therapeutically. CPC is often sold as lyophilized, water-soluble powder and the higher the purity of CPC, the higher the cost. Figure 5 shows the price of CPC sold at different purities in various amounts by five manufacturers: Soley Institute (Turkey), Delhi Nutraceuticals PVT (India), Biotechnology Co. (China), Qingdao Haosail Science Co. (China), Sigma Aldrich (UK). At a purity classified as food grade the price of CPC ranges from 4.8 -7.3 THB per gram. At a reactive grade purity the price of CPC ranges from 20-40,000 THB per gram. Analytical grade CPC can sell for 4,000-4,000,000 THB per gram.

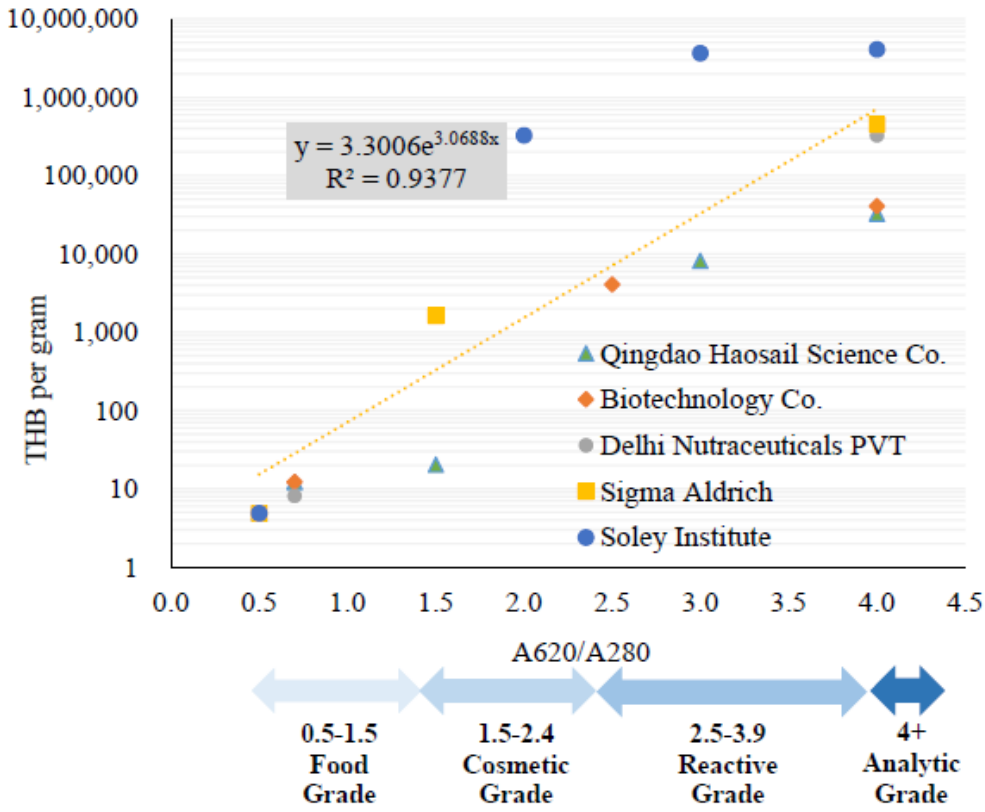

Figure 5 Scatter plot of the price of CPC of various grades.

Source: Modified from (Brain, 2017)

Several methods have been developed to extract and purify CPC, such as precipitation, ion-exchange chromatography, and gel-filtration chromatography, but these are tedious and time-consuming (Chaiklahan et al., 2011; Liao et al., 2011; Niu et al., 2007). The major drawback of almost all such methods is the large number of steps involved, high cost, low loading quantities, low recovery rates, and complexities and difficulties in up-scaling.

2.4.1 Precipitation

Proteins precipitation occurs due to salting out effect, as a result of the competition between protein and saline ions for water molecules, leading to hydration water removal from protein. A greater protein-protein interaction happens, which becomes stronger than protein-water interaction, resulting in aggregation of

protein molecule followed by their precipitation. However many proteins precipitate in a narrow salt concentration range, making this method efficient for fractionation.

2.4.2 Membrane filtration

As a method of separation, membrane processes are relatively new. Thus membrane filtration was not considered a technically important separation process until 30 years ago. Today membrane processes are used in a wide range of applications and their importance is growing day by day. Membrane processing is an emerging technology and because of its multidisciplinary character it can be used in a large number of separation processes. However, comparison between different separation processes is difficult.

The membrane processes are broadly classified into two types namely pressure driven membrane processes and non pressure driven membrane processes. In pressure driven processes, the membrane process can be distinguished based on membrane pore size and consequently on the particle size of the solute. These processes are microfiltration (MF), ultrafiltration (UF), nanofiltration (NF) and reverse osmosis (RO). During these processes, the transport through the membrane takes place as a result of applied pressure (pressure gradient) on the feed side. Because of this driving force, the solvent and various solute molecules permeate through the membrane, whereas other molecules or particles are rejected to various extents depending on the pore size of the membrane.

Microfiltration (MF) is the membrane process which most closely resembles conventional coarse filtration with respect to the pore sizes of membranes (0.05 to 10 μm). Transmembrane pressure of less than one bar is required to run such process, and is mainly used for separating colloidal and suspended particles of size range, of 0.05 to 10 microns. The other applications of this process include: cell harvesting from bioreactors, virus removal for solutions, clarification of fruit juice and beverages, air filtration and sterilization.

Ultrafiltration (UF) the pore size of the membrane lies between nanofiltration (NF) and microfiltration, that is, in the range of 0.05 μm (near MF) to 1 nm (near NF). Pressure in the range of 1 to 10 bar is required to run this process. It is used to

separate extremely small particles and dissolved molecules in fluids. In addition to size of the molecule, other factors such as molecule shape and charge can also play a role in the efficacy of this process. Molecules larger than the membrane pores will be retained near the surface of the membrane and get concentrated during the ultrafiltration process.

Nanofiltration (NF) falls between UF and RO and constitutes a relatively new class of membrane separation process. The pore size of the membrane is < 2 nm and the pressure range required to run this process is in the range of 10 to 25 bar. Most of NF membranes are composites and mainly used in separation applications such as demineralization, color removal and desalination. It also used in concentration of organic solutes, suspended solids, polyvalent ions, permeate contains monovalent ions and low molecular weight organic solutions like alcohol.

2.4.3 Ion exchange chromatography

Ion exchange is probably the most frequently used chromatographic technique for the separation and purification of proteins, polypeptides, nucleic acids, polynucleotides, and other charged biomoleules. The reasons for the success of ion exchange are its widespread applicability, its high resolving power, its high capacity, and the simplicity and controllability of the method. (Khan, 2012)

Purification using ion exchange chromatography depends upon the reversible adsorption of charged solute molecules to immobilized ion exchange groups of opposite charge. Most ion exchange experiments are performed in five main stages. These steps are illustrated schematically.

The first stage is equilibration in which the ion exchanger is brought to a starting state, in terms of pH and ionic strength, which allows the binding of the desired solute molecules. The exchanger groups are associated at this time with exchangeable counter-ions (usually simple anions or cations, such as chloride or sodium). The second stage is sample application and adsorption, in which solute molecules carrying the appropriate charge displace counter-ions and bind reversibly to the gel. Unbound substances can be washed out from the exchanger bed using starting buffer. In the third stage, substances are removed from the column by

changing to elution conditions unfavorable for ionic bonding of the solute molecules. This normally involves increasing the ionic strength of the eluting buffer or changing its pH.

2.5 Aqueous two phase extraction (ATPE)

Among the numerous protein downstream processes described above, liquid-liquid extraction has been established as an interesting alternative purification method since several features of the early processing steps (recovery, concentration and purification) can be combined into a single operation (Mazzola et al., 2008). Generally, liquid-liquid extraction is defined as the transfer of certain components from one phase to another when immiscible or partially soluble liquid phases are brought into contact with each other. Due to its simplicity, low costs and ease of scale-up this process has widely been employed in chemical industry. Compared to other separation techniques, extraction is considered to have special advantages when handling labile substances or when distillation is impossible for economic reasons or product properties. Nevertheless, liquid-liquid extraction systems applied in industry usually involve the use of organic solvents which are not suitable for protein recovery as most proteins are either insoluble in organic solvents or are denatured irreversibly (Kula et al., 1982). Therefore, the production of recombinant proteins and enzymes requires the development of an adequate separation technique at reasonable cost. Liquid-liquid binary systems can also be formed using two polymers or polymer/salt solutions. These so-called Aqueous Two-Phase Extraction (ATPE) were first discovered in 1896 by the Dutch microbiologist M. Beijernick who noticed the separation of two phases when solubilizing gelatin and agar or starch in water (Beijerinck, 1910). However, the first report of ATPE remained unnoticed until 1956 when a Swedish biochemist, P. A. Albertsson, rediscovered the phenomenon and developed the phase separation technique (Albertsson, 1956). Since then, ATPE have found widespread application. They have proven to be highly suitable for the gentle separation of cell membranes and organelles from crude cell lysates as well as for the selective purification of proteins and enzymes from protein

mixtures or cell extracts (Agasoster, 1998; Albertsson, 1956, 1986; Gündüz, 2000; Rito-Palomares, 2004; Roobol-Bóza et al., 2004; Walter and Johansson, 1994).

In general, ATPE are composed of either two incompatible polymers (e. g. polyethylene glycol (PEG) and dextran) or one polymer and a salt (e. g. PEG and a phosphate salt) in aqueous solution. If these phase-forming compounds are solubilised above a critical concentration in aqueous solution, the separation of two phases occurs. Each phase contains predominantly water (70-90 %) and is enriched with regard to one of the phase-forming components. Both polymer/polymer and polymer/salt ATPE provide advantages over conventional extraction methods using organic solvents. Due to the aqueous nature of the phases and the low interfacial tension (between 0.0001 and 0.1 dyne/cm), ATPE allow one phase to disperse into the other and thus create a high interfacial contact area for efficient mass transfer. Moreover, the polymers have been reported to exhibit stabilizing effects on the biological activity and structure of proteins and enzymes (Albertsson, 1986). The mild process conditions as well as the fast phase separation allow the purification of biomolecules by providing a biocompatible environment and reducing protein denaturation and enzyme inactivation.

2.5.1 Phase diagram

Phase diagram data are commonly used in order to delineate the potential working area for a particular two-phase system. The phase diagram provides information about (1) the concentration of the phase-forming components necessary to form a system with two phases which are in equilibrium, (2) the subsequent concentration of phase components in the top and bottom phase, and (3) the ratio of phase volumes. This information can be drawn from the binodal curve and the tie-lines which are characteristic for a phase diagram of an investigated ATPE (Figure 6). The top phase ‘polymer 1’ is plotted on the abscissa and the bottom phase ‘salt or polymer 2’ is plotted on the ordinate. Usually, the axes are labelled with polymer and salt concentrations, in the units of weight of the substance per 100 weight units of the mixture (percent by weight; wt %). The binodal curve separates the one-phase region, located below the binodal, from the two-phase region, above the curve.

Component concentrations from the region above the binodal curve will form two immiscible aqueous phases, while those from below the binodal will provide only a one-phase system. Information about the final concentration of phase components in the top and bottom phases of a generated ATPE can be drawn from the tie-line that connects two nodes (T and B in Figure 6) on the binodal. The ratio of the segments PB (top phase) and PT (bottom phase) can be approximated graphically by the volume ratio of the two phases. The points P1, P2, and P3 represent the total compositions of three systems lying on the same tie-line with different volume ratios. ATPE prepared by component concentrations along the tie-line will provide systems with the same final concentration of phase components in the top and bottom phases, but a differing total composition and volume ratio between the phases. Just above the so-called critical point (C_P) the composition and volume of both phases are almost equal.

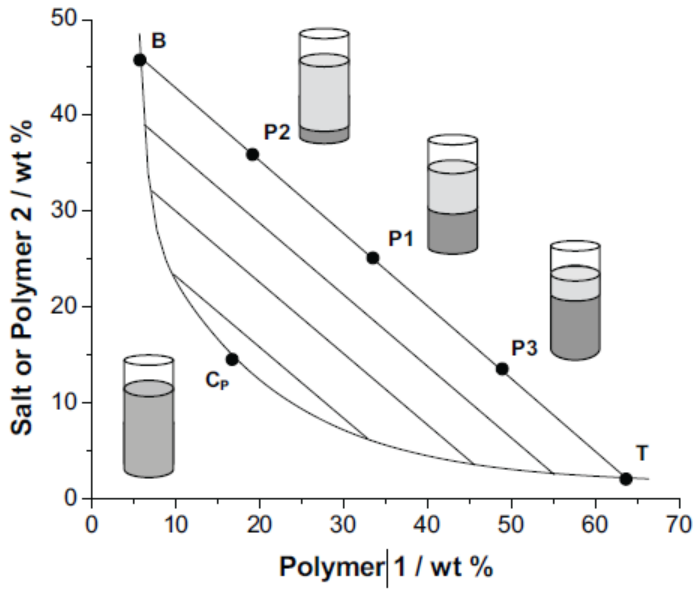

Figure 6 Schematic illustration of a phase diagram for ATPE

Source: Dreyer, (2008)

2.5.2 Process of phase formation

The state of knowledge on the theory of phase formation in aqueous two-phase systems is still characterised by a huge variety of ideas, models and methods (Cabezas, 1996). This fact is reflecting the relatively poor understanding of the process itself. Still, for polymer/polymer ATPE, phase formation has been generally attributed to the hydrated surfaces of each species which are sufficiently incompatible to generate phase separation (Albertsson, 1986; Rito-Palomares, 2004). From a thermodynamical point of view, phase separation can be explained by consideration of the Gibbs free energy. A closed aqueous two-phase system at constant temperature and pressure reaches equilibrium when the total Gibbs free energy is at minimum. The change of Gibb's free energy is defined by ΔH_m (Enthalpy change), ΔS_m (Entropy change) and T (Absolute temperature) according to Eq.7

$$\Delta G_m = \Delta H_m - T\Delta S_m \qquad \text{Eq. (7)}$$

The value of ΔG_m must be negative for mixing of components to occur and consists of an entropy and an enthalpy term. The entropy term, ΔS_m is a measure of the degree of disorder in the system as a result of the mixing process. Summation of individual net enthalpy changes associated with the interaction of unlike components defines the enthalpy of mixing, ΔH_m Phase separation occurs, when the interaction energy between unlike components becomes slightly positive (ΔH_m increases). For ATPE, the large size of the polymer reduces the entropy of mixing and results in the decrease of the term $T\Delta S_m$. Hence, the enthalpy of mixing dominates the Gibbs free energy, resulting in a positive change of ΔG_m. As a consequence, the system becomes unstable and the formation of two phases takes place due to a reduction of interactions between unlike molecules which is needed to reach equilibrium. Phase separation in polymer/salt systems remains largely unclear. It was initially proposed to be associated with differing interactions with the ether dipoles of the polymer chain but this theory has not been widely adopted (Huddleston et al., 1991). However, the relative effectiveness of various salts in promoting phase separation is seen to follow the Hofmeister series.

2.5.3 System variables influencing partitioning

Several factors are known to influence the properties of ATPE and partitioning of biomolecules therein. In this regard, system variables affecting the composition of ATPE, and therefore partitioning are discussed in this section. These have to be distinguished from protein-related properties which also exhibit a strong influence on the partition behavior.

Partitioning between the phases of ATPE is dependent on the chemical difference between the phases and thus the polymer concentrations. In general, with increasing polymer concentration, the partitioning of a substance towards the polymer-enriched phase will be enhanced due to an increased chemical difference between the phases (Albertsson, 1986; Johansson et al., 1998; Walter and Johansson, 1994). Additionally, the molecular weight of the polymer used influences ATPE formation; the greater the molecular weight, the lower the concentration required for phase separation. This effect has been attributed to the interaction of the PEG chain with water molecules. For low molecular weights only tightly bound water molecules are associated with the PEG chain. Increasing the molecular weight, however, results in the chain beginning to fold on itself (adopting a secondary structure), as it shares loosely bound water between adjacent segments (Harris, 1992). As a consequence the interaction reduces the contact of the PEG chain with water molecules and phase formation is facilitated (Zijlstra et al., 1996).

The most commonly used polymers for the formation of ATPE are polyethylene glycol (PEG) and dextran. Since both of these polymers are non-toxic and have been intensively tested for food and pharmaceutical use, they are also classified as safe for the recovery of therapeutic proteins. A wide variety of other polymers have been investigated for the formation of ATPE, including e. g. random copolymers of ethylene oxide (EO) and propylene oxide (PO) or ficoll (Aldred et al., 1993; Alred et al., 1994; Berggren et al., 1995; Harris et al., 1991; Johansson et al., 1996).

Studies on PEG/salt ATPE have revealed that the location of the binodal and tie-lines for a particular pair of components depends on the system's temperature.

Since PEG possesses a low cloud point of approximately 100°C in water, a raise of temperature above 100°C results in insolubility of PEG and the formation of two phases. Moreover, it has been reported that the cloud point temperature can be changed by the addition of salt to the PEG solution. With increasing salt concentration, the cloud point temperature is decreased, resulting in the fact that lower concentrations of PEG and salt are needed to obtain phase separation (Aldred et al., 1993; Harris, 1992). The relative effectiveness of salts in promoting phase separation has been reported to follow the Hofmeister series, which is a classification of ions based on their salting-out ability.

2.5.4 Protein properties affecting partitioning

The basis of aqueous two-phase extraction is the selective distribution of substances between the two phases. The partition coefficient (K) of a protein is defined as the concentration of the biomolecules in the top phase divided by the concentration in the bottom phase

1. Protein surface properties

Generally, protein partitioning in ATPE is a process wherein the exposed groups on a protein surface come into contact with the phase components and therefore represents a surface dependent phenomenon (Albertsson, 1986; Asenjo and Andrews, 1989; Lamarca et al., 1990). It can be proposed that the distribution of hydrophobic and hydrophilic residues in combination with charged and other polar groups on a protein's surface determine protein solubility in the aqueous phases and partitioning therein.

The discovery that the surface of globular proteins contains non-polar hydrophobic groups has led to increasing interest in the involvement of hydrophobic interaction during protein partitioning in ATPE (Hachem et al., 1996; Lee and Richards, 1971). Several approaches have been used in order to study the effect of hydrophobicity on partitioning in ATPE. Examples comprise the coupling of hydrophobic tails to PEG in order to increase the hydrophobicity of the phase rich in that polymer or the hydrophobic modification of proteins that were partitioned in a

number of ATPE to investigate the effect of hydrophobicity as a single property on partitioning (Franco et al., 1996; Shanbhag and Axelsson, 1975). In general, high correlations could be found between the surface hydrophobicity of proteins and their partition coefficient in PEG/salt ATPE as well as PEG/dextran ATPE.

Besides protein hydrophobicity, the protein surface charge plays a distinctive role in the partition process. The solubility of proteins in aqueous solutions is determined by a combination of different interactions such as polar interactions with the solvent, ionic interactions with the salt present and repulsive electrostatic forces between molecules of the same charge (Scopes, 1994). Since proteins are composed of sequences of amino acids that carry charged groups (depending upon their acidic or basic character), the net electric charge on a protein surface represents the sum of all electric charges present on the amino acids. At the so-called 'isoelectric point' the net surface charge of a protein is neutral. If the pH value of an aqueous solution containing protein is above the isoelectric point, proteins carry a negative net charge while below the isoelectric point their charge is positive. Hence, the pH value within an ATPE directly influences the charge at a protein's surface. A general rule of thumb recommends to select a system pH above the isoelectric point (pI) of the target compound. As a consequence, an electrochemical affinity is generated between the negatively charged product and PEG, which has a positive dipolar momentum due to its terminal hydroxyl groups (Benavides and Rito-Palomares, 2008; Nerli et al., 2001). However, the pH value should not be increased unnecessarily (e. g. 4-5 units above the pI) since an increasing amount of contaminants will also obtain electrochemical affinity towards the recovering phase.

Furthermore, partitioning in ATPE has been reported to be dependent on the biomolecules' molecular weight. Generally, small molecules such as amino acids tend to distribute evenly between the phases, while larger particles such as proteins or DNA get enriched in one of the phases. Even larger biomolecules like whole cells generally distribute between the interface and one of the two phases or collect entirely at the interface between the phases (Albertsson, 1986; Sasakawa and Walter, 1972). These observations can be explained by the greater contact area between high molecular weight biomolecules and the system components. According to the

biomolecules' characteristics and the kind of interaction, partitioning will tend preferentially to one of the phases.

2. Interaction of proteins and phase-forming compounds

The influence of molecular weight of PEG is related to the molecular weight and hydrophobic character of the target compound. Therefore, its selection must be done according to two physicochemical properties: (1) It has been reported that the purification of hydrophilic high molecular weight compounds (>10000 g/mol) is favored by the application of low molecular weight PEG (<4000 g/mol) within ATPE. (2) On the other hand, the recovery of hydrophilic compounds of low molecular weight (<10000 g mol^{-1}) is improved by applying high molecular weight PEG (>4000 g/mol). This behaviour is related to the free volume available within the top and bottom phase (Cabezas, 1996). An effect of salts on proteins has already been reported more than a century ago by Franz Hofmeister, who noticed that ions exhibited various abilities of precipitating proteins (Hofmeister, 1888). The so-called Hofmeister series classifies ions in order of their ability to change water structure and their effect on the stability of the secondary and tertiary structure of proteins. Ions which exhibit strong interactions with water molecules and thereby increase the structuring of water are called 'kosmotrope', while ions that decrease the structuring of water are named 'chaotropes'. Kosmotropic salts are usually small and highly charged, while chaotropic salts are large and low charged (Zhao, 2006). Nevertheless, the mechanism of the Hofmeister series is not entirely clear. Recent reports postulate that the mechanism does not result from changes in general water structure but instead from more specific interactions between ions and proteins and ions and the water molecules directly contacting the proteins (Zhang and Cremer, 2006).

2.5.5 Application of ATPE

Aqueous two-phase systems have been applied in two main areas: as an analytical tool and for product recovery. These applications as well as selected examples thereof will be discussed in more detail in the following two sections.

1. Analytical application

The dependence of partitioning in ATPE from surface properties and conformation of proteins has rendered the technique a useful tool for a variety of analytical applications. Beside the sensitivity and the rapidity of the method, a particular advantage lies in the possibility to analyses both macromolecular and cellular structures. Basically, analytical applications of ATPE can be divided in two main categories, (1) interactions between biomolecules and (2) studies of protein surface properties.

(1) When biomolecules interact with each other, their partitioning behavior in ATPE is affected due to changes in properties such as size, net surface charge and hydrophobicity (Lundberg and Backman, 1994; Middaugh and Lawson, 1980; Walter and Johansson, 1994). Mattiasson and coworkers have exploited this concept in order to develop an immunoassay format in ATPE called 'partition affinity ligand assay' for rapid quantification of antigen (Mattiasson, 1986). The concept is based on the change in partitioning of one of the reactants as a function of increasing concentration of the other and can be used for the calculation of dissociation constants. Moreover, it has been shown that interactions between molecules can be used to separate enantiomers in ATPE. The preferential partitioning of bovine serum albumin towards the bottom phase in PEG/dextran systems could be used to separate L- and D-tryptophan due to the fact that the protein binds selectively to one of the enantiomeric forms (L-tryptophan) of the racemic mixture (Ekberg et al., 1985).

(2) ATPE have also been applied for studying changes on protein surfaces. Examples comprise e. g. the estimation of surface charges and the isoelectric point of proteins by varying conditions of pH and salt during partitioning in ATPE, or the determination of surface hydrophobicity and conformational changes in proteins by partitioning in the presence of hydrophobic and affinity ligands (Walter and Johansson, 1994). Moreover, changes in the protein surface as a result of point mutations were reported to be predictable from partition coefficients of peptides (Berggren et al., 2000).

2. Product recovery in biotechnology

Representing a technically simple, easily scalable, energy-efficient and mild separation technique ATPE provide a useful tool for product recovery in biotechnology. They are utilized predominantly as primary recovery steps in purification processes. Since most biotechnological products are typically manufactured in large, dilute, multiphase fermentation broths, the first desirable step for their recovery is concentration. Aqueous Two-Phase systems are particularly suitable for this application due to the biocompatible environment and the possibility to include cells or cell debris in the extraction. The usage of ATPE for protein downstream processes is not only restricted to intracellular enzymes from microbial cells but also proteins from more complex raw materials like animal tissues and mucilaginous plant material (Jordan and Vilter, 1991). Moreover, ATPE have been applied for the isolation of membrane proteins which normally are rather difficult and time-consuming to purify, the isolation of DNA and the extraction of small molecular weight compounds such as amino acids (Cole, 1991; Ramelmeier et al., 1991; Sanchez-Ferrer et al., 1989; Sikdar et al., 1991). Further interesting applications of ATPE include the so-called ‘extractive bioconversion’. Since the productivity of biotechnological processes is often very low due to either inhibition or toxicity of the product to the producer-organism or the instability of the product itself, ATPE can be applied to combine product removal and bioconversion. While the bioconversion takes place in one phase, the product is extracted to the other (Kuboi et al., 1995; Kwon and Okano, 1996; Zijlstra et al., 1996). Additional alternative applications of ATPE are exemplarily summarized in Table 2.

Table 2 Alternative applications of aqueous two-phase systems

ATPE	New application	Reference
PEG/dextran	Separation of polymerase chain reaction (PCR)-inhibitory substances from bacterial cells	Lantz et al., 1996
PEG/phosphate	Recovery of viral coat proteins from recombinant *E. coli*	Rito-Palomares and Middelberg, 2002
	Preparation of highly purified fractions of small inclusion bodies	Walker and Lyddiatt, 1998
	Recovery of aroma compounds under product inhibition conditions	Rito-Palomares et al., 2000
PEG/sulphate	Drowning-out crystallization of sodium sulphate	Taboada et al., 2000
	Recovery of metal ions from aqueous solutions	Rogers et al., 1996
	Recovery of food coloring dyes from textile plant wastes	Huddleston et al., 1998
	Partition of small organic molecules	Rogers et al., 1998

The purification of proteins using ATPE has been successfully carried out in large-scale for more than a decade. Scaling up an ATPE process is relatively straightforward since the same partitioning can be obtained both in small laboratory scale and in large-scale extractions. One major advantage lies in the fact that the conventional extraction equipment as used for organic-aqueous extraction can be applied in chemical industry (Hart et al., 1994; Kula, 1990; Kula and Selber, 2009; Raghavarao et al., 1995; Strandberg et al., 1991). Examples for largescale protein extractions include among others the application of PEG/salt systems for purification of recombinant proteins from *E. coli* and the purification of cholesterol oxidase by surfactant-based cloud point extraction systems (Minuth et al., 1997; Minuth et al., 1996; Strandberg et al., 1991). However, limitations in the industrial application of ATPE arise from the incomplete theoretical understanding of phase equilibrium and protein partitioning, as well as the cost of polymers and the isolation of protein from the phase-forming compounds. The latter can be achieved by ion-exchange chromatography or back-extraction though (Asenjo et al., 1994; Johansson, 1994).

Additionally, ultrafiltration can be used to recycle both polymer and salt thereby rendering the process itself more economical (Hustedt, 1986; Veide et al., 1989).

2.6 Mathematical model of Aqueous Two-Phase Extraction behavior

At the present time, there are quite a few mathematical models for phase equilibria in Aqueous Two-Phase Extraction available. The diversity they offer comes from the different concepts and ideas behind the models. Each model has its own strength and limitations because each model is typically best at representing only a few aspects of system behavior. Hence, these aspects must be considered well before a suitable model is selected to predict and represent the phase behavior.

2.6.1 Osmotic Virial Expansions

Edmond and Ogston, (1968) used the osmotic virial expansion in modeling the thermodynamic behavior of ATPE. These expansions are mathematically simple and have model parameters with relatively simple physical interpretations (Cabezas, 1996). There are two different expansions, one is based on the work of (McMillan and Mayer, 1945) and the other on the work of (Hill, 1986). As the expansions are expressed in terms of composition variables, the theories are applicable only at very low solute concentrations, which is the criteria of an ATPE.

The thermodynamic properties of a multicomponent system are represented by a power series in solute concentration in mole volume-1 or molarity by the McMillan and Mayer theory. This is superficially similar to theory of Hill. However, Hill developed chemical potentials at constant temperature and pressure rather than at constant solvent chemical potential which, as a result, does not need any osmotic pressure correction.

2.6.2 Integral Equation Theory

This new approach combines the Omstein-Zemike integral equation (Ornstein, 1914) , Boublik and Mansoori et al. equation of state, perturbation theory (Boublík, 1970; Mansoori et al., 1971), the McMillan Mayer osmotic virial expansion and other elements to come up with a general expression for a modified excess Hernholtz free energy for an ATPE. The model is perhaps the most complete and sophisticated available, however is a very complex model and requires many experimental parameters.

2.6.3 Lattice Theory

The idea of this theory is to model a liquid mixture to be solid-like, as in a quasicrystalline lattice. This is attractive because the macromolecules and the small molecules can be distributed and redistributed until all possible arrangements or configurations have been inspected. The Gibbs energy, for the mixture is then derived from the entropy of the system contributed by the number of possible configurations and the enthalpy contributed by the number of interactions between the molecules. As this theory is based on the assumption of concentrated polymer solutions, the problem faced in osmotic virial expansions with applicability for solution of high concentration is avoided. However, validity remains an open question in very dilute solutions with large number of solvent molecules present between the polymer coils.

The classical polymer solution theory of Flory and Huggins that is based on the lattice theory has been exploited in modeling of the phase behavior of ATPE due to its relative simplicity (Flory, 1942; Huggins, 1942). It provides a good mechanistic insight into the phase formation process as well as qualitatively good predictions or correlations for the phase equilibrium and partitioning behavior.

The Flory-Huggins theory approaches the polymer solution as a lattice of sites; a regular array in space, and supposes that the sites are occupied by either a solvent molecule or a polymer segment. In accordance, the theory defines volume fractions as representations of the fraction of lattice sites occupied by each

substance. Flory and Huggins proposed that the polymer segments in the solution behave like chains with links of the same size as a molecule of the solvent. Thus, a polymer segment and a solvent molecule occupy the same volume. Note that a polymer segment may not correspond with a monomer unit. Further, the segments and solvent can be interchanged with no change in the lattice; that is, no volume change occurs upon mixing and the solution behaves ideally with ideal entropy of mixing and zero excess entropy. Interaction parameters take into account any deviation from ideal solution behavior.

The theory is applied in accordance with a few additional assumptions.

- the aqueous solution is sufficiently represented by the liquid lattice model;
- the aqueous solution posses an ideal entropy of mixing;
- deviations from ideal solution behavior are accounted for in terms of (enthalpic) solute-solvent and solute-solute interaction parameters; and
- the phase-forming polymer chains are flexible.

The mathematical expressions for the Gibbs energy of mixing for each component in the mixture are written based on the theory and the formulation of the difference between the chemical potential of each component and that in the standard state are derived using MATLAB.

The thermodynamic consistency relations given by the cross derivative equality for chemical potentials of each component,

$$\left.\frac{\partial \mu_i}{\partial n_j}\right|_{T,P,n_{k\neq j}} = \left.\frac{\partial \mu_j}{\partial n_i}\right|_{T,P,n_{k\neq j}} \qquad \text{Eq. (8)}$$

$$\sum_i n_i du_i \Big|_{T,P} = 0 \qquad \text{Eq. (9)}$$

The Flory-Huggins theory for solvent-polymer solutions was first extended by Scott and Tompa (Jiang and Prausnitz, 2000; Scott, 1949) to ternary solutions. The Gibbs energy of mixing for the mixture composed of two polymers and a solvent derived is given by

$$\frac{\Delta G_m}{RT} = \left\{ \sum_{i=1}^{3} \frac{\phi_i}{r_i} \ln \phi_i + \sum_{i=1}^{3} \sum_{j=i+1}^{3} \chi_{ij} \phi_i \phi_j \right\} \sum_{i=1}^{3} r_i n_i \qquad \text{or} \qquad \text{Eq. (10)}$$

$$\frac{\Delta G_m}{RT} = n_1 \ln \phi_1 + n_2 \ln \phi_2 + n_3 \ln \phi_3 + (n_1 + n_2 r_2 + n_3 r_3)(\chi_{12}\phi_1\phi_2 + \chi_{13}\phi_1\phi_3 + \chi_{23}\phi_2\phi_3)$$

Eq. (11)

Here n_i is the number of moles of each component.

r_i is the number of segments per polymer.

ϕ_i is the volume fraction of component i in the mixture.

$$\phi_i = \frac{x_i v_i}{\sum_{i=1}^{3} x_i v_i} \qquad \text{Eq. (12)}$$

where the subscripts 1, 2, 3 represent water, a phase-forming polymer and a second phase-forming polymer (or salt); x_i the mole fraction of component i; v_i the specific volume; $\chi_{ij,i\neq j}$ and is the Flory-Huggins interaction parameter between component i and j at 25°C. In this work, it is assumed that the χ_{ij} are independent of composition.

The difference between the chemical potential of each component in the mixture and that in the standard state is defined by

$$\frac{(\mu_i - \mu_i^0)}{RT} = \frac{1}{RT} \left(\frac{\partial (n_1 + n_2 + n_3) \Delta G_m}{\partial n_i} \right)_{T, n_{j\neq i}} \qquad \text{Eq. (13)}$$

Using Eq. 10 and Eq. 13, the following expressions for the chemical potential difference of a component, valid in both the top and bottom phases, are obtained

$$\frac{\Delta \mu_i}{RT} = \ln \phi_i + 1 - r_i \sum_j \frac{\phi_j}{r_j} + r_i \sum_j \chi_{jk} \phi_j - r_i \sum_j \sum_{k>j} \chi_{jk} \phi_j \phi_k \qquad \text{Eq. (14)}$$

Thus,

$$\frac{\Delta \mu_1}{RT} = \ln \phi_1 + \left(1 - \frac{r_1}{r_2}\right)\phi_2 + \left(1 - \frac{r_1}{r_3}\right)\phi_3 + r_1 \left(\chi_{12}\phi_2 (1 - \phi_1) + \chi_{13}\phi_3 (1 - \phi_1) - \chi_{23}\phi_2\phi_3 \right)$$

Eq. (15)

$$\frac{\Delta\mu_2}{RT} = \ln\phi_2 + \left(1-\frac{r_2}{r_1}\right)\phi_2 + \left(1-\frac{r_2}{r_3}\right)\phi_3 + r_2\left(\chi_{12}\phi_1\left(1-\phi_2\right) + \chi_{13}\phi_1\phi_3 - \chi_{23}\phi_3\left(1-\phi_2\right)\right)$$

Eq. (16)

$$\frac{\Delta\mu_3}{RT} = \ln\phi_3 + \left(1-\frac{r_3}{r_1}\right)\phi_1 + \left(1-\frac{r_3}{r_1}\right)\phi_2 + r_3\left(-\chi_{12}\phi_1\phi_2 + \chi_{13}\phi_1\left(1-\phi_3\right) + \chi_{23}\phi_2\left(1-\phi_3\right)\right)$$

Eq. (17)

At equilibrium, under constant temperature and pressure, the difference of chemical potential of the component i (i = 1, 2, 3) must be equal in both phases

$$\Delta\mu_1^{\,t} = \Delta\mu_1^{\,b} \quad , \quad \Delta\mu_2^{\,t} = \Delta\mu_2^{\,b} \quad , \quad \Delta\mu_3^{\,t} = \Delta\mu_3^{\,b}$$ Eq. (18)

where the superscripts t and b indicate top and bottom phases, respectively.

2.7 Mass transfer models

The mass transfer model is based on the equations proposed by (Weinstein et al., 1998) Mathematical model assumptions are the following:

- Variation of average rate and concentrations in the radial direction in each phase are negligible.
- Volumetric flow rate is independent of mass transfer and solute concentration.
- Drops in the disperse phase behave as spheres with uniform diameter.
- The solute is fully miscible in the solvent.
- Global mass transfer coefficient per area unit is constant for each phase.
- Axial dispersion coefficients are independent of height.
- Equilibrium is linear.

2.7.1 Disperse phase

The different terms entering and leaving the differential section which have to be defined for the development of the model show in Figure 7. Mass transfer for the system under study occurs from the continuous phase to the disperse phase.

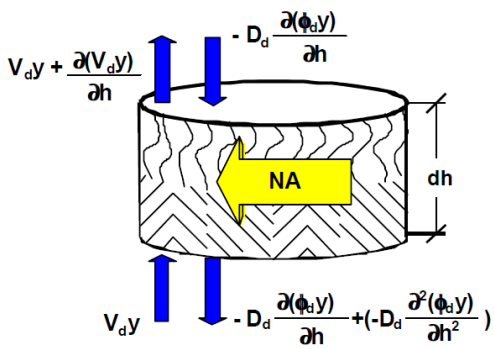

Figure 7 Differential section with axial mixing for the disperse phase.

Source: Modified from Blanco et al., (2000)

The following terms can be observed in the differential section in Figure 7:

Input

$$V_d y - D_d\left(\frac{\partial(\phi_d y)}{\partial h}\right) + N_A.a.dh \qquad \text{Eq. (19)}$$

Output

$$V_d y + \frac{\partial(V_d y)}{\partial h}dh - D_d\left(\frac{\partial(\phi_d y)}{\partial h}\right) - D_d\frac{\partial^2(\phi_d y)}{\partial h^2}dh \qquad \text{Eq. (20)}$$

Accumulation = Input- Output

$$\left(\frac{\partial(\phi_d y)}{\partial h}\right)dh \qquad \text{Eq. (21)}$$

Mass transfer molar flow:

$$N_A.a = K_d a\left(y^* - y\right) \qquad \text{Eq. (22)}$$

Equilibrium equation:

$$y^* = mx \qquad \text{Eq. (23)}$$

The result after a mass balance of each component in the disperse phase is:

$$\frac{\partial(\phi_d y)}{\partial t} = -\frac{\partial(V_d y)}{\partial h} + D_d\left(\frac{\partial^2(\phi_d y)}{\partial h^2}\right) + K_d a(mx - y) \qquad \text{Eq. (24)}$$

Additional considerations were taken to simplify the previous equation:

- Surface rate in the disperse phase is constant throughout the column.
- Disperse phase hold-up is constant throughout the column (it is neither function of time nor of height).

These two considerations arise from the fact that measurement of surface rates and hold-up throughout the column filled with a structured packing is very difficult, if not impossible.

- Axial mixing is negligible.

This last consideration can be explained based on Peclet number.

$$Pe = \frac{U * d_{vs}}{D} \qquad \text{Eq. (25)}$$

Numerator product in Eq. 25 is constant, because surface rates and average drop size were assumed as constant for the development of the model. In addition, Peclet number is inversely proportional to the turbulent diffusion coefficient. This means that at high Peclet numbers diffusion coefficient should be low, which results in a decrease in axial mixing. Applying these assumptions to Eq. 24

$$\phi \frac{\partial y}{\partial t} = -V_d \frac{\partial y}{\partial h} + K_d a(mx - y) \qquad \text{Eq. (26)}$$

2.7.2 Continuous phase

The different inlet and outlet terms in the differential section in Figure 8 are also defined for this phase.

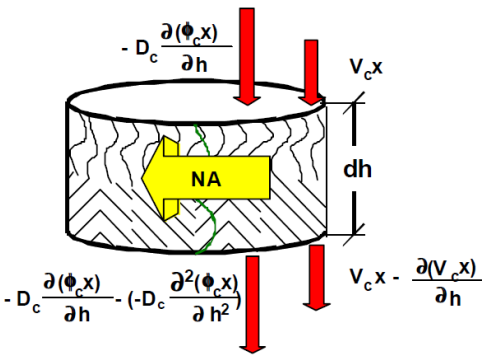

Figure 8 Differential section with axial mixing for the continuous phase

Source: Modified from Berenice et al. (2000)

Input

$$V_c x - D_c\left(\frac{\partial(\phi_d x)}{\partial h}\right) \qquad \text{Eq. (27)}$$

Output

$$V_c x + \frac{\partial(V_c x)}{\partial h}dh - D_c\left(\frac{\partial(\phi_c x)}{\partial h}\right) - D_c\frac{\partial^2(\phi_c x)}{\partial h^2}dh + N_A.a.dh \qquad \text{Eq. (28)}$$

Accumulation = Input- Output

$$\left(\frac{\partial(\phi_c x)}{\partial t}\right)dh \qquad \text{Eq. (29)}$$

A mass balance for each component in the continuous phase results in:

$$\frac{\partial(\phi_c x)}{\partial t} = -\frac{\partial(V_c x)}{\partial h} + D_c\left(\frac{\partial^2(\phi_c x)}{\partial h^2}\right) + K_d a(mx - y) \qquad \text{Eq. (30)}$$

The same assumptions as for the disperse phase were considered to simplify the solution of Eq. 16, resulting in:

$$\phi\frac{\partial x}{\partial t} = -V_c\frac{\partial y}{\partial h} + K_d a(mx - y) \qquad \text{Eq. (31)}$$

Border conditions for differential Eq. 26 and 31 are:

$$h = z \qquad \frac{\partial x}{\partial h} = 0 \qquad x = x_F \qquad \text{Eq. (32)}$$

$$h = 0 \qquad \frac{\partial y}{\partial h} = 0 \qquad y = y_0 \qquad \text{Eq. (33)}$$

Interphase area, a, is calculate as follows:

$$a = \frac{6\varepsilon\phi_d}{\partial_{vs}} \qquad \text{Eq. (34)}$$

2.7.3 Hydrodynamic parameters and mass transfer coefficients

Diffusion coefficients (D_{AB})

When a temperature gradient is applied to a mixture or a solution, molecular segregation occurs and a resulting concentration gradient appears. The sense and intensity of this concentration gradient are linked to the sign of the thermal diffusion coefficient of the reference component in the mixture and to the value of its Soret coefficient.

In 1879, the Swiss scientist Charles Soret discovered that a salt solution contained in a tube with the two ends at different temperatures generated a salt flux and temperature gradient, resulting in steady-state conditions in a concentration gradient. Although German scientist, Ludwig, described the same phenomenon several years before in a one-page report, the name "Soret effect" is usually attributed to mass separation induced by temperature gradients (Platten, 2006). The Soret coefficient (S_T) in binary systems is defined as:

$$S_T = \frac{D_T}{D_i} \qquad \text{Eq. (35)}$$

where D_i is isothermal diffusion coefficient (D_i)

D_T is the thermal diffusion coefficient, which both enter the mass flux equation defined as:

$$J_x(\mathrm{x,t}) = -\rho \mathrm{D}_i \frac{\partial c}{\partial x} - \rho D_T c(1-c)\frac{\Delta T}{a} \qquad \text{Eq. (36)}$$

Using this approximation, if the concentration difference remains small, the thermal diffusive contribution is ruled out of Eq. (36) (Costesèque et al., 2004), but is reintroduced via the boundary conditions that also use the same approximation. Then, Eq. (37) becomes:

$$\frac{\partial c}{\partial t} = \mathrm{D}_i \frac{\partial^2 c}{\partial x^2} \qquad \text{Eq. (37)}$$

The particular solutions of the diffusion equation, besides the stationary one written as $c_\infty = c(x, t=\infty)$, are typically of the form:

$$c(x,y) = (A_n \cos \lambda_n x + B_n \sin \lambda_n x)\mathrm{e}^{-\lambda_n^2 D_t} \qquad \text{Eq. (38)}$$

Finally, the general solution, which is the sum of all the particular solutions is:

$$c(x,y) = c_\infty(x) + \sum_{n=1}^{\infty} A_n \cos\left(\frac{n\pi x}{a}\right)\exp\left(-n^2 \frac{t}{\tau_D}\right) \qquad \text{Eq. (39)}$$

with:

$$c_\infty(x) = c_0 + \frac{D_T}{D_i} c_0(1-c_0)\frac{\Delta T}{h}\left(\frac{h}{2} - x\right) \qquad \text{Eq. (40)}$$

$$A_n = -\frac{4}{n^2\pi^2}\frac{D_T}{D_i} c_0(1-c_0)\Delta T \qquad \text{(with n odd)} \qquad \text{Eq. (41)}$$

Knowing $c(x,y)$, the concentration difference between the bottom and the top $c(o,t)$-$c(h,t)$ within the cell is:

$$\frac{\Delta c(t)}{\Delta T} = \frac{D_T}{D_i} c_0(1-c_0)\left[1 - \frac{8}{\pi^2}\sum_{n\ odd}\frac{e^{-n^2\frac{t}{\tau_D}}}{n^2}\right] \qquad \text{Eq. (42)}$$

with:

$$\tau_D = \frac{(V/A)^2}{\pi^2 D_i} \qquad \text{Eq. (43)}$$

CHAPTER 3

METHODOLOGY

The overall flow of the research methodology of this study is presented and ensured by detail description on each experimental procedure and research designs. The flow and overall research methodology with their respective and interrelationship is presented in Figure 9. The chemicals and equipment used for these studies are summarized below.

Chemical

1. Sodium di-hydrogen phosphate (NaH_2PO_4) (Ajax, Australia)
2. Di- Sodium hydrogen phosphate (Na_2HPO_4) (Ajax, Australia)
3. Sodium bicarbonate ($NaHCO_3$)
4. Sodium nitrate ($NaNO_3$)
5. Sodium chloride (NaCl)
6. Magnesium sulfate ($MgSO_4$)
7. Polyethylene glycol 4000 (PEG4000)
8. Potassium di-hydrogen phosphate (KH_2PO_4) (Ajax, Australia)
9. Di-Potassium hydrogen phosphate (K_2HPO_4) (Ajax, Australia)

Equipment

1. Ultrasonic bath (Honda, W-113, Japan)
2. Sartorius CPA3202S Competence analytical balance, 3200 g x 0.01 g
3. Magnetic stirrer
4. Hot bath
5. Cooling bath
6. Cylinder 100 mL
7. Universal centrifuge, PLC – 012E, Taiwan
8. Spectrophotometer (Model SPECTRO SC, U.S.A.)
9. Spectroquant Move 100 (Merck, Germany)

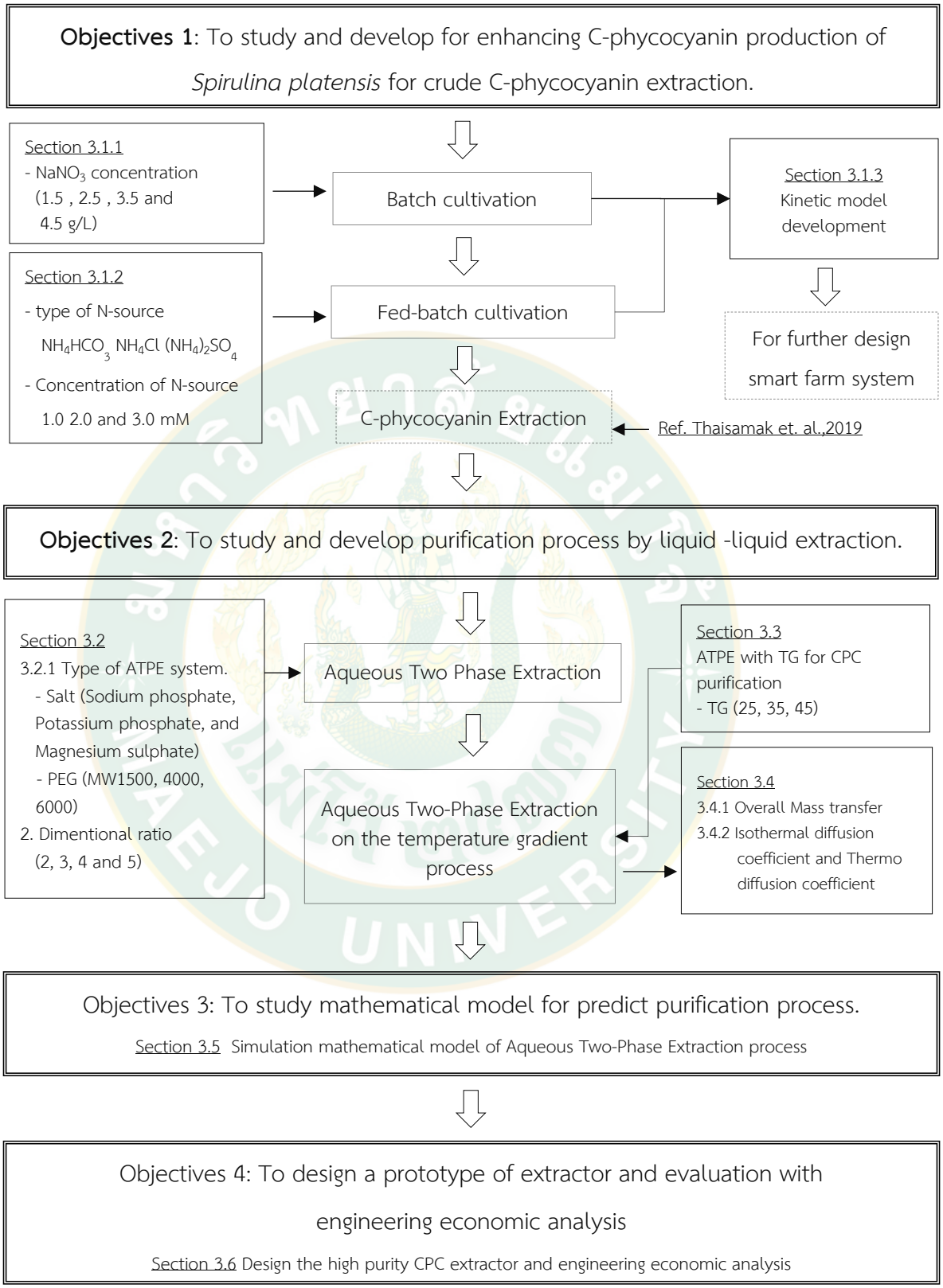

Figure 9 Flow chart of overall research methodology

Analytical method

1. Determination of cell growth

The biomass concentration was determined by measuring the optical density of the sample at wavelength of 680 nm (denoted as OD_{680}) using a UV/Vis spectrophotometer (Model SPECTROSC, USA). The OD_{680} values were converted to wet biomass concentration by following equation. (the moisture content in the wet basis was 83.59 ±0.66 %) via appropriate calibration between OD_{680} and cell weight.

$$W = 5.8667 \times OD_{680} - 2.5563 \qquad \text{Eq. (44)}$$

The specific growth rate (μ) of Spirulina culture was obtained by following calculation.

$$\mu = \frac{\ln(W / W_0)}{t} \qquad \text{Eq. (45)}$$

Where W and W_0 are indicated the biomass concentration (g/L) at initial and cultivation time (days:d), respectively. The biomass productivity (P_w) during the culture period was calculated from the Eq. 46.

$$P_w = \frac{\Delta W}{\Delta t} \qquad \text{Eq. (46)}$$

2. Determination of ammonium and nitrate concentration

Samples from cultivation systems were collected for ammonium and nitrate concentration at 11 am every day during the batch and fed-batch. The concentration profile were measured using a Spectroquant Move 100 (Merck, Germany)

3. Determination of CPC concentration

A fixed amount of the biomass (5 g) was mixed with 25 mL of 0.1 M sodium phosphate buffer (pH = 7.0), then keep in freezing condition (-10 ^{o}C) for overnight and thawing next in room temperature. After that the ultrasound-assisted extractions based on research of (Thaisamak et al., 2019) was used as extraction method. The cell debris was removed by centrifugation at 3,500 rpm for 30 minutes, and the supernatant (blue color) was collected to CPC analysis. The supernatant (crude

extract) was measured the absorbance by using UV/Vis spectrophotometer at the wavelengths of 620 nm and 652 nm for calculating the concentration of CPC (g/L) according to the following Eq. 47 (Bennett and Bogorad, 1973). The content of CPC (%) was calculated according to (Boussiba and Richmond, 1979) following Eq.48. The yield (mg/g) and productivity of CPC (g/L·d) according to the following Eq. 49 and Eq. 50.

$$CPC\ concentration = \frac{A_{620} - 0.474A_{652}}{5.34} \quad \text{Eq. (47)}$$

$$\%CPC = \frac{A_{620} \times V \times 100}{3.39 \times W \times \%DW} \quad \text{Eq. (48)}$$

$$Y_{CPC} = \frac{CPC \times V}{D_w} \quad \text{Eq. (49)}$$

$$P_{CPC} = \mu \times W \times \%CPC \quad \text{Eq. (50)}$$

4. Determination of CPC purity

The CPC and total protein concentrations in top and bottom phase were analyzed to estimate the purity (EP), purification factor (PF) and partition coefficient (K) of the process.

$$EP = \frac{A_{620}}{A_{280}} \quad \text{Eq. (51)}$$

where A_{620} and A_{280} are the absorbance of the sample at 620 and 280 nm, respectively. This relationship is indicative of the CPC extract purity with respect to most forms of contaminating proteins (Chethana et al., 2015). Absorbance at 620 nm indicates the CPC concentration, while absorbance at 280 nm indicates the total protein concentration in the solution.

$$PF = \frac{EP_p}{EP_c} \quad \text{Eq. (52)}$$

where PF is the purification factor, EP_c is crude extract purity, and EP_p is the pure extract purity.

$$K = \frac{CPC^t}{CPC^b} \quad \text{Eq. (53)}$$

where K is the partition coefficient, and CPC^t and CPC^b represent the CPC concentration in the top phase and the bottom phase, respectively. The recovery yield (RC, %) describes the efficiency of purification operations, where the identity of the material is the same before and after the process. The recovery yield of the CPC from the sample was calculated using Eq. 54 (Chew et al., 2019), in which V_r is the volume ratio, and V^t and V^b represent the volumes of the top and bottom phase, respectively, according to the following Eq.55

$$RC = \frac{KV_r}{1+KV_r} \times 100 \quad \text{Eq. (54)}$$

$$V_r = \frac{V^t}{V^b} \quad \text{Eq. (55)}$$

Statistical analysis

The data were analyzed by conducting a one-way analysis of variance (One-way ANOVA) using statistic software. All values are shown as mean ± standard deviation. Statistical differences were establish according to probability threshold ($p<0.05$)

3.1 Enhancing cell growth and CPC production of *Spirulina platensis*

In this research, the cultivation system employed were customarily designed by the author as shown in Figure 10. The microalgae were pre-cultured and inoculated in the bottle, the medium use for strain culture was adapted from Zarrouk medium consisting of (per liter): 16 g $NaHCO_3$, 2.5 g $NaNO_3$, 1 g NaCl , 0.5 g K_2HPO_4 , 0.2 g $MgSO_4$ The initial biomass was maintained as 0.37 g/L. and the culture were controlled at 28 - 30 °C, pH 9-10 (Algae Connect, Model ALS-SPARC-2A, USA), and LED illumination (BASTVA, Model GW-AQM55W, China) with the ratio of red and blue as 3:1 with lighting period of 16 hours per day at 350 μmol/m^2.s

(Jaturonglumlert et al., 2017). During the cultivation, the CO_2 either pure from tank was bubbled into the bottle to control when the pH at 9.0-9.5 as the carbon source.

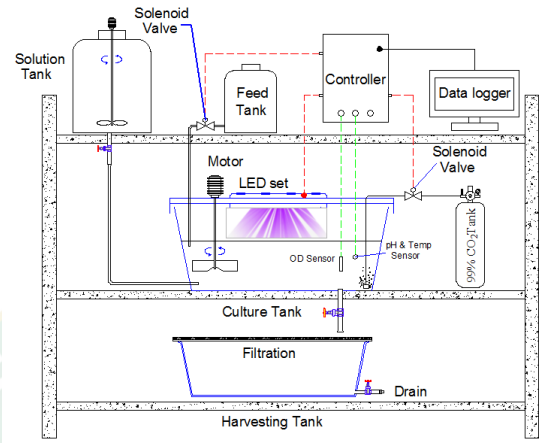

Figure 10 Operation of batch and fed-batch cultivation

3.1.1 Operation of batch cultivation

This experiment has investigated the effect of sodium nitrate as nitrogen source. Four levels different of sodium nitrate were employed to investigate the nitrogen consumption of Spirulina (1.5 2.5 3.5 and 4.5 g/L). During cultivation liquid samples were collected at set time intervals to determine the cell concentration, CPC concentration and residual nitrogen source concentration.

3.1.2 Operation of fed-batch cultivation

Three type ammonium salts (NH_4HCO_3, NH_4Cl, $(NH_4)_2SO_4$) were selected for adding nitrogen sources during *Spirulina platensis* cultivation. Three levels in each salt is containing the range of high medium and low (1.0 2.0 and 3.0 mM), meaning of 1.0 mM is minimum concentration which *Spirulina platensis* use for growing, and 3.0 mM is concentration at toxicity phenomena in cultivation (Li et al., 2012). All treatment was carried out in 2 L of culture tank which was controlled the medium of culture (per litter) that include: 16 g $NaHCO_3$, 2.5 g $NaNO_3$, 1 g NaCl , 0.5 g K_2HPO_4 , 0.2 g $MgSO_4$. The initial biomass was maintained as 0.37 g/L. For fed-batch cultivation, time regulator was set up for pulse-feeding nitrogen source during the experiment.

Liquid samples were collected at set time intervals to determine the cell concentration, CPC concentration and residual nitrogen source concentration.

3.1.3 Kinetic model development

Monod model and Haldane model is widely used for describing the effect of substrate concentration (C_s) on specific growth rate (μ), Eq. 56 and Eq. 57.

$$\mu = \mu_m \left(\frac{C_S}{C_N + C_S} \right) \qquad \text{Eq. (56)}$$

$$\mu = \mu_m \left(\frac{C_S}{C_N + C_S + \frac{C_S^{\,2}}{C_I}} \right) \qquad \text{Eq. (57)}$$

Where C_N and C_I are optimal substrate concentration and inhibit concentration at the maximum specific growth rate. In this study, the kinetic model is modified from the Monod model and the Haldane model for simulating the kinetic parameters of *Spirulina platensis* cultivation namely specific growth rate (μ) and CPC productivity (P_{CPC}). In these equations, the maximum growth rate constant (μ_m) and maximum CPC productivity constant ($P_{CPC,m}$) are assumed to be a function of nitrate concentration (C_{S1}) and ammonium concentration (C_{S2}) as shown in Eq. (58) and Eq. (59). Furthermore, in fed-batch cultivation, the kinetic model would considered to account the substrate inhibition of growth at higher substrate concentrations as shown in Eq. (60) and Eq. (61).

$$\mu = \mu_m \left(\frac{C_{S1}}{C_{N1} + C_{S1}} \right) \left(\frac{C_{S2}}{C_{N2} + C_{S2}} \right) \qquad \text{Eq. (58)}$$

$$P_{CPC} = P_{CPC,m} \left(\frac{C_{S1}}{C_{N1} + C_{S1}} \right) \left(\frac{C_{S2}}{C_{N2} + C_{S2}} \right) \qquad \text{Eq. (59)}$$

$$\mu = \mu_m \left(\frac{C_{S1}}{C_{N1} + C_{S1} + \frac{C_{S1}^{\ 2}}{C_{I1}}} \right) \left(\frac{C_{S2}}{C_{N2} + C_{S2} + \frac{C_{S2}^{\ 2}}{C_{I2}}} \right) \qquad \text{Eq. (60)}$$

$$\mu_{CPC} = P_{CPC,m} \left(\frac{C_{S1}}{C_{N1} + C_{S1} + \frac{C_{S1}^{\ 2}}{C_{I1}}} \right) \left(\frac{C_{S2}}{C_{N2} + C_{S2} + \frac{C_{S2}^{\ 2}}{C_{I2}}} \right) \qquad \text{Eq. (61)}$$

3.2 Purification of CPC extracted from *Spirulina platensis* by Aqueous Two - Phase Extraction

The study examined the partitioning of CPC in an Aqueous Two-Phase Extraction (PEG 4000–salt system). Their protein partitioning data was used to generate correlations that were used to describe how CPC and impurities partition between the top and bottom phases during the process. The phase equilibria data for then used in the process model to describe the aqueous two-phase system phase equilibria during process simulations, as shows in Figure 11.

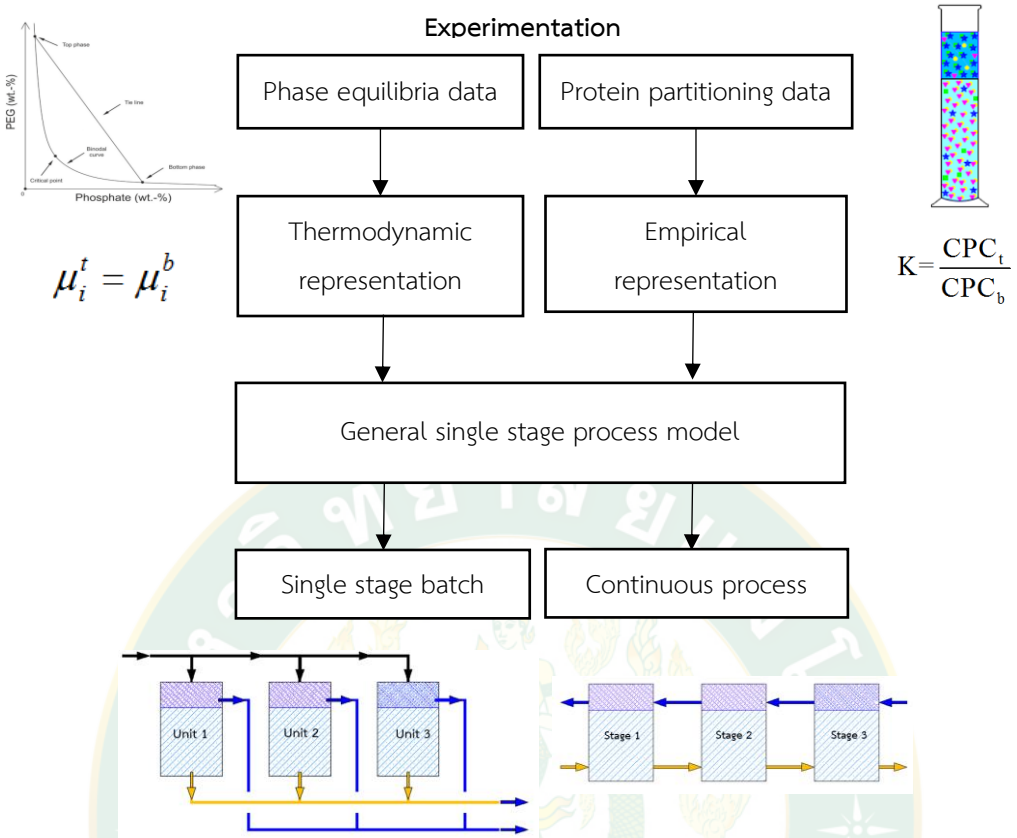

Figure 11 Overview of experiment framework for ATPE

ATPE was carried out by adding predetermined quantities of polymer (6%w/v) and salt (15 % w/w) from the reported phase diagrams (Chethana et al. ,2015). Weighing polyethylene glycol and salt to a specified amount, mixing it with the crude extract by making the total weight of the system to 100% w/w basis. The mixture was stirred thoroughly for about two hours to equilibrate and allowed for phase separation. Concentrations of CPC and total protein in the both phases were analyzed for estimating the purity and yield of CPC

The backward extraction, the top phase of the system was taken and to this equal volume of 1.2 M sodium chloride (NaCl) solution was added. Sample was kept for 0.5 hours and observed for the CPC separation to the bottom phase was also separated for further study.

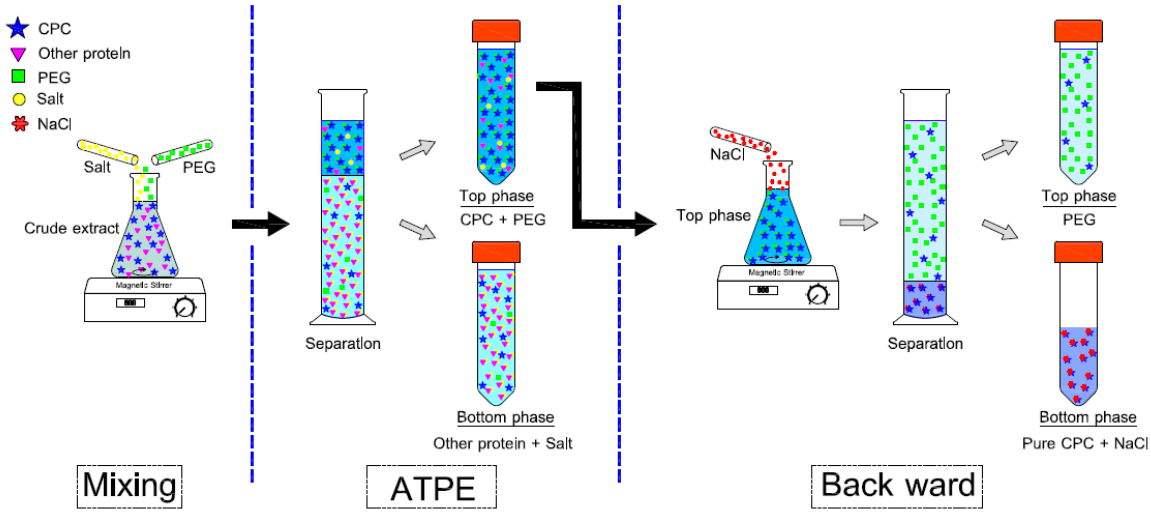

Figure 12 Schematic diagram of the ATPE procedure

3.2.1 Selection of type of Aqueous Two-Phase System.

In order to identify the suitable system for purification of CPC, ATPE experiments were carried out by adding predetermined quantities of polymer (6%w/w) and salt (15 % w/w) from the reported phase diagrams (Chethana et al. , 2015). Three different molecular weight of polyethylene glycol (1500, 4000 and 6000) and three different phase forming salts (Sodium phosphate, Potassium phosphate, and Magnesium sulphate), weighing polyethylene glycol and salt to a specified amount, mixing it with the crude extract by making the total weight of the system to 100% w/w basis. Other parameters such as phase composition, phase volume ratio, temperature and pH of system were kept constant.

3.2.2 Effect of dimension ratio (H/D) on Aqueous Two - Phase Extraction.

In order to know the influence of height and diameter ratio on CPC concentration and purity. The experiments were performed at four different height and diameter ratio (2 3 4 and 5). Other parameters such as phase system, phase volume ratio, temperature and pH of system were kept constant.

3.3 Application of Aqueous Two-Phase Extraction on the temperature gradient process

3.3.1 Effect of the temperature gradient (TG) on ATPE process

The extraction column was set up in the equipment as shown in Figure 13. A column with a working capacity of 100 mL was used for this purpose. The internal diameter of the reactor was 10 cm, placed in a water bath which was maintained temperature by the thermostatic water circulator. The all sample preparation as a same previously study. The mixture was stirred thoroughly for about two hours to equilibrate and allowed for phase separation at the specified temperature gradient (TG=0 [control], TG15, TG25, and TG35), TG is the temperature gradient, which is the difference between top temperatures (T_1) and bottom (T_2). The control treatment is the same process at room temperature 25±3 (without temperature gradient effect). The CPC and total protein concentrations in each phase were analyzed to estimate the purity (EP) purification factor (PF) and partition coefficient (K) of the process.

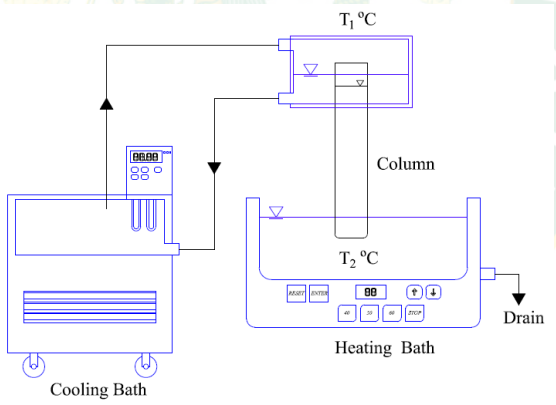

Figure 13 Schematic diagram in experiment of ATPE

The partition coefficient of CPC is giving by the ratio between the equilibrium concentration in the top and bottom phase as shown in Eq. 8 (Section 2.5.4)

3.3.2 Effect of temperature gradient (TG) on phase partitioning in the ATPE process

The ATPE system considered in this study consists of five components water (component 1), PEG 4000 (component 2), salt (component 3) establish the ATPE into which the CPC (component 4), is distributed. The salt content was determined by flame photometry (PerkinElmer model PFP7 & PFP7/C, PerkinElmer, England). The water was quantified by vacuum drying at 50°C for 8 h. The amount of water was obtained from the variation of the sample weight before and after the drying process, corresponding to the mass of water evaporated. The quantity of PEG was determined from the difference between the mass of the dried sample and the amount of the salt, as shown by Eq. 62.

$$m_{PEG} = m_{DS} - m_s \qquad \text{Eq. (62)}$$

where m_{PEG}, m_{DS}, and m_S are the masses of PEG, dried sample, and salt, respectively. All measurements were made in triplicate.

3.4 Mass transfer studies on Aqueous Two-Phase Extraction on the temperature gradient process

3.4.1 Prediction of overall mass transfer coefficients (k_La)

The experiments to determine the mass transfer coefficient of CPC purification by using Aqueous Two-Phase Extraction on the temperature gradient process. The mass transfer rate of CPC concentration in the PEG described as

$$\frac{dCPC}{dt} = k_L a\left(CPC_s - CPC\right) \qquad \text{Eq. (63)}$$

The magnitude of the interfacial area is $\frac{\pi d^2}{4}$ where d is the diameter of the reactor (because the liquid–liquid interface was maintained flat in our experiments). Eq.33 is integrated with the condition, $CPC=CPC_0$ at t = 0. Upon integration, we get,

$$-\ln(CPC_s - CPC_t) = -k_L a\, t + \ln(CPC_s - CPC_0) \qquad \text{Eq. (64)}$$

The volumetric mass transfer coefficient (k_La) was calculated. Here, CPC_t and CPC_s are the concentration of CPC in the PEG and the equilibrium concentration of CPC in the PEG, respectively. If we plot $-\ln(CPC_s - CPC)$ against time, the volumetric mass transfer coefficient is obtained from the slope of the graph. The whole experiment was repeated three times to ensure the reliability of the data.

3.4.2 Prediction of diffusion coefficients

Estimation of the isothermal diffusion coefficient (D_i) for CPC in both phases of ATPE utilized the correlation for protein diffusion coefficients proposed by Novak *et al*. (2015), which is based on the solute's molecular weight (M) and radius of gyration (R_G):

$$D_i = \frac{6.85 \times 10^{-15} \times T}{\eta \cdot \sqrt{M^{1/3} R_G}} \qquad \text{Eq. (65)}$$

where η is the dynamic viscosity of the solvent in Pa.s (dependent on operating temperature) and T is the temperature in K. For CPC, M and R_G were 18,500 Da and 54.1 Å , respectively (Thaisamak et al.,2020)

Estimation of the thermal diffusion coefficient (D_T), it is necessary to collect experimental variations of concentration $\Delta c(t)$ from initial to separation completely. The measured values are then divided by the corresponding ΔT and the experimental curve is drawn. Next, a curve fitting procedure using statistical software is used to set two parameters the Soret coefficient (S_T) and mass diffusion time (τ_D) of Eq. (42), and adjusted until Eq. (42) fits the experimental curve best. So, the S_T and τ_D values are evaluated using the mathematical fitting procedure.

The enhancement factor (EF) was used to quantify the thermal diffusion effect. EF is defined by the ratio of the diffusion coefficient of the conventional process (D_0) and the diffusion coefficient of Aqueous Two - Phase Extraction coupled

with different temperatures (D_{dT}) (summation of isothermal and thermal diffusion coefficient). The equation is defined as:

$$EF = \frac{D_{dT}}{D_0} \qquad \text{Eq. (66)}$$

3.5 Simulation mathematical model of Aqueous Two-Phase Extraction process

In order to generate the binodal curves and tie lines that represent the phase equilibrium behavior, the problem is formulated as an optimization routine, where the equilibrium phase separation concentrations are obtained by minimizing the chemical potential differences of each component between the phases. The binodal curve for an ATPE is constructed by top and bottom concentrations of phase-forming components that give the least chemical potential differences between the phases. Firstly, the concentration (in terms of volume fraction) of water in the top phase is fixed and by varying the value of the concentration of one phase-forming polymer (concentration of the third component is determined from the material balance), the optimizer minimizes the chemical potential differences between the phases to solve for the concentrations of the bottom phase. Next, the water composition is changed and the value of the concentration of the phase-forming polymer is varied in order to find the bottom phase concentrations that give the minimum chemical potential differences

A procedure was written to model the partitioning behavior of CPC in the system by calculating the partition coefficient of a specific protein using the top and bottom phase concentrations of the phase-forming components at equilibrium. The simulation requires the new end points determined for the feed tie line and the interaction parameters between the protein and water and the polymers as inputs. The partition coefficient value is unique for a given protein in a particular ATPE. The determination of partition coefficient for the CPC in an ATPE that consists of water, polymer and salt. Using the end points at the top and bottom phase generated by the simulation, the ionic strength of the aqueous solution for the particular salt concentration and thus, the contribution to the partitioning, are taken into consideration.

3.6 Design the high CPC purity extractor and the engineering economic analysis

There is a large number of extraction equipment that can be classified, as shown Figure 14. In all liquid–liquid extraction apparatus, the phase contact occurs when one phase is dispersed in the other. This phase contact enables the mass transfer, which can be carried out in one or more stages. Single mixer–settlers are operated in single-stage mode, while several mixer settlers connected in series can also be operated in so-called batteries in countercurrent or cross-current mode. The most common extraction apparatuses that work in countercurrent mode are columns. A distinction is made here between columns without energy supply, such as spray columns or packed columns, and columns with energy supply, which include pulsed or stirred columns.

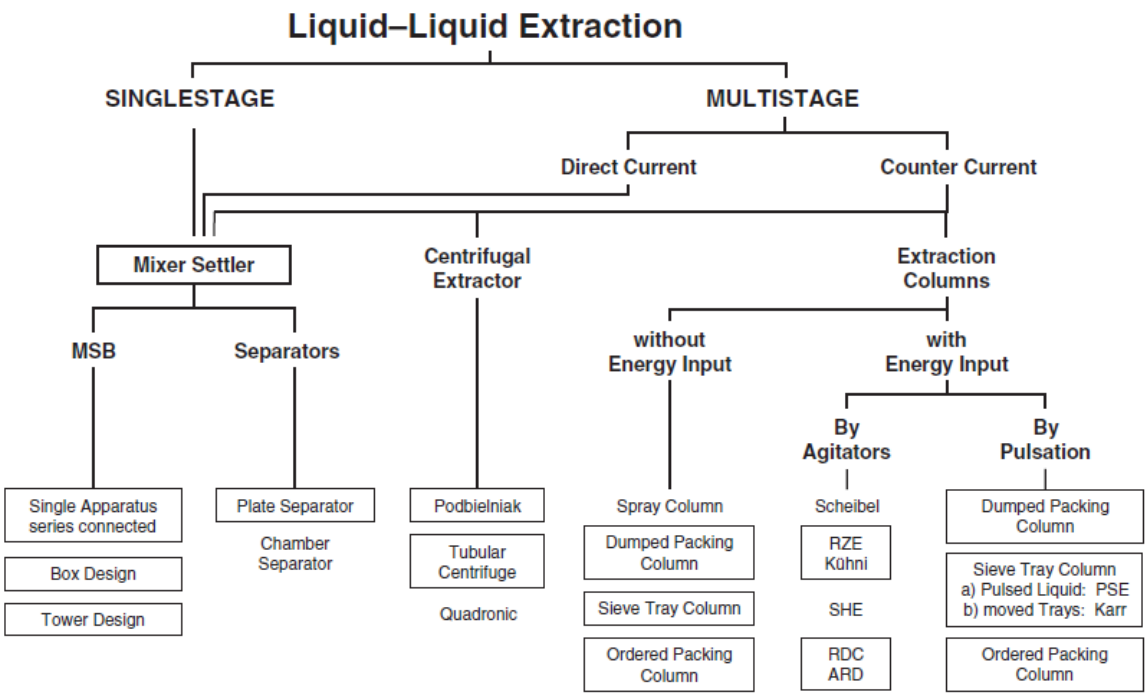

Figure 14 Extraction equipment overview

An extraction column can be divided into three areas. In the lower part of the column is the column bottom. In the column bottom, the heavy phase is removed from the column and the light phase is added. When inserting the light phase, care must be taken to ensure that the drops are optimally sized and distributed over the

entire column cross section. The size of the drops has a significant influence on the separation efficiency of a column. Large droplets have a poor surface to volume ratio and thus may lead to an insufficient mass transfer. If the drops become too small, there is a risk that a stable emulsion will form, which cannot be separated during the process. The contact zone is located in the middle area, where the mass is transported from the heavy phase to the light phase. In the upper area, also called column head, the drops coalesce and can be removed from the column. In the column head, the heavy phase is also fed into the column.

In extraction columns, the countercurrent is caused by the difference in density between the two phases. If the light phase is dispersed, it rises up in through a vertical cylindrical body and coalesces at the head of the column. If the heavy phase is dispersed, then the phase separation area is correspondingly located at the bottom of the column. This applies to both static columns (without external energy supply) and to columns with external energy supply, which include stirred and pulsed columns. Moreover, as reported by (Luo et al., 2016) apply vortex fluidic device (VFD) intensify ATPE for CPC purification, processing in the VFD tracks toward turbulent flow with high Reynolds number >2000. The VFD-intensified ATPE continuous flow processing has spontaneous phase separation of the liquid exiting the 20 mm diameter tube inclined at 45° and rotating at 6550 rpm for a 0.2 mL/min flow rate. This method can be applied with ATPE which the slow demixing rate due to the small difference in densities between the two-phase. (Guo et al., 2015) study an Aqueous Two - Phase Extraction couple with ultrasound was employed to extract lignans from *Zanthoxylum armatum*. The results showed ultrasonic-assisted ATPE can be a suitable method for extraction and enrichment of lignans from *Z. armatum*. The main advantages of the approach in this work to developing aqueous two-phase extraction are applied to the different temperatures to supply energy for the extractor. Different temperature affects the solvent density in two-phase to improve the mass transfer.

For column design, the active height is calculated on the basis of the mass transfer unit notion. In the hypothesis of the plug flow, the height of the column is:

$$H = NTU \times HTU \qquad \text{Eq. (67)}$$

where NTU is the number of transfer units relative to the dispersed and to the continuous phase respectively, when expressing the mass transfer rate as the overall mass transfer coefficients. HTU is the height of the transfer unit relative to the overall mass transfer coefficient in the same phases.

NTU is calculated taking into account the equilibrium data. The relationships given in Eq. 68 (Koncsag and Barbulescu, 2011) is related to the extract and the raffinate and it is to see which equation applies to the continuous phase or the dispersed phase (e.g. the raffinate can be dispersed phase in one application and continuous phase in another one):

$$NTU = \int_{x_1}^{x_2} \frac{dx}{x - x_e} \qquad \text{Eq. (68)}$$

where:

x_1, x_e, are the solute concentration in the extract respectively in the flow entering (1) or exiting (2) the column. x_e is the solute concentrations in the extract, in equilibrium conditions in every point along the column. The volumetric overall mass transfer coefficients related to the dispersed phase k_La are correlated with the height of the mass transfer unit HTU and the superficial velocity of the dispersed phase v_d which The phase between phosphate and PEG4000 is in the range of 0.42-1.64 mm/s. (Igarashi et al., 2004)

$$HTU = \frac{v_d}{k_L a} \qquad \text{Eq. (69)}$$

In practice, the height of the column is calculated starting with the experimental determination of mass transfer coefficients, continuing by the calculation of HTU with Eq. 69.

CHAPTER 4

RESULT AND DISCUSSION

4.1 Enhancing cell growth and CPC production of *Spirulina platensis*

4.1.1 Effect of Sodium nitrate on cell growth and CPC production

Nitrogen source is an important factor that affect to the viability and productivity of microalgae in batch cultivation. The final *Spirulina platensis* biomass in different sodium nitrate concentration were given in Figure 15. The result show that, a rapid increase on biomass production was observed in medium containing of 3.5 g/·L sodium nitrate that was presented the maximum biomass concentration (4.859 g/L). At 3.5 g/L sodium nitrate was presented the maximum biomass concentration, both CPC productivity and significantly increased when the concentration of sodium nitrate was increased from 1.5 to 3.5 g/L (Table 3).

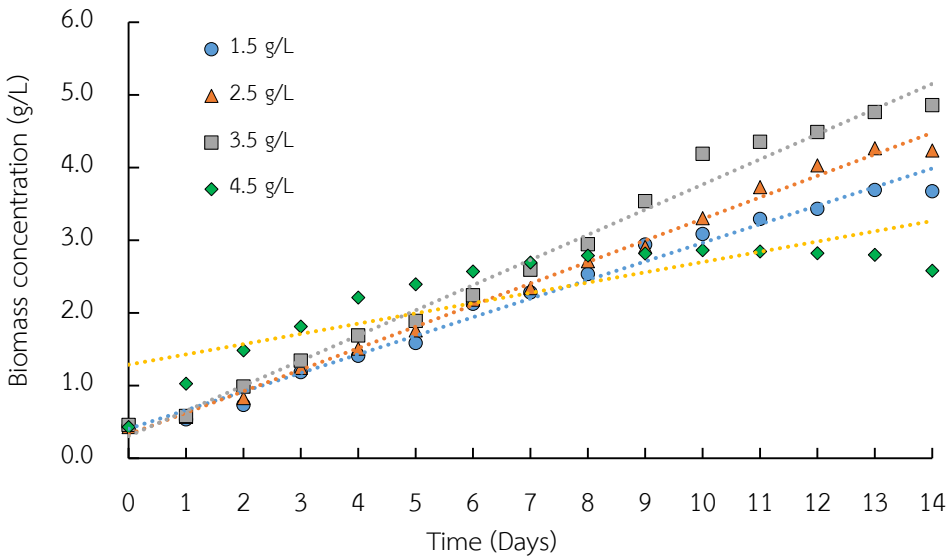

Figure 15 The effect of sodium nitrate concentration on cell growth

However, a sharp decrease was observed when the concentration of sodium nitrate reached to 4.5 g/ L, which is this level fall inhibition region. This could be directly supported by the observation of changing cells color from green to white during cultivation interval the first five days. The growth rate was began to decline in

the third day. Thus, 3.5 g/L sodium nitrate seemed to be the optimal concentration of sodium nitrate for the growth and CPC accumulation of *Spirulina platensis*, with the maximum biomass productivity of 0.314 g/L.d, specific growth rate of 0.169 d^{-1}, CPC productivity of 44.59 mg·/L.d and 14.20% of yield.

Table 3 The effect of sodium nitrate concentration on kinetic parameters

Nitrate concentration (g/L)	W (g/L)	P_w (g/L.d)	μ (d^{-1})	P_{CPC} (mg/L.d)
1.5	3.692	0.231	0.151	25.55
2.5	4.237	0.272	0.163	30.71
3.5	4.859	0.314	0.169	44.59
4.5	2.865	0.154	0.128	8.79

The cellular component of microalgae usually varies with the cell growth phase. In this work spirulina was cultivated in a batch culture around 14 days to investigate variation in CPC production (Figure 16).

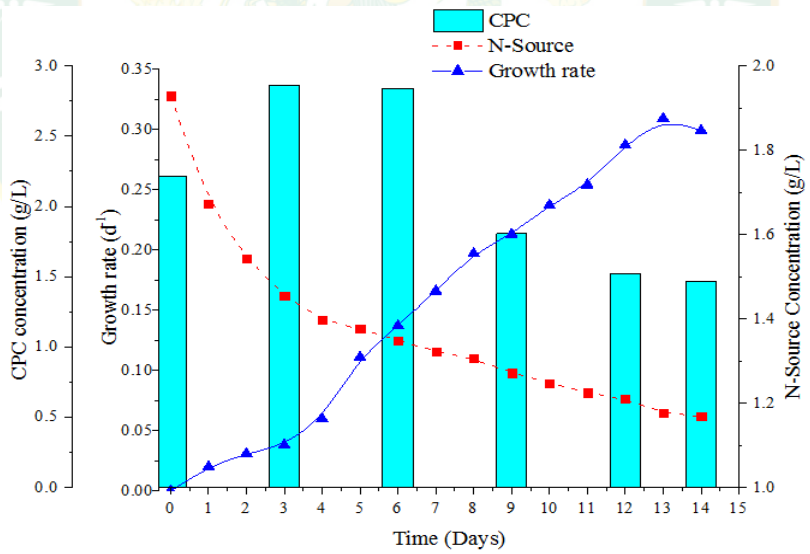

Figure 16 Time-course profiles of growth rate, nitrate concentration and CPC concentration during the batch cultivation of *Spirulina platensis*.

The CPC concentration increased simultaneously along with nitrogen consumption and the maximum values (2.840 g/L) was obtained at the beginning of nitrogen depletion. This trend is well in agreement with the report of Chen et al.

(2013). It has been suggested that CPC belongs to a family of phycobiliproteins which have obtained a secondary role as intracellular nitrogen storage compounds and mobilized for other purposes in times of nitrogen shortage. Therefore, in order to attain the maximum CPC concentration, the beginning of nitrogen depletion period should be the optimal time for adding nitrogen source to cultivate and enhance the cell growth rate, and CPC concentration. Thus, it is necessary to develop an effective strategy that could enhance the biomass production, and achieve the high CPC concentration simultaneously.

4.1.2 Improvement of CPC production of *Spirulina platensis* by using fed-batch operation

On the basis of batch culture results, different pulse-feeding fed-batch protocols were investigated with the aim of increasing the total availability of the supplied nitrogen source (N-source) as well as avoiding the above inhibitory level. All experiment was carried out using $NaNO_3$ because it was particularly important as nitrogen source at the beginning of the cultivation. Then, the concentrated ammonium solution was used as N-source pulse feeding every day to reach concentration in the medium including 1, 2 and 3 mM. Ammonia is preferentially assimilate over nitrate because the above mention is describe it is favorable nutrient of *Spirulina platensis* in term of energy situation. The results of the fed-batch process were shown in Figure 17 and Table 4.

Spirulina platensis responses were varied with different ammonium solution. The biomass production and productivity of *Spirulina platensis* were increased significantly when increasing the NH_4HCO_3 concentration. Since nitrogen was required for synthesis of the amino acid, which was used for make proteins up. Additionally, increasing of nitrogen concentration might be cause of an increasing in protein biosynthesis. The maximum biomass concentration and growth rate were obtained in the culture of pulse-fed with 3 mM NH_4HCO_3, but decrease in both were observed when increase the NH_4Cl and $(NH_4)_2SO_4$ concentration (2 and 3 mM) indicating that the inhibition phenomena of growth was appeared by high level of ammonium.

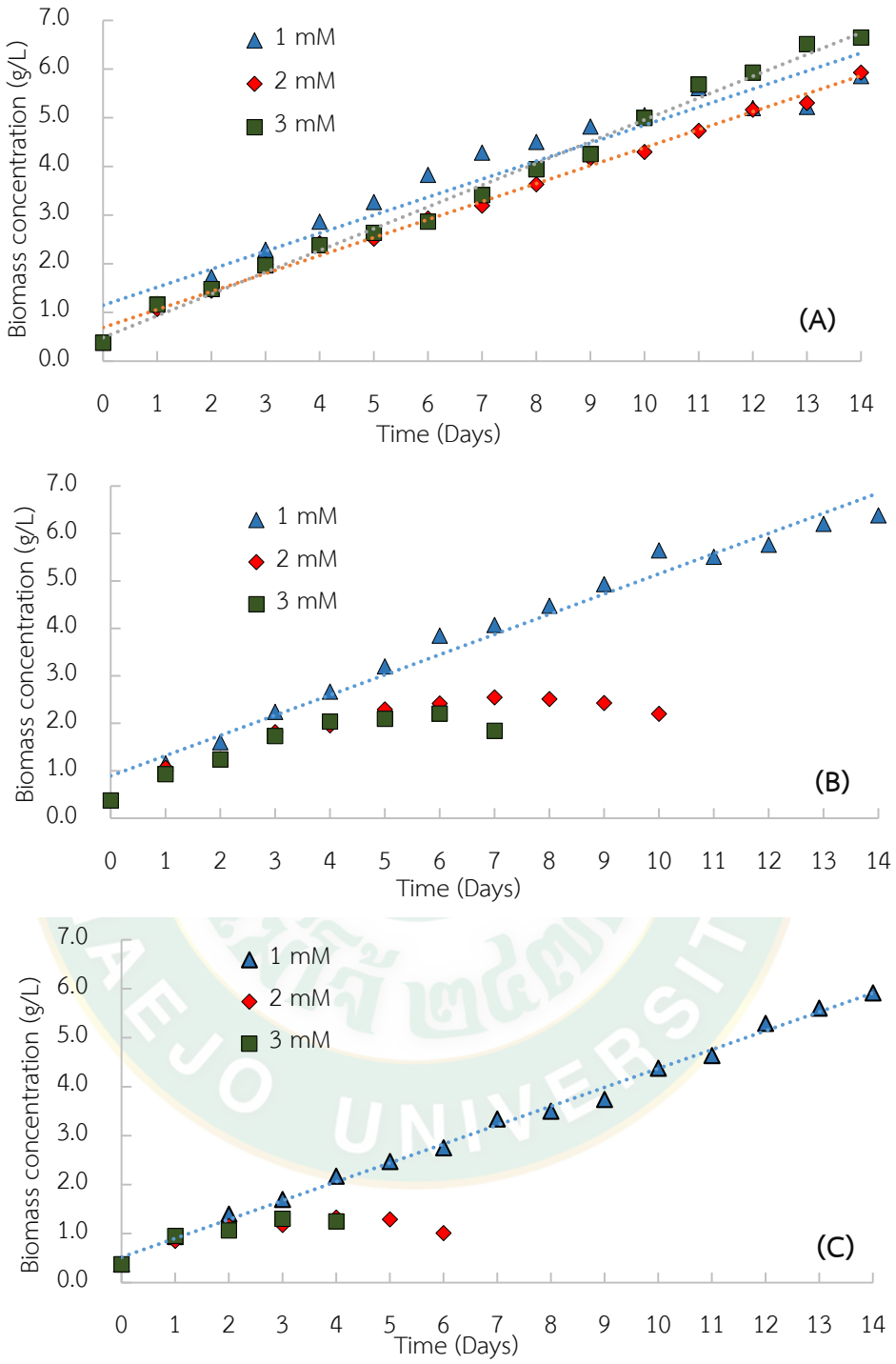

Figure 17 Biomass concentration of fed-batch cultivation of *Spirulina platensis* by pulse-feeding everyday (A) Ammonium bicarbonate (NH_4HCO_3) (B) Ammonium Chloride (NH_4Cl) and (C) Ammonium sulfate $(NH_4)_2SO_4$

Table 4 The effect of ammonium concentration on kinetic parameters of fed-batch cultivation of *Spirulina platensis*.

Ammonia Concentration (mM)		W (g/L)	P_w (g/L.d)	μ (d^{-1})	P_{CPC} (mg/L.d)
NH_4HCO_3	1.0	5.857	0.391	0.196	176.7
	2.0	5.927	0.396	0.197	192.1
	3.0	6.649	0.448	0.205	217.7
NH_4Cl	1.0	6.385	0.429	0.202	150.6
	2.0	2.548	0.210	0.176	123.9
	3.0	2.207	0.182	0.168	n/a
$(NH_4)_2SO_4$	1.0	5.915	0.396	0.197	113.2
	2.0	1.327	0.219	0.164	n/a
	3.0	1.304	0.106	0.101	n/a

Note: n/a is cannot found because of ammonium inhibition during culture.

Moreover, to investigate performance of fed-batch operation, four strategies were defined that for reducing times of feeding and increase concentration of a solution. For the time-course profiles of growth rate, four strategies were defined namely: pulse-fed with 3 NH_4HCO_3 everyday; 3 NH_4HCO_3 every two days; 6 mM NH_4HCO_3 everyday and 6 mM NH_4HCO_3 every two days, respectively (Figure 16-17). Figure 18-19 shows the growth rate in fed-batch with 3 mM NH_4HCO_3 everyday (1.187 d^{-1}) was slightly higher than 6 mM NH_4HCO_3 every two days feeding (1.143 d^{-1}). However, the growth rate was decrease in case of fed-batch with 6 mM NH_4HCO_3 everyday indicating that this level is over toxicity limit.

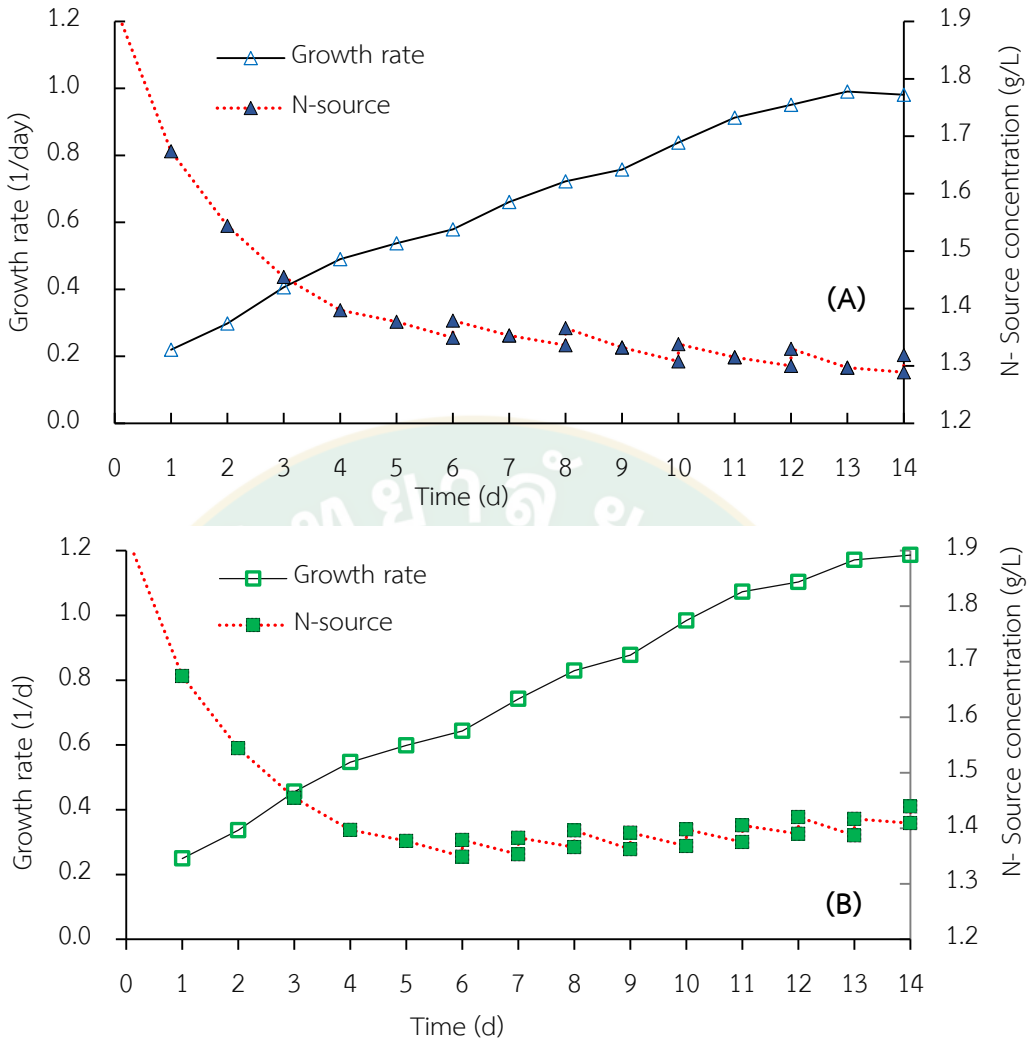

Figure 18 Time-course profiles of growth rate, N-source concentration during the culture fed-batch with (A) 3 mM NH_4HCO_3 every two days (B) 3 mM NH_4HCO_3 everyday

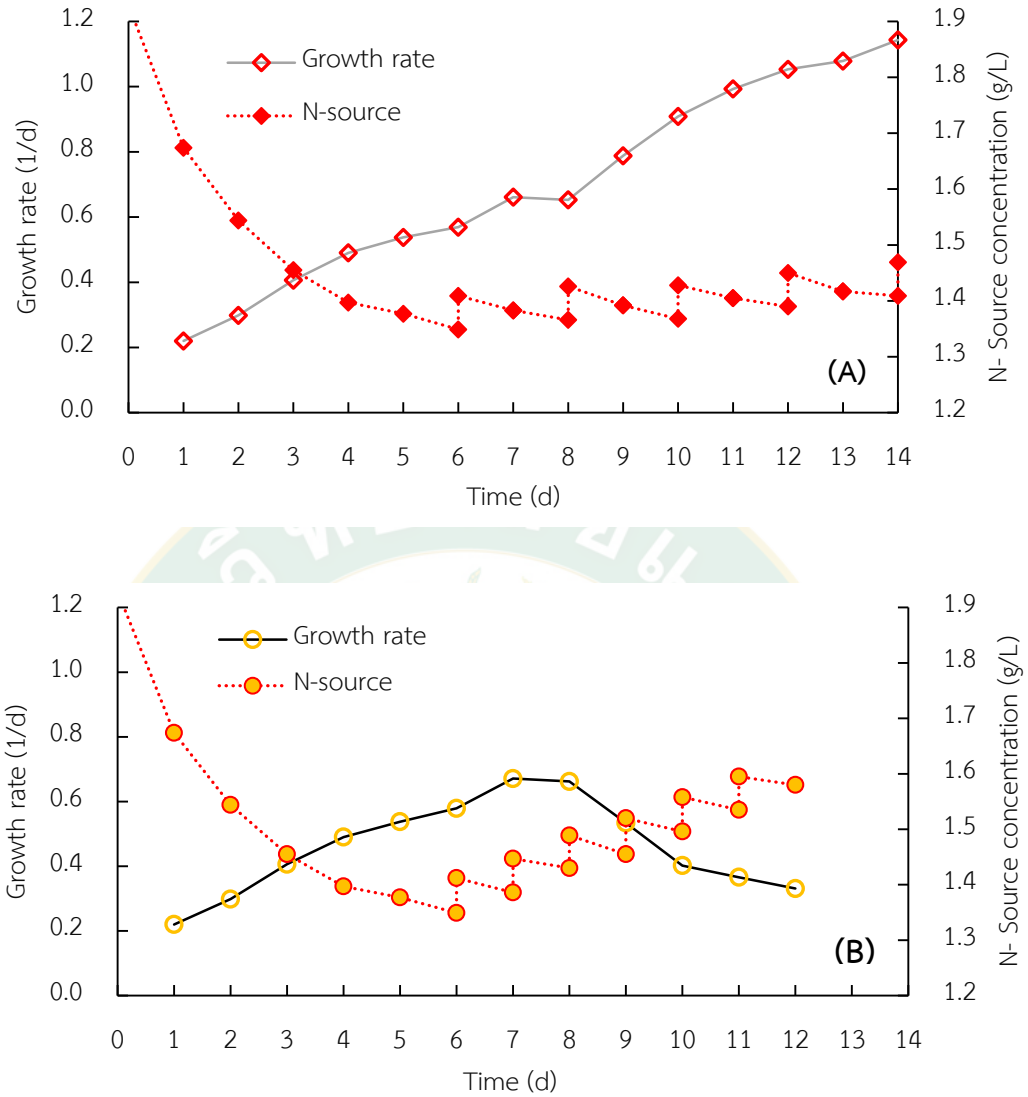

Figure 19 Time-course profiles of growth rate, N-source concentration during the culture fed-batch with (A) 6 mM NH_4HCO_3 every two days (B) 6 mM NH_4HCO_3 everyday.

Figure 20 show that the CPC concentration of *Spirulina platensis* was increased with the prolonged time of fed-batch operation (3 mM NH_4HCO_3 everyday). This CPC concentration was higher than that obtained in the batch culture with sodium nitrate concentration 3.5 g/L around 53% (Table 3). These result was indicated that adjusting the feeding ammonium concentration could enhance the accumulation of CPC, and fed-batch cultivation with the NH_4HCO_3 of 3.0 mM seemed to be a feasible strategy for enhance CPC accumulation.

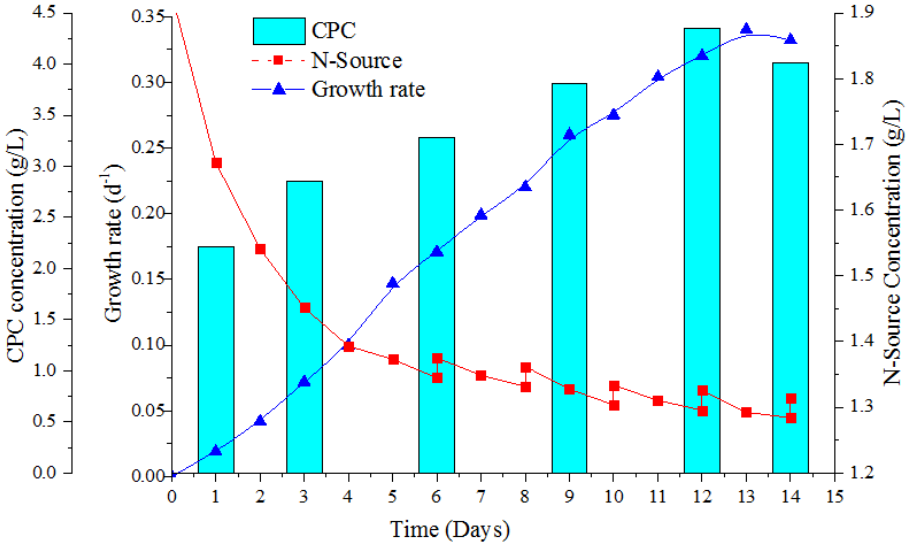

Figure 20 Time-course profiles of growth rate, N-source concentration and CPC concentration (column) during the fed-batch with 3 mM NH_4HCO_3.

Table 5 was present the comparison of the performance of biomass production, biomass productivity, CPC production, CPC productivity between this result and the literature. The biomass production and biomass productivity from 3 mM NH_4HCO_3 feeding was higher than other study and indicated that biomass production not only requires nitrogen sufficient condition but also need other nutrients. However, The CPC production obtained from 3 mM NH_4HCO_3 feeding was enhanced around 75% from reported in previous literatures.

Table 5 Comparison of kinetic parameters under fed-batch operation from this work with those reported in the literature.

Operation strategies	Biomass production (g/L)	Biomass productivity (mg/L.d)	CPC productivity (mg·/L.d)	Reference
Batch	0.770	92.4	67	Sassano et al., 2007
Batch	2.250	740.0	125	Chen et al., 2013
Batch	3.114	n/a	14	Leema et al., 2010
Fed-batch	1.759	113.9	n/a	Nascimento et al., 2014
Fed-batch	6.780	588.2	94	Xie et al., 2015
Fed-batch	6.649	448.0	98	This study

4.1.3 Kinetic model for CPC production

The changes in biomass concentration and CPC production with cultivation time in batch and fed-batch cultivations were plotted in Figure. 16 and Figure 20, then the experimental data was fitted by regression tool as function of non-linear regression in statistic program, the following kinetic models were established in this work given as following equation:

Batch cultivation

$$\mu = 0.600\left(\frac{C_{S1}}{0.414 + C_{S1}}\right)\left(\frac{C_{S2}}{0.056 + C_{S2}}\right) \qquad r^2 = 0.938 \qquad \text{Eq. (70)}$$

$$P_{CPC} = 0.335\left(\frac{C_{S1}}{0.413 + C_{S1}}\right)\left(\frac{C_{S2}}{0.055 + C_{S2}}\right) \qquad r^2 = 0.937 \qquad \text{Eq. (71)}$$

Fed-Batch cultivation

$$\mu = 0.400\left(\frac{C_{S1}}{0.414 + C_{S1} + \frac{C_{S1}^2}{13{,}885.6}}\right)\left(\frac{C_{S2}}{0.056 + C_{S2} + \frac{C_{S2}^2}{0.190}}\right) \qquad r^2 = 0.992 \qquad \text{Eq. (72)}$$

$$P_{CPC} = 0.223\left(\frac{C_{S1}}{0.413 + C_{S1} + \frac{C_{S1}^2}{17{,}234.4}}\right)\left(\frac{C_{S2}}{0.055 + C_{S2} + \frac{C_{S2}^2}{0.188}}\right) \qquad r^2 = 0.993 \qquad \text{Eq. (73)}$$

The experimental data fitted the model quite well (r^2 =0.937-0.992). The maximum growth rate constant (μ_m) and maximum CPC growth rate constant ($P_{CPC,m}$) in fed-batch was higher than batch cultivation. The concentration of nitrate (C_{N1}) and concentration of ammonium (C_{N2}) are 0.41 and 0.05 g/L, respectively.

These result was an illustration of *Spirulina platensis* cultivation that refer about the nitrogen source was not only show adverse impact on growth rate, productivity of *Spirulina platensis*, but also significantly in term of increasing the CPC formation. For nitrate inhibition on growth, the value of nitrate inhibit (C_{I1}) is 17,234.4

g/L, which means that when the nitrate concentration was lower than the result, it would not occur the inhibition on the growth rate and CPC growth rate. Moreover, the value of ammonium inhibition (C_{I2}) was 0.188 g/L, indicating that the amount of ammonium concentration should be lower than this value and it could use as the optimal inhibition ammonium concentration for fed-batch cultivation.

In commercial scale cultivation, the controlling is well relative for establish "Smart Farm" culture modelling, production controlling and feed monitoring that are invariable underpinning by sensors and sensor networks. In control system, a controller unit would record continuously such as the culture temperature, pH, and biomass growth by sensor. These information of cultivate were continuously transferred to the computer data logger where the data would be analyzed, displayed and recorded.

$$\frac{d(C_{NN})}{dt} = (0.615 - 2.030\ P_{CPC})C_{S1}C_{S2} \quad r^2 = 0.902 \qquad \text{Eq. (74)}$$

The kinetic model in fed-batch cultivation was used for estimated nitrogen consumption (C_{NN}) according to the relationship between the CPC growth rate and N-source concentration as shown in Eq. (74). When the nitrogen consumption exceeded the pre-set value, the nutrients feeding system was activated for a predefined period, so that the nitrogen source feeding solution could fed into the culture. This system was verified by comparison with the constant feeding method. When the constant feeding was used, owing to the amount of ammonium fed being larger than of the cell growth demanded, the ammonium in the medium accumulated to a certain concentration to inhibit cell growth.

4.2 Purification of CPC extracted from *Spirulina platensis* by ATPE

In ATPE, the purification of the protein is mainly due to the differential partitioning of the target protein to one phase and the contaminant proteins to the other phase. Which is dependent on many factors such as type of ATPE (phase forming salt and molecular weight of the phase forming polymer) phase volume ratio pH temperature and column dimension. A properly designed systematic approach is

required in order to reduce this large number of experiments. Selection of key parameters is an important task and requires thorough knowledge of solute to be studied. In view of this, experiments were planned through a systematic approach as shown in Figure 13. Wherein all the parameters, that are expected to affect the partitioning of the proteins and enhance the purification of CPC, are considered in a logical sequence. Details of selection of each of these parameters and their effect on protein partitioning have been discussed in the following sections.

4.2.1 System selection for ATPE

In order to identify the suitable system of ATPE for purification of CPC, the experiments were carried out by adding predetermined quantities of polymer (6%w/w) and salt (15 % w/w) from the reported phase diagrams (Chethana et al., 2015). Three different molecular weight of polyethylene glycol (1500, 4000, and 6000) and three different phases forming salts (Sodium phosphate, Potassium phosphate, and Magnesium sulphate), the results are shown in Table 6.

Table 6 Effect of different salt and PEG on ATPE

Salt	PEG (MW)	CPC concentration in top phase (g/L)	Recovery (%)	PE of CPC		
				K	in top phase	PF
Soduim phosphate	1500	4.263±0.15	58.91±0.28	2.151±0.02	1.287±0.01	1.160±0.08
	4000	5.453±0.14	64.72±0.50	2.753±0.06	1.428±0.04	1.284±0.06
	6000	4.879±0.12	62.14±0.53	2.463±0.06	1.428±0.04	1.161±0.03
Potassium phosphate	1500	5.180±0.13	63.53±1.70	2.622±0.19	1.346±0.07	1.218±0.15
	4000	7.017±0.15	70.23±1.40	3.550±0.24	1.839±0.07	1.663±0.18
	6000	5.480±0.03	64.83±1.20	2.770±0.14	1.653±0.27	1.508±0.36
Magnesium sulphate	1500	2.390±0.49	44.14±2.30	1.220±0.31	1.035±0.35	1.056±0.38
	4000	3.152±0.36	51.31±1.70	1.585±0.11	1.204±0.10	1.092±0.17
	6000	2.878±0.57	48.72±1.79	1.441±0.22	1.088±0.27	1.004±0.32

It is observed that, the most of CPC concentrated in the PEG phase (Top). The concentration and purity of CPC in top phase was considered as the response

variable to evaluate the effect of different systems. The phosphate salts have shown maximum purity of CPC for all the molecular weights of PEG when compared to the other salts. This is mainly due to the favorable biocompatible phase environment by the phosphate salts. Further, among phosphate salts, potassium phosphate showed better results in terms of purity and overall yield when compared to that of sodium phosphate. In view of this PEG/potassium phosphate system was chosen for further experiments.

4.2.2 Effect of dimension ratio (H/D) on ATPE

This parameter was conducted by using optimal condition from previous experiment. The experiments were studied the different of H/D ratio that are 2, 3, 4 and 5 by varying the height and diameter of column. The results shown in Table 7, the H/D ratio have effect to CPC concentration. The highest CPC was obtained by using the H/D ratio at 4. The result also showed, the trend of CPC in top phase was increased by increasing the H/D ratio.

Table 7 The results of effect of height and diameter column ratio (H/D)

H/D	CPC concentration in top phase (g/L)	Recovery (%)	K	EP of CPC in top phase	PF
2	6.210±0.56	60.09±1.67	3.148±0.43	1.751±0.16	1.585±0.15
3	6.591±0.43	63.67±1.83	3.311±0.45	1.753±0.09	1.586±0.15
4	7.024±0.31	72.27±1.43	3.561±0.37	1.865±0.11	1.688±0.19
5	6.131±0.42	67.55±1.24	3.127±0.33	1.853±0.08	1.677±0.36

However, CPC was showed lowest at 5 of H/D ratio that may cause of high ratio is big volume of solution which not suitable for this diameter column in experiment. In the same way as the partition coefficient, the H/D ratio from 2 to 4 were better than 5 of H/D ratio. The partition coefficient is an important index of ATPE which can descript the performance of process, this index is the ratio of the concentration between top phase and bottom phase. Thus, the 4 of H/D ratio was chosen due to this ratio was show highest that was 7.024 g/L of the CPC

concentration, and together with this ratio was took short time to partition and achieved equilibrium.

4.3 Application of Aqueous Two-Phase Extraction on the temperature gradient process

4.3.1 Effect of the temperature gradient (TG) on ATPE process

Experiments were performed at three levels of temperature gradient (TG15 TG25 and TG35), while the other parameters were kept constant (PEG4000 saturation 6% [w/v], potassium phosphates 15 % [w/v], pH 7.0, total volume 100 mL, and separation time of 2 hours). The control treatment is the same process at room temperature 25±3 (without temperature gradient effect). Figure 21 shows the results of the effect of TG on CPC concentration in the top phase at complete separation. The highest concentration and purity were found at TG25 (13.932 g/L), significantly higher than the conventional method. According to the results, the highest purity and yield values were 2.337 and 91.18, respectively, which were obtained under the condition of TG25 (Table 8).

Table 8 Effect of different temperature on concentration and purity in ATPE

	Control	TG15	TG25	TG35
CPC Concentration (g/L)				
Top Phase	7.012±0.29	7.840±0.54	13.932±1.25	9.069±0.84
Bottom Phase	1.975±0.23	1.112±0.25	0.758±0.14	1.028±0.36
Partition coefficient (K)	3.550	7.050	18.380	8.822
V_r and RC				
Volume of top phase (V_T, mL)	48 ± 2	39 ± 3	36 ± 3	43 ± 4
Volume of bottom phase (V_B, mL)	52 ± 3	61 ± 2	64 ± 3	57 ± 3
Volume ratio (V_r)	0.92	0.64	0.56	0.75
Recovery yield (RC,%)	76.62	81.84	91.18	86.94
EP				
Top Phase	1.839±0.04	1.889±0.29	2.337±0.20	1.918±0.33
Bottom Phase	0.812±0.05	0.856±0.18	0.569±0.13	0.746±0.17
Purification factor (PF)	1.663	1.708	2.113	1.734

The reason for this a potential phenomenon which decreases the viscosity of the mixture and enhances the solvent solubility and diffusion capacity (Zhang et al., 2015). Meanwhile, when the TG greater than 35, the purity of CPC extracted in ATPE of PEG4000 and potassium phosphates decreased sharply due to an observed significant reduction in the absorption strength at 620 nm, the characteristic absorption band of the CPC protein. Conversely, this means that the hydrogen bonding which interacted between the surface water of protein was destroyed at high temperatures.

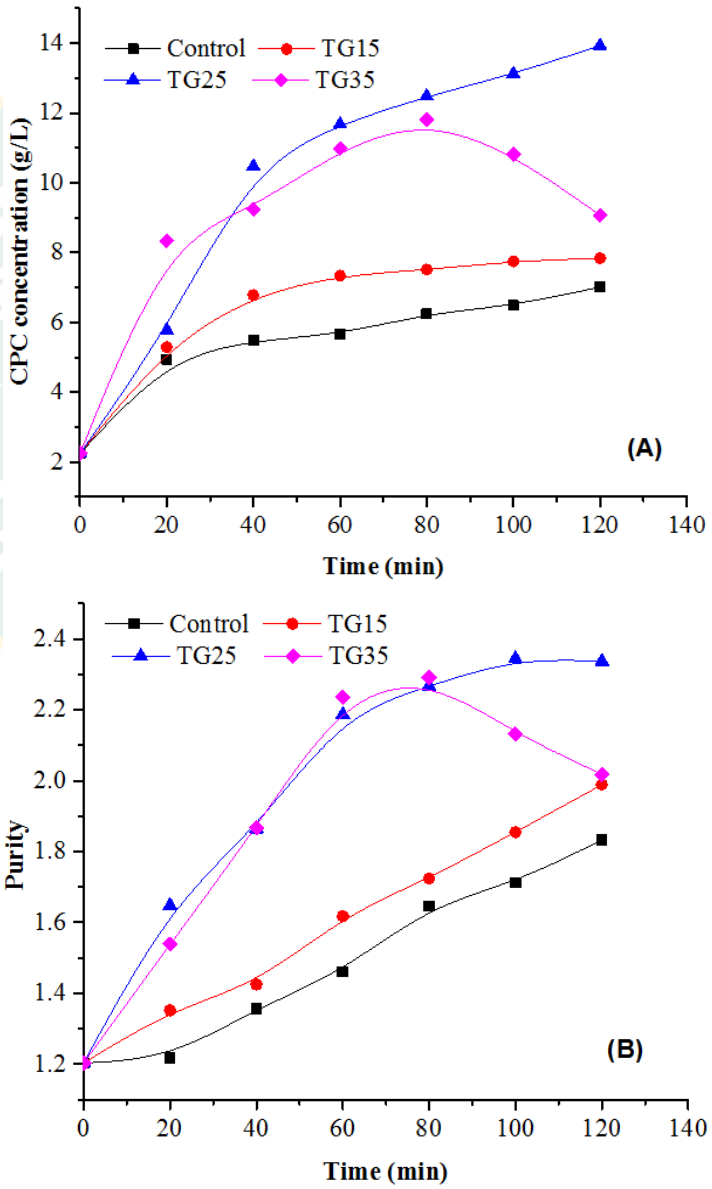

Figure 21 (A) Concentration profiles and (B) purity of CPC in top phase

From the experiment, it can be seen that TG can improve the purification rate of the process. Which can be used to analyze in the term of process time as shown in Table 9. It was found that the use of TG significantly reduced the processing time compared to the conventional process at the same CPC purity. At CPC purity 1.5 (initial in cosmetic grade), the processing time in the conventional process about 60 min, TG25 can reduce the time to 14 min or 76%. In other words, It can help reduce time costs and reduce the cost of production.

Table 9 Process efficiency in terms of time

Time of process (min)	Control	TG15	TG25	TG35
@ PE=1.5	61	46	14	15
@ PE=1.8	114	92	31	33
@ PE=2.0	-	123	46	70

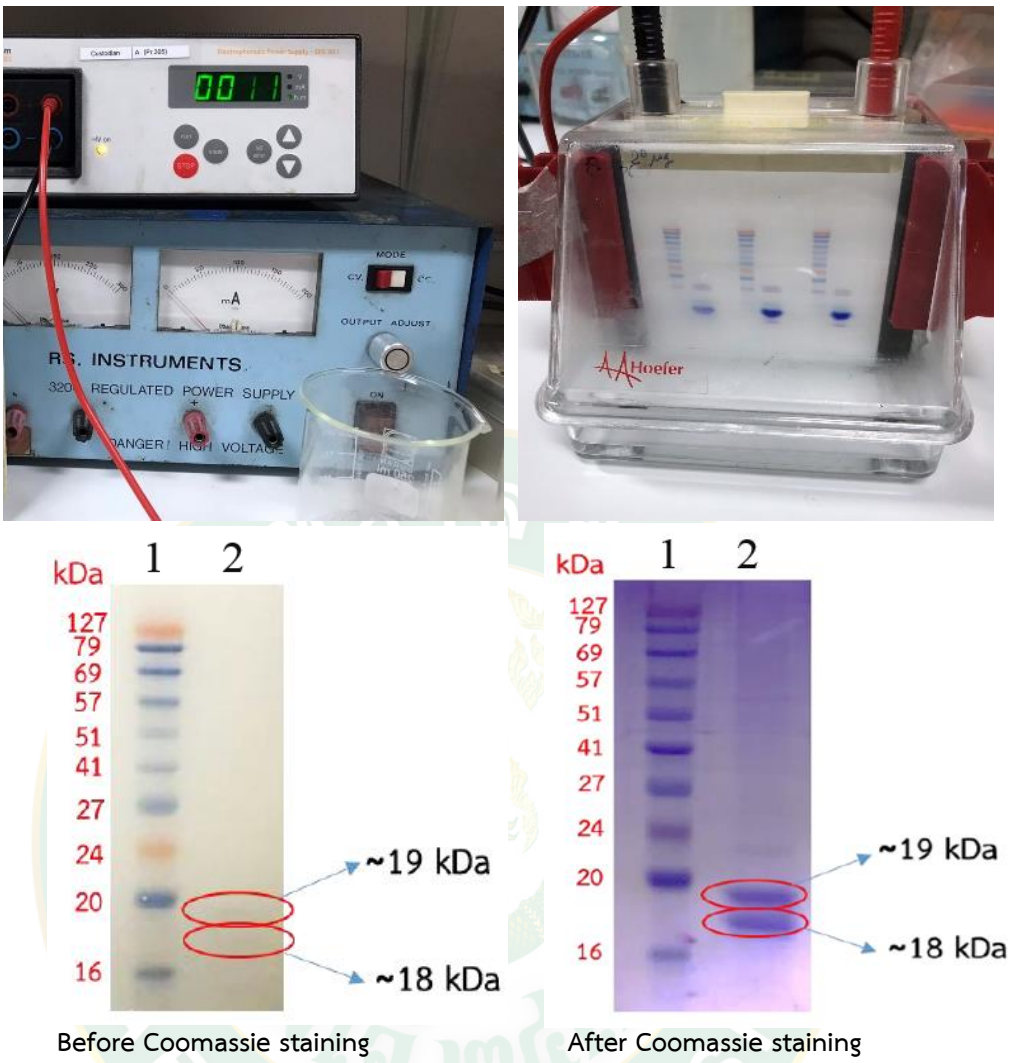

Figure 22 SDS-PAGE analysis of CPC

SDS-PAGE analysis was used to confirm the purity of CPC and is shown in Figure 22. Lane 1 indicates the molecular marker, while Lane 2 shows the pure CPC which is clearly visible in a band. This is potentially that during ATPE, the majority of the contaminant protein present in the crude extract was partition to the bottom phase, resulting in increased CPC purity. The molecular weights of CPC show two bands α and β with approximate sizes of 18 and 19 kDa, respectively. These results are similar to those obtained by Patil et al. (2006) and Chethana et al. (2015) who presented the molecular weight of CPC from *Spirulina platensis* by SDS-PAGE.

Table 10 presented the comparison of the performance of purification between this result and the literature. The purity of CPC using Aqueous Two-Phase

Extraction on the temperature gradient process was higher than the precipitation method around 136% higher than dialysis and conventional ATPE around 10%. Although the purity value is less than that of multi-step APTE and ion-exchange chromatography, the recovery yield is still 6 times higher and has medium-cost level, which is suitable for use in the food and cosmetics industry. It has also been shown that in the development of CPC purification to analytical grade, it should be developed into multi-stage Aqueous Two-Phase Extraction on the temperature gradient process. Due to its high efficiency in both purity and yield

Table 10 Comparison of the result from this work with those reported in the literature.

Process	EP	RC%	Cost	Reference
Precipitation	0.99	88.6	low	Moraes and Kalil, 2009
Dialysis	2.145	36.0	high	Jerley and Prabu, 2015
ATPE	2.110	89.5	medium	Zhao et al., 2014
Multi step ATPE (3 step)	4.05	85.0	high	Patil and Raghavarao, 2007
Ion exchange chromatography	4.58	14.0	very high	Kumar et al., 2014
ATPE	1.839	76.62	medium	This study
ATPE on TG process	2.337	91.18	medium^{+}	This study

Note: EP= Extracted Purity and RC% = Recovery yield
medium^{+} = The ATPE process with utility additions.

4.3.2 Effect of temperature gradient (TG) on phase partitioning

The partition coefficient (K) of purification increased monotonically with TG, as shown in Table 8 and Figure 23, to fully understand this behavior, it is important to investigate the effect of the TG on the CPC concentrations. Since the partition coefficient (K) is the ratio of the concentration in the top phase to the bottom phase. Therefore, when the K value changes, it also affects the purity of the CPC. That is the K value increase, the purity increase.

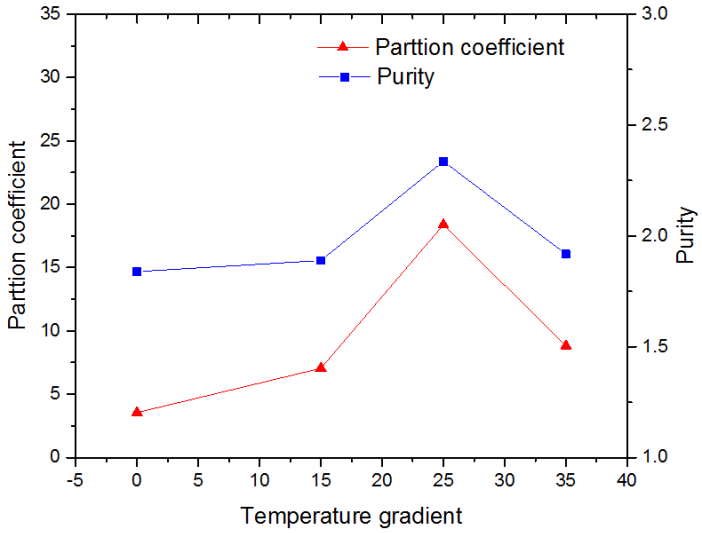

Figure 23 Effect of TG on phase partitioning in the ATPE process

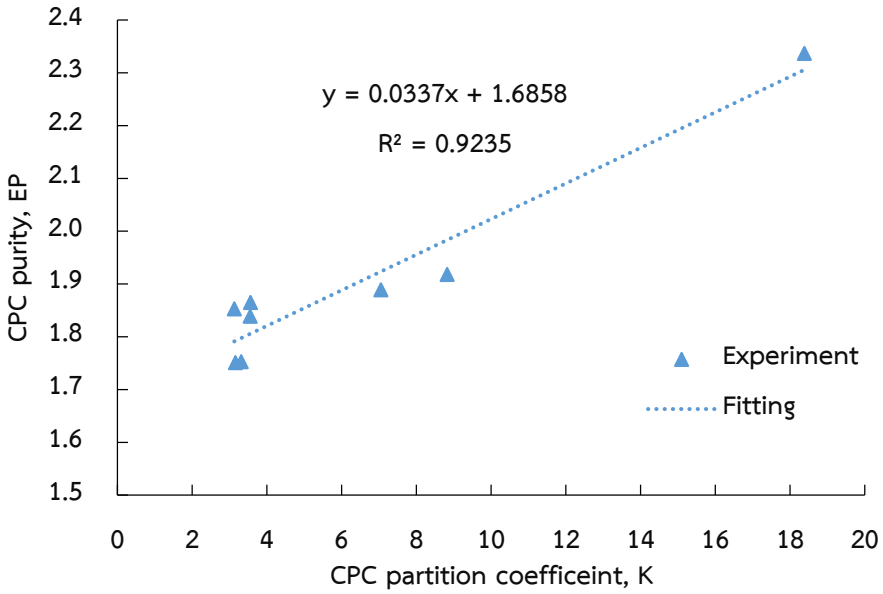

Figure 24 Effect of TG on phase partitioning in the ATPE process

The relationship between the partition coefficient and the purity as shown in Figure 24. The correlation equation can be found by the fitting curve and equation shown in Eq.75. This relationship is used to predict the purity of the additional process (section 4.5.2).

$$EP = 0.0337K + 1.6858 \qquad \text{Eq. (75)}$$

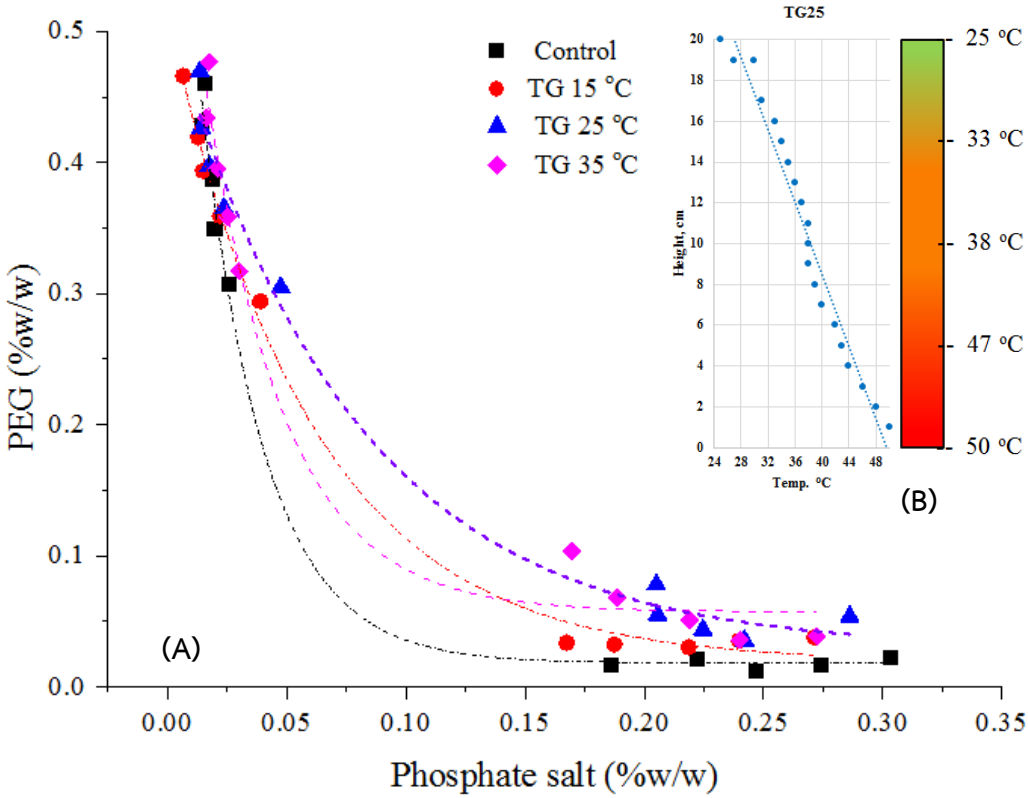

Figure 25 Modified binodal curve of PEG4000 and potassium phosphates in ATPE

Then, determine the concentration of salt and PEG in both phases. A set of experiments were subsequently conducted to generate binodal curves at TG varying from 15 to 35. Binodal curves obtained by plotting the concentrations of PEG and phosphate salt in the top and bottom phases are shown in Figure 25A. In the control treatment, the process separation in isothermal condition (without TG). The partitioning depends on the preferential binding of the molecules between the phases. In Aqueous Two-Phase Extraction on the temperature gradient process, the partitioning improved by a temperature gradient. The distribution of the temperature at TG25 within the system as shown in Figure 25B. The temperature gradient affects the viscosity and density of the system. Which the binodal moves away from the origin when the TG increases, causing the tie line length (TLL) over time to increase. (Figure 26). This can be said to result in a faster and more complete separation due to the preferential binding of the water molecules to the polar salt surface instead of the PEG at a higher temperature difference. Several authors have also observed these results. (Carvalho et al., 2007; Gautam and Simon, 2006; Sé and Aznar, 2002).

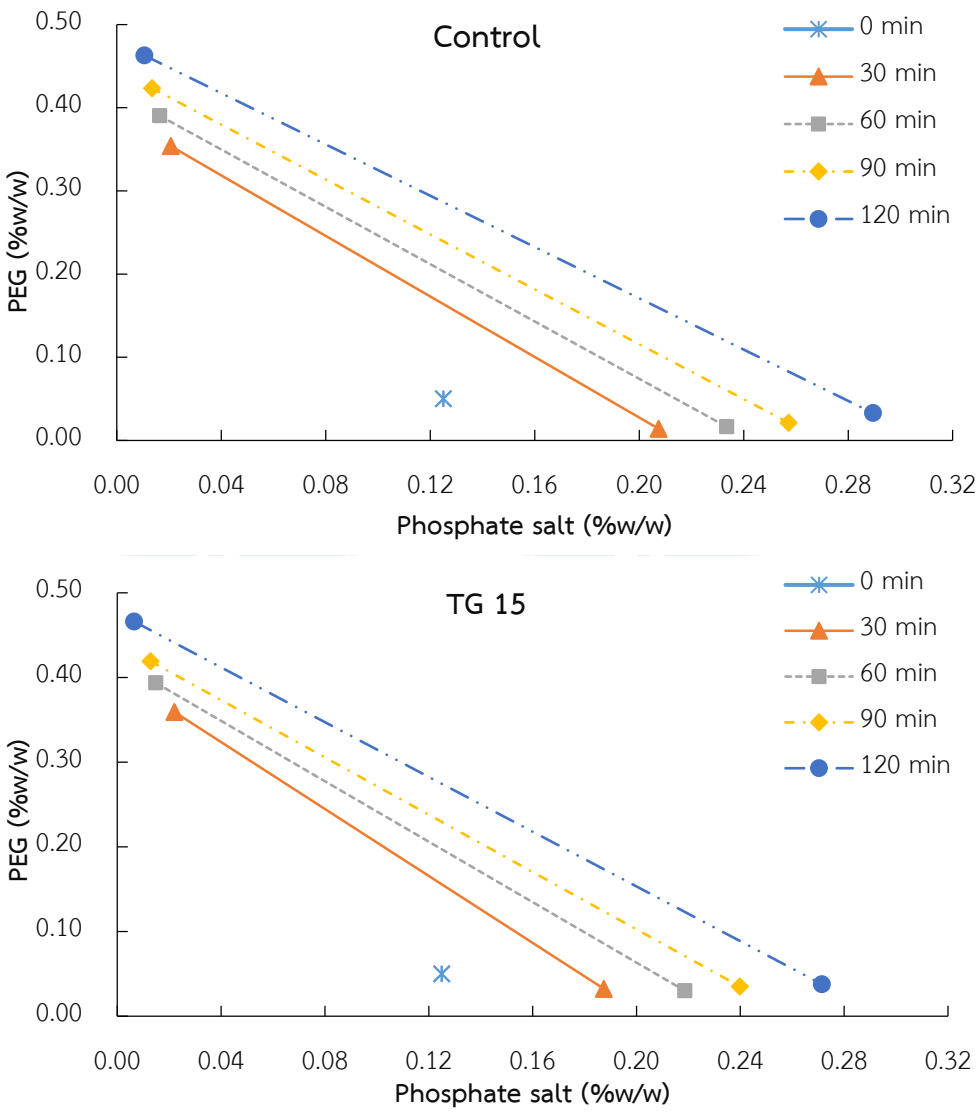

Figure 26 TLL of ATPE process over time in different TG.

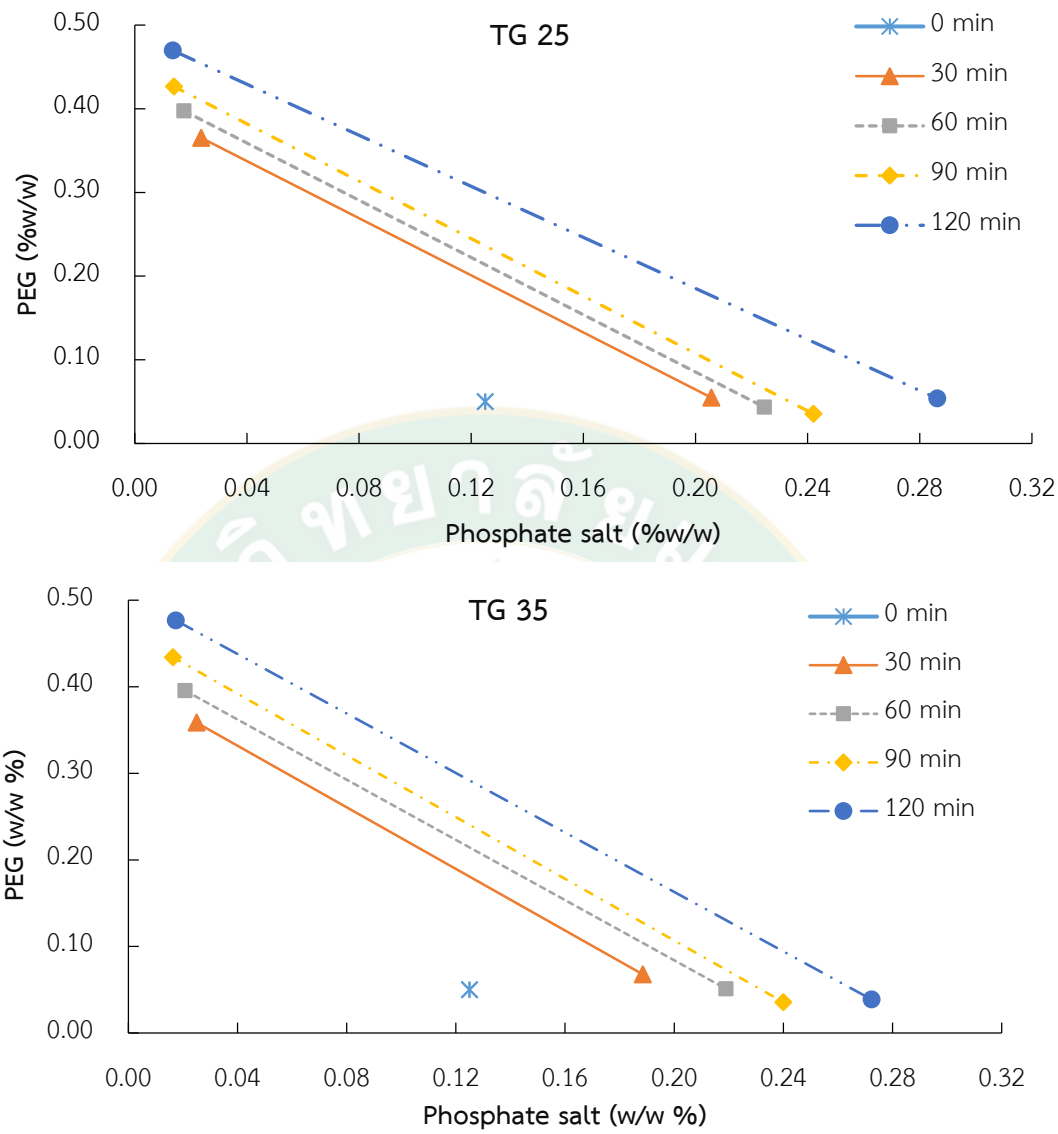

Figure 26 TLL of ATPE process over time in different TG. (Continue)

Figure 26 shows the change in TLL over time, with TLL becoming longer over time. This represents a change in the weight fraction of components (PEG and salt) in the ATPE system. In addition, the system with different TG affects differently the weight fraction of components. Therefore can be analyzed for the relationship of weight fraction in a function of time and TG, as shown in Eq. 76 to 79. This relationship is further used to predict the purity of the process (Section 4.5.2).

$$\phi_2^t = 0.155 + 3.01\times10^{-3}t + 2.10\times10^{-3}TG \qquad \text{Eq. (76)}$$

$$\phi_2^b = 0.083 - 7.82\times10^{-4}t + 1.09\times10^{-4}TG \qquad \text{Eq. (77)}$$

$$\phi_3^t = 0.333 - 9.57\times10^{-5}t + 6.64\times10^{-4}TG \quad \text{Eq. (78)}$$

$$\phi_3^b = 0.148 - 1.19\times10^{-3}t - 3.05\times10^{-4}TG \quad \text{Eq. (79)}$$

4.4 Mass transfer studies of Aqueous Two-Phase Extraction on the temperature gradient process

4.4.1 Prediction of overall mass transfer coefficients (k_La)

The experiments to determine the overall mass transfer coefficient (k_La) of Aqueous Two - Phase Extraction were under flat-interface condition. A glass column with a working capacity of 100 mL. The internal diameter of the reactor was 10 cm. A glass column was placed in a water bath which was maintained temperature by the thermostatic water circulator that mentioned in Figure 13. The k_La was calculated. Here, CPC_t and CPC_s are the concentration of CPC in the PEG and the equilibrium concentration of CPC in the PEG, respectively. If we plot –ln (CPC_s-CPC_t) against time, the volumetric mass transfer coefficient is obtained from the slope of the graph as shown in Figure 27.

Temperature gradient has a significant effect on k_La, Which is observed from Table 11. k_La at TG25 and conventional method were 0.027 and 0.020 min^{-1}, respectively. It can observed that Aqueous Two-Phase Extraction on the temperature gradient process is an effective driving force to the mass transfer CPC concentration in ATPE due to it might be the relative importance of buoyancy forces due to temperature variations.

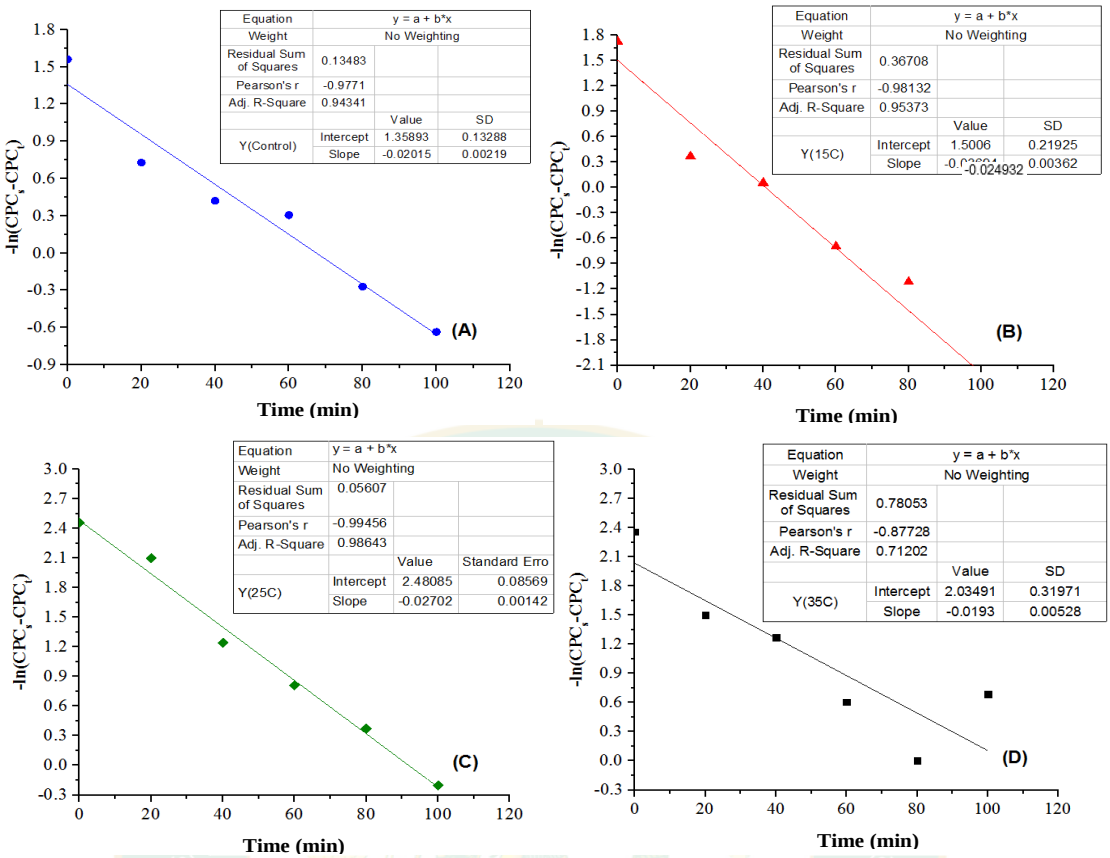

Figure 27 Determination of overall mass transfer coefficient

(A) Control (B) TG15 (C) TG25 (D) TG35

Table 11 The overall mass transfer coefficient

Treatment	k_La (min^{-1})	R^2
Control	0.0202	0.943
TG15	0.0249	0.954
TG25	0.0270	0.986
TG35	0.0193	0.712

4.4.2 Prediction of diffusion coefficients

The experiments to determine the isothermal diffusion (from Eq. 65) thermal diffusion and Soret coefficients (from Eq. 42) of Aqueous Two-Phase Extraction on the temperature gradient process, the corresponding Soret coefficients, mass diffusion times, and deduced isothermal diffusion and thermo diffusion coefficients.

Temperature gradient have a significant effect on diffusion coefficient, as observed in Table 12 which shows that the isothermal diffusion coefficient (D_i) at TG25 and the conventional method were 2.281 × 10^{-12} and 2.104 × 10^{-12} m^2/s, respectively. The Soret coefficient and thermal diffusion were found to be highest at TG25. This is why the Aqueous Two-Phase Extraction on the temperature gradient process is an effective driving force for the mass transfer of the CPC concentration. It might be the relative importance of the diffusion coefficient due to temperature variations. (Schimpf and Semenov, 2000) extended the relation between the thermal diffusion coefficient and viscosity, in which reducing the viscosity resulted in the thermal diffusion coefficient increasing. Therefore, the Aqueous Two-Phase Extraction on the temperature gradient process affects viscosity and buoyancy forces, thereby resulting in improved mass transfer efficiency between the processes.

Table 12 The mass diffusion times, Soret coefficient, the isothermal diffusion coefficient, and the thermal diffusion coefficient of ATPE on TG process

	τ_D (min)	S_T (1/K)	D_i (m^2/s) × 10^{-12}	D_T ($m^2/s{\cdot}K$) × 10^{-13}	EF
Control			2.104		-
TG15	23.325	0.162	2.210	3.580	1.220
TG25	52.797	0.211	2.281	4.813	1.313
TG35	16.753	0.192	2.351	2.398	1.231

The value of isothermal diffusion and thermal diffusion coefficients were different in each experiment. From their values, it is possible to deduce that the enhancement factor (EF) is the factor that characterizes the efficiency of a process compared with the conventional method, as shown in Table 12. TG25 was enhanced around 30% from the conventional method. This result indicates that different temperature not only affects efficiency of the ATPE process, but it also enhances the efficiency of the transport phenomena during the process. This finding is similar to Chan et al. (2003) who concluded that the Soret coefficient and isothermal diffusion coefficient are driven by temperature gradients and concentration gradients.

4.5 Mathematical model of Aqueous Two-Phase Extraction process

4.5.1 The fitting of binodal curve

The optimal binodal curve at TG25 (from section 4.3.2) for the selected PEG and phosphate salt was obtained through the experimental (Figure 25A). Further, the experimental bimodal data were fitted by modifying the constants and coefficients of the expressions available in the literature equations by using computer programs. (MATLAB, Math Work Inc.) (Figure 28)

```
>> Binodal
Regupathi Equation

mdl =


Nonlinear regression model:
    y ~ p1 + ((p2*(Ws^0.5))) + (p3*Ws)

Estimated Coefficients:
          Estimate       SE        tStat       pValue
          ________    ________    _______    _________

    p1     0.39569    0.082993     4.7677    0.0020411
    p2    -0.79388     0.48252    -1.6453      0.14391
    p3     0.31878     0.55822    0.57107      0.58581


Number of observations: 10, Error degrees of freedom: 7
Root Mean Squared Error: 0.026
R-Squared: 0.959,  Adjusted R-Squared 0.947
F-statistic vs. constant model: 81.7, p-value = 1.41e-05
----------------------------------------------------
```

```
Hu Equation

mdl =


Nonlinear regression model:
    y ~ p1 + ((p2*(Ws^0.5))) + (p3*Ws) + (p4*(Ws^2))

Estimated Coefficients:
          Estimate       SE        tStat       pValue
          ________    _______    ________    _______

    p1    0.19375     0.19177     1.0103     0.35133
    p2    0.69768      1.3676    0.51015     0.62817
    p3    -2.3848      2.3902   -0.99773     0.35693
    p4     2.0965      1.8047     1.1617     0.28949


Number of observations: 10, Error degrees of freedom: 6
Root Mean Squared Error: 0.0254
R-Squared: 0.966,  Adjusted R-Squared 0.95
F-statistic vs. constant model: 57.6, p-value = 8.16e-05
----------------------------------------------------
```

```
Maria Equation

mdl =


Nonlinear regression model:
    y ~ exp(p1 + ((p2*(Ws^0.5))) + (p3*(Ws^3)))

Estimated Coefficients:
          Estimate       SE        tStat       pValue
          ________    _______    _______    ________

    p1    -1.1119     0.34985    -3.1782     0.01553
    p2     -1.497      1.5467   -0.96788     0.36535
    p3    -34.952      18.084    -1.9328    0.094537


Number of observations: 10, Error degrees of freedom: 7
Root Mean Squared Error: 0.0244
R-Squared: 0.964,  Adjusted R-Squared 0.953
F-statistic vs. zero model: 154, p-value = 9.44e-07
----------------------------------------------------
```

```
Graber Equation

mdl =


Nonlinear regression model:
    y ~ 1/(p1 + (p2*(Wp^0.5)) + (p3*(Wp)))

Estimated Coefficients:
          Estimate       SE        tStat       pValue
          ________    _______    _______    ________

    p1     3.1674     0.93296     3.395    0.011521
    p2    -18.778      10.923   -1.7191     0.12928
    p3     97.069      30.107    3.2242    0.014569


Number of observations: 10, Error degrees of freedom: 7
Root Mean Squared Error: 0.0254
R-Squared: 0.985,  Adjusted R-Squared 0.981
F-statistic vs. zero model: 413, p-value = 3.09e-08
```

Figure 28 Nonlinear regression for binodal curve by MATLAB program

Four equations, Regupathi Hu Marai and Graber equation, are used to predict the coefficients to describe the relationship of the weight fractions of PEG (W_P) and salt (W_S) in the ATPE system. The determination coefficient (R^2) is a statistical value indicating the accuracy of prediction. From nonlinear regression by using the MATLAB

program, found that all equations were able to accurately predict correlation, which R^2 value greater than 0.950. The highest is shown 0.981 by Graber equation as shown in Table. 13

Table 13 Literatures empirical of correlation

Equations	Constants				R^2
	a	b	c	d	
Regupathi et al., 2012: $W_P = a + bW_S^{0.5} + cW_S$	0.396	-0.794	0.318	-	0.947
Hu et al., 2004: $W_P = a + bW_S^{0.5} + cW_S + dW_S^2$	0.194	0.698	-2.385	2.096	0.950
Maria et al., 2001: $\ln W_P = a + bW_S^{0.5} + cW_S^3$	-1.112	-1.497	-34.952	-	0.953
Graber et al., 2001: $\frac{1}{W_S} = a + bW_P^{0.5} + cW_P$	3.167	-18.778	97.069	-	0.981

The coefficients obtained from the analysis were as follows in Eq. 80, which will be used to further predict the phase behavior on the ATPE process.

$$\frac{1}{W_S} = 3.167 - 18.778W_P^{0.5} + 97.069W_P \qquad \text{Eq. (80)}$$

4.5.2 The simulation of phase equilibrium behavior

The ATPE model in this work is water-PEG4000-salt systems. When a system reaches equilibrium, the energy content is at the lowest possible state. This applies to an ATPE, where the equilibrium state attained would enable it to partition into two distinguishable phases, namely the top and the bottom phase, with respective components in each phase achieving the following:

1. Minimize in the difference of Gibbs energy of mixing $(\min \Delta G^{two-phase})$
2. Equal chemical potentials $(\mu_i^t = \mu_i^b, \quad \text{where} \quad i = 1, 2, 3, ..., n)$
3. Equal fugacity $(f_i^t = f_i^b, \quad \text{where} \quad i = 1, 2, 3, ..., n)$

The theory for water-PEG4000-salt systems, it has been shown by Kenkare et a!. (1995) that Coulombic interactions among salt ions contribute towards phase separation in aqueous systems containing salts. Thus, we chose a simple, application oriented mathematical model of phase behavior of the salt-polymer ATPE systems that includes the effect of Coulombic interactions among salt ions.

In this model, the expression for Gibbs energy of mixing combines the extended Eq. 10 for ternary systems, and an electrostatic contribution given by Pitzer's extension of the Debye-Hiickel function (1973), as follows

$$\frac{\Delta G_m}{RT} = \frac{\Delta G^{DH}}{RT} + \frac{\Delta G^{FH}}{RT} \qquad \text{Eq. (81)}$$

where superscripts DH and FH denote Debye-Hiickel and Flory-Huggins contributions, respectively. Thus, we assumed that the volume fractions of the components are equal to the segment fractions, and expressed Eq.81 using the conventional expression for Flory-Huggins contribution. For a ternary water-PEG4000-salt systems, the general expression for Gibbs energy is:

$$\frac{\Delta G_m}{RT} = \left\{ \phi_1 \left(\frac{MW_1}{W_1} \right) \left[-A_\varphi \left(\frac{4I}{b} \right) \ln\left(1 + bI^{0.5}\right) \right] \right\} + \{ n_1 \ln \phi_1 + n_2 \ln \phi_2 + n_3 \ln \phi_3 + \left(n_1 + n_2 n_2 + n_3 n_3\right)\left(\chi_{12}\phi_1\phi_2 + g_{13}\phi_1\phi_3 + \chi_{23}\phi_2\phi_3\right) \} \qquad \text{Eq. (82)}$$

where MW_1 is the molecular weight of water

W_1 is the weight of water,

χ_{12} is the interaction parameter between water and PEG4000

χ_{23} is the interaction parameter between PEG4000 and ion (salt)

I is the ionic strength of that aqueous system given by

$$I = \frac{1}{2}\left[\frac{\phi_3 \left(W_1 / MW_1\right)}{1 - \phi_3} \right] \left| z_A z_B \right| \qquad \text{Eq. (83)}$$

z_A and z_B are the valences of the cation and anion.

A_φ and b are the Debye-Hiickel constants

g_{13} is an empirical function of interaction parameter between water and salt in terms of the mixture composition of the salt, g_{13} given by

$$g_{13}(\phi_3) = \sum_{k=1}^{n} c_k \phi_3^{k-1} \qquad \text{Eq. (84)}$$

c_k is coefficients regressed

For this system, the difference between the chemical potential of component i in the mixture and that in the standard state would be

$$\mu_i - \mu_i^0 = \left(\frac{\partial (n_1 + n_2 + n_3) \Delta G_m}{\partial n_i} \right)_{T, N_{j \neq i}} \qquad \text{Eq. (85)}$$

where n_i ; is the number of moles of component i. From Eq. 81 and 84 $\Delta\mu_i$ are given by

$$\frac{\Delta\mu_1}{RT} = \frac{2A_\varphi \sqrt{I}}{1+b\sqrt{I}} \left(\frac{MW_1}{W_1} \right) + \ln\phi_1 + \left(1 - \frac{r_1}{r_2}\right)\phi_2 + \left(1 - \frac{r_1}{r_3}\right)\phi_3 + r_1 \left(\chi_{12}\phi_2 (1-\phi_1) + g_{13}(1-\phi_1) - g'_{13}\phi_1\phi_2\phi_3 - \chi_{23}\phi_2\phi_3 \right) \qquad \text{Eq. (86)}$$

$$\frac{\Delta\mu_2}{RT} = -A_\varphi |z_A z_B| \left[\frac{\sqrt{I}}{1+b\sqrt{I}} + \frac{2}{b}\ln\left(1+b\sqrt{I}\right) \right] + \ln\phi_2 + \left(1 - \frac{r_2}{r_1}\right)\phi_1 + \left(1 - \frac{r_2}{r_3}\right)\phi_3 + r_2 \left(\chi_{12}\phi_1 (1-\phi_2) - g_{13}\phi_1\phi_3 + g'_{13}\phi_1\phi_3 (1-\phi_2) + \chi_{23}\phi_3 (1-\phi_2) \right) \qquad \text{Eq. (87)}$$

$$\frac{\Delta\mu_3}{RT} = -A_\varphi |z_A z_B| \left[\frac{\sqrt{I}}{1+b\sqrt{I}} + \frac{2}{b}\ln\left(1+b\sqrt{I}\right) \right] + \ln\phi_3 + \left(1 - \frac{r_3}{r_1}\right)\phi_1 + \left(1 - \frac{r_3}{r_2}\right)\phi_2 + r_3 \left(-\chi_{12}\phi_1\phi_2 + g_{13}\phi_1 (1-\phi_3) - g'_{13}\phi_1\phi_3\phi_4 + \chi_{23}\phi_2 (1-\phi_3) \right) \qquad \text{Eq. (88)}$$

$$\frac{\Delta\mu_4}{RT} = -A_\varphi |z_A z_B| \left[\frac{\sqrt{I}}{1+b\sqrt{I}} + \frac{2}{b}\ln\left(1+b\sqrt{I}\right) \right] + \ln\phi_4 + r_4 \left\{ \phi_1 \left(\chi_{14} - \frac{1}{r_1} \right) + \phi_2 \left(\chi_{24} - \frac{1}{r_2} \right) + \phi_3 \left(\chi_{34} - \frac{1}{r_3} \right) - \chi_{12}\phi_1\phi_2 - g_{13}(\phi_3)\phi_1\phi_3 - g'_{13}(\phi_3)\phi_1\phi_2\phi_3 - \chi_{23}\phi_2\phi_3 \right\} \qquad \text{Eq. (89)}$$

The partition coefficient of the CPC in ATPE is:

$$K_4 = \exp\left\{-A_{\varphi}\left|z_A z_B\right|\left\{\left(\left(\frac{\sqrt{I}}{1+b\sqrt{I}}\right)^t - \left(\frac{\sqrt{I}}{1+b\sqrt{I}}\right)^b\right) + \left(\frac{2}{b}\left\{\ln\left(1+b\sqrt{I}\right)^t - \ln\left(1+b\sqrt{I}\right)\right\}\right)\right\}\right.$$

$$\left. + r_4\left(\left(\phi_1^t - \phi_1^b\right)\left(\chi_{14} - \frac{1}{r_1}\right) + \left(\phi_2^t - \phi_2^b\right)\left(\chi_{24} - \frac{1}{r_2}\right) + \left(\phi_4^t - \phi_4^b\right)\left(\chi_{34} - \frac{1}{r_3}\right)\right)\right\} + f(TG) \quad \text{Eq. (90)}$$

Figure 29 show how the MATLAB coding is written in order to solve the chemical potential different. At equilibrium, the difference of chemical potential of component 4 must be equal in both phase as shown in Eq. 91

$$\mu_4^t = \mu_4^b \qquad \text{or} \qquad \Delta\mu_4 = \min\ (10^{-6}) \qquad \text{Eq. (91)}$$

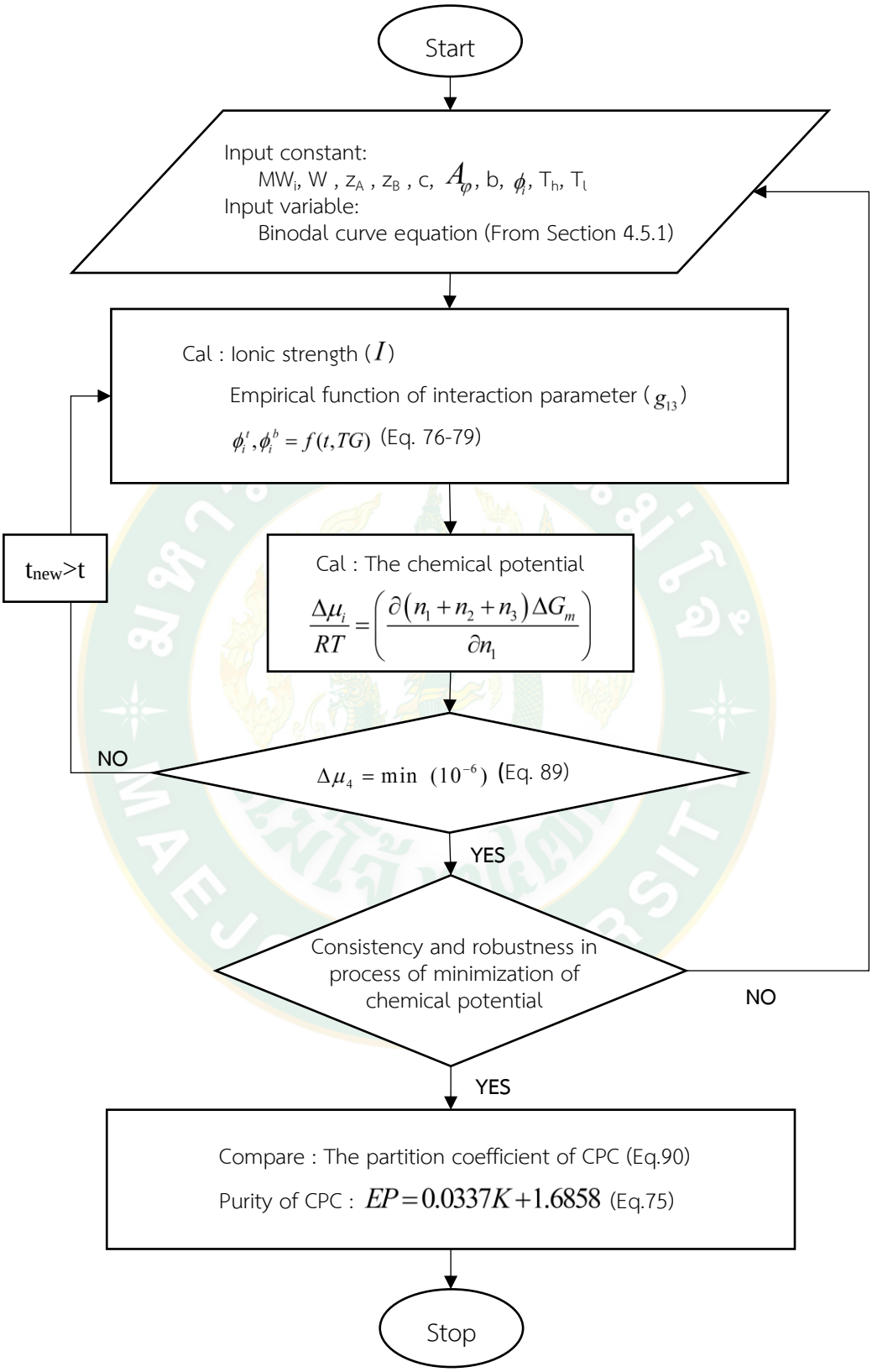

Figure 29 The algorithm calculation and simulation flow chart

The MATLAB script for simulation of phase equilibrium behavior is included and show in Appendix A, the script is estimate. The script is the applicability of the minimization of chemical potential approach in calculation of the ATPE behavior and protein partitioning behavior using the empirical data, when input variable and constant: Molecular weight of component (MW_i), Weight of water (W), The valences of cation and anion for a salt (z_A and z_B), The coefficients regression (c_k) by (Partanen et al., 2003), A_φ and b are the Partanen constant. The initial fraction of component (ϕ_i), the temperature gradient (TG). The model parameters used for the four components in the ATPE mixture of PEG4000 + Salt (potassium phosphate + water + CPC (at TG25), including the factor for the objective function of the model, are to be predetermined.

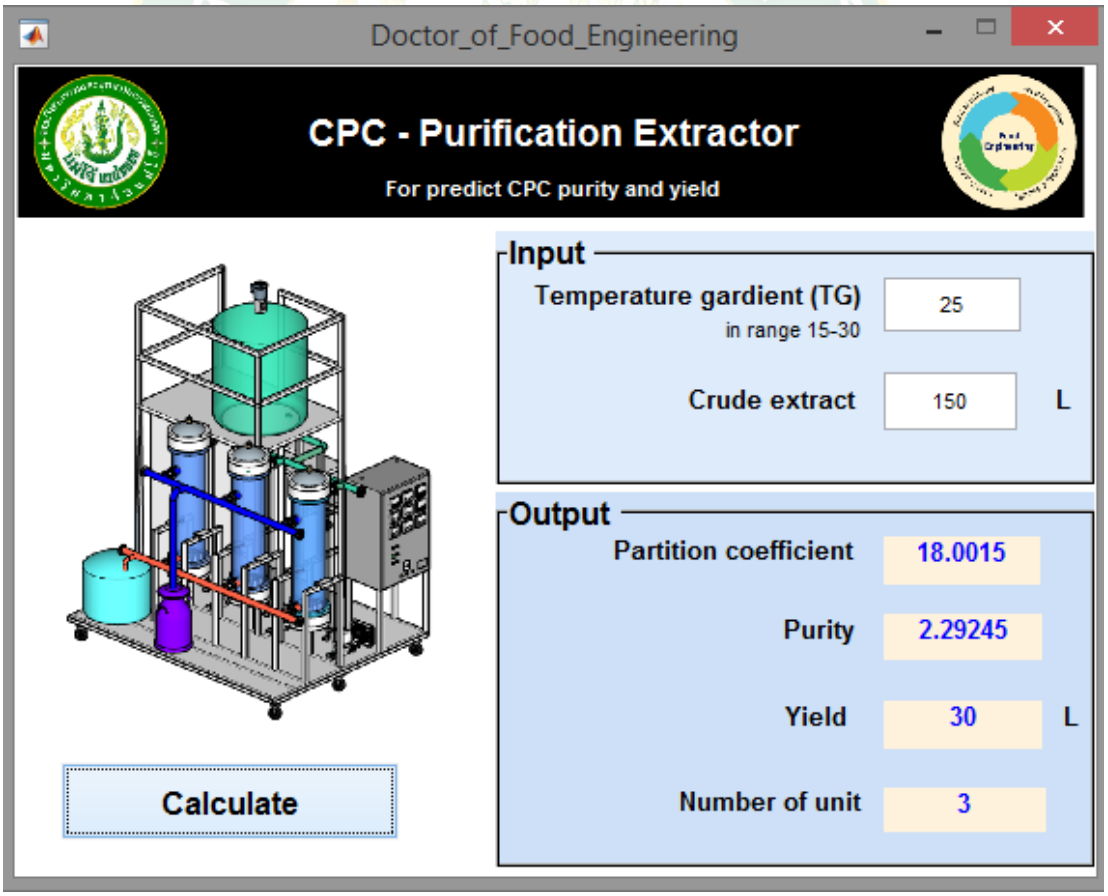

Figure 30 Screen example of a MATLAB program to simulate the phase equilibrium behavior.

The Graphic User Interface (GUI) was created with the simulation MATLAB script to simulate the process in case for the limitation of this simulation. The boundary condition was including the temperature gradient should be performing 15-30, because it is an optimal range for constructing a temperature distribution and does not affect the CPC which is sensitive at high temperatures.

The GUI predicted the partition coefficient from Eq. 90, and from the correlation between partition coefficient and purity (From section 4.3.2), the figure of GUI is shown in Figure 30. The result of the partition coefficient of the system which the model can predict, the purity of CPC, and yield of the product. Table 14 shows the comparison of experimental and predicted values, it was found that the model can predict in purity value accurately with an error of less than 10% which is acceptable. Although in the case of the partition coefficient there is a high error which may be the result of some constants (z_A, z_B, c_k, A_φ) cannot vary according to the temperature gradient. The model should be developed by further determining the relationship between the constant value and TG.

Table 14 Comparison of the values obtained from experiments and simulation

Process	Partition Coefficient, K			Purity, EP		
	Experiment	Simulate	Error (%)	Experiment	Simulate	Error (%)
Control	3.550	6.518	83.60	1.839	1.905	3.61
TG15	7.050	9.319	32.18	1.889	2.000	5.87
TG25	18.380	18.002	2.06	2.337	2.292	1.91
TG35	8.822	4.147	52.99	1.918	1.826	4.82

4.6 Design the high CPC purity extractor and the engineering economic analysis

4.6.1 Food machine concept design

For our experimental study with a specific separation the explained mathematical procedure is applied. The required heights of column are derived for different conditions. The calculated height using equation as shown in Table 15

From Table 16 shows the comparison calculated heights of the column between the conventional method (without TG) and Aqueous Two-Phase Extraction

on the temperature gradient process. As can be seen in the first row is the height of the column from the conventional method. The calculated height is 1.58 which more than the Aqueous Two-Phase Extraction on the temperature gradient process in the second row. Showed that Aqueous Two-Phase Extraction on the temperature gradient process which can help to reduce the height of the column and the efficiency of the extractor is comparable to the conventional method. Because the effect of the temperature difference helps to increase the mass transfer coefficients (k_La) during the process.

Table 15 Calculated height using equation

	NTU	HTU (m)	H (m)
Convectional method	1.263	1.25	1.58
ATPE on TG process	1.061	0.93	0.99

The column design as shown in Figure 31. The column diameter can be calculated from the experimental data in section 4.2.2, where the optimum height and dimeter ratio is 4, when the height is 1 meter (from Table 14). The calculated diameter is 25 centimeters. The internal volume is 50 L. In the design of heating and cooling units based on the principle of heat transfer using fin to increase the efficiency of the system by increasing the area for heat transfer. And to comply with food hygiene design principles. The prototype is designed to be disassembled to reduce the dead space and convenient for cleaning.

According to the company requirement, the prototype capacity must be more than 30 L/batch, so from the column designed above, the approximate product is only 10 liters (25-30% of volume), The prototype designed to 3 columns for produce pure CPC 30 liters per time as shown in Figure 32

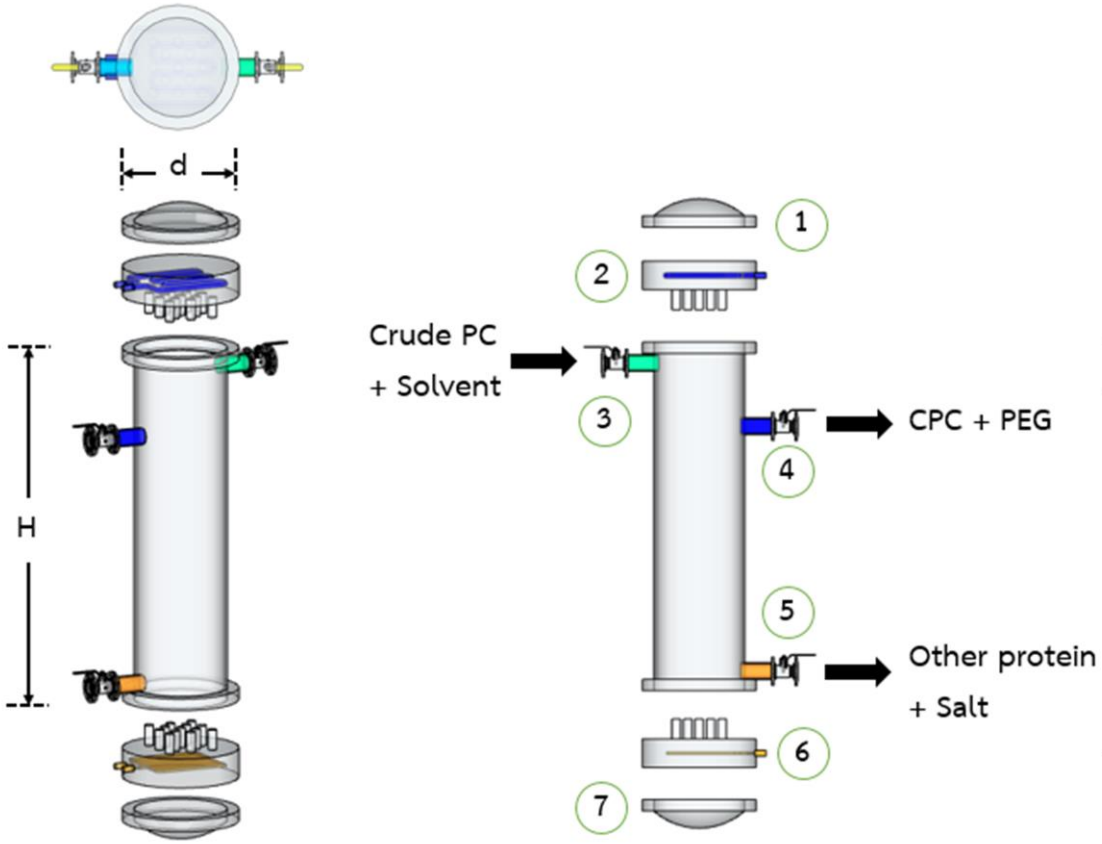

NO.	Assembly
1	Top Cover
2	Cooling Unit
3	Feed Valve
4	Extract Valve
5	Drain Valve
6	Heating Unit
7	Bottom Cover

Figure 31 Assembly view of column

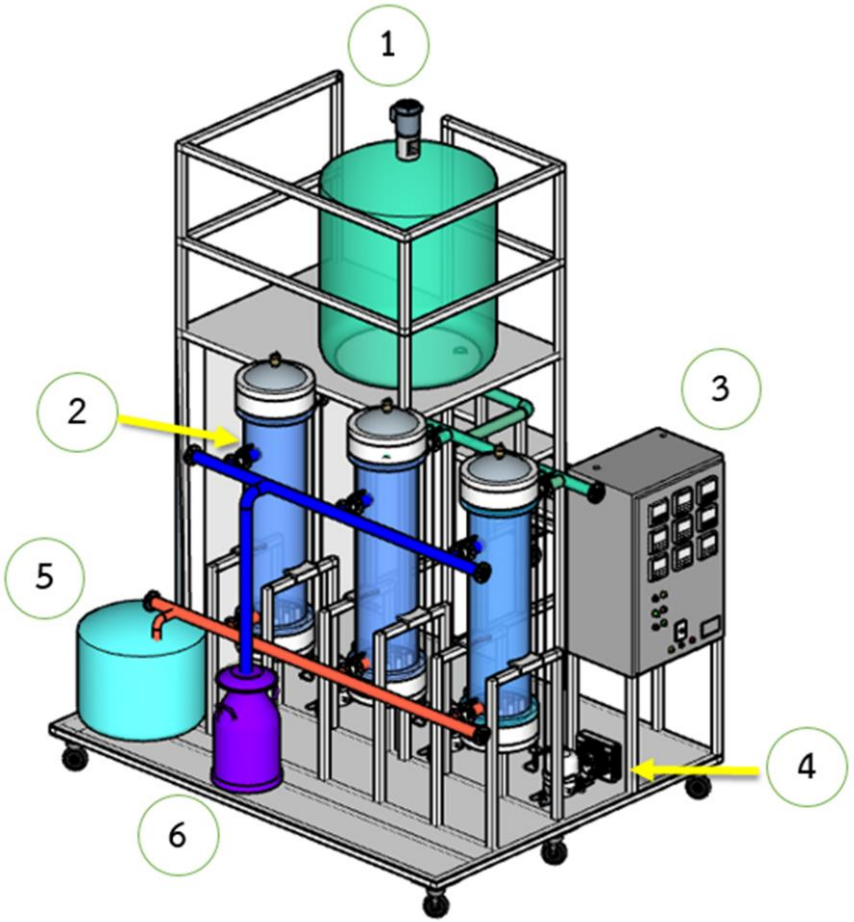

NO.	Component
1	Mixing tank
2	Column
3	Controller
4	Cooling system
5	Residual tank
6	Product tank

Figure 32 Conceptual prototype machine design

4.6.2 Engineering economic analysis

The cost of the Aqueous Two-Phase Extraction on the temperature gradient extractor was estimated as shown in Table 16, following the concept design, the assembly details as shown in this table, and can estimate ATPE extractor price about 1,200,000 THB.

Table 16 The assembly details and cost of extractor machine

Detail	Description	Q'TY	Unit	Unit price	Cost
1. Column					
Stainless tube SUS316	Sch.40 Dia 10 inch	1	pieces	50,000.00	50,000.00
Stainless tube SUS316	Dia. 1 inch	4	tubes	5,000.00	20,000.00
Ball valve stainless	Dia. 1 inch	3	set	1,800.00	9,000.00
Automatic valve	Dia. 1 inch	6	set	10,000.00	60,000.00
Cover and frame		6	set	10,000.00	60,000.00
Frame		2	pieces	50,000.00	100,000.00
2. Heating-Cooling Unit					
Copper tube		3	tubes	10,000.00	30,000.00
Insulation		3	pieces	10,000.00	30,000.00
Cooling set		3	set	20,000.00	60,000.00
Electric water heater	2000 W	3	set	12,000.00	36,000.00
Fin set		3	set	10,000.00	45,000.00
3. Control system					
Chemical pump	Food grade	1	set	10,000.00	30,000.00
Control unit		1	set	300,000.00	300,000.00
Flow meter		3	set	15,000.00	45,000.00
4. Chemical Tank					
Chemical Tank	Volume 200 L	2	set	5,000.00	20,000.00
Stirring set		1	set	50,000.00	50,000.00
Product Tank	Volume 500 L	1	set	10,000.00	10,000.00
Total cost					**955,000.00**
After-sale service and warranty 10% of total cost					**95,500.00**
Total					**1,050,500.00**
Sale price of prototype					**1,200,000.00**

Table 17 shows the engineering economic analysis of the Aqueous Two-Phase Extraction on the temperature gradient extractor which was produced the pure CPC

as powder, the selling price 275 THB/g (purity> 2.0) which was defined following the global market reviews. The daily product calculated from the final product as a powder is 1,200 g/day. Monthly expense is the summation cost of extraction, purification, and drying process. From the net benefit per month, as shown in the table, the simple payback period for the ATPE extractor was as 1.53 years or about 2 years.

Table 17 The economic analysis of extractor full capacity 30 L

Cost investment information	Price	Unit
1. Monthly income		
1.1 CPC powder (purity> 2.0)	1,200	g/day
1.2 Selling price of pure CPC (cosmetic grade) as 275 THB/g, so the monthly income (20 days)	6,600,000	THB/month
2. Monthly expense		
2.1 Raw material		
- Crud PC (2,000 THB/Liter)	6,000,000	THB/month
2.2 Purification Cost		
- Chemical and others cost for purification	356,400	THB/month
2.3 Drying Cost		
- Chemical and others cost for drying	178,200	THB/month
3. Economic analysis		
3.1 Price of extractor	1,200,000	THB
3.2 Monthly expense	6,534,600	THB/month
3.3 Monthly profit	65,400	THB/month
3.4 Yearly profit	784,800	THB/year
3.5 Simple payback period	1.53	Years

CHAPTER 5
CONCLUSION

5.1 General conclusion

The purpose of this research to study and develop the CPC purification process from the cultivation process to the final step, the result as shown the following:

5.1.1 Enhancing cell growth and CPC production of *Spirulina platensis*

The fed-batch cultivation proved to be an effective strategy to further enhance CPC production of *Spirulina platensis*. The results indicate that the maximum CPC production (4.354 g/L) and productivity (97.53 mg/L.d) was obtained when using fed-batch with the NH_4HCO_3 3.0 mM. A kinetic model to describe the *Spirulina platensis* culture system including cell growth, CPC formation, as well as nitrogen consumption was proposed.

Batch cultivation

$$\mu = 0.600\left(\frac{C_{S1}}{0.414 + C_{S1}}\right)\left(\frac{C_{S2}}{0.056 + C_{S2}}\right)$$

$$P_{CPC} = 0.335\left(\frac{C_{S1}}{0.413 + C_{S1}}\right)\left(\frac{C_{S2}}{0.055 + C_{S2}}\right)$$

Fed-Batch cultivation

$$\mu = 0.400\left(\frac{C_{S1}}{0.414 + C_{S1} + \frac{C_{S1}^2}{13,885.6}}\right)\left(\frac{C_{S2}}{0.056 + C_{S2} + \frac{C_{S2}^2}{0.190}}\right)$$

$$P_{CPC} = 0.223\left(\frac{C_{S1}}{0.413 + C_{S1} + \frac{C_{S1}^2}{17,234.4}}\right)\left(\frac{C_{S2}}{0.055 + C_{S2} + \frac{C_{S2}^2}{0.188}}\right)$$

5.1.2 Purification of CPC extracted from *Spirulina platensis* by Aqueous Two - Phase Extraction

The suitable aqueous two phase system for purification of CPC. The concentration and purity of CPC in the top phase were considered as the response variable to evaluate the effect of different systems. It can be observed that phosphate salts have shown maximum purity of CPC for all the molecular weights of PEG when compared to the other salts. The optimal aqueous two phase system is PEG4000 6% and potassium phosphate 15% which value of the CPC concentration and purity in the top phase were recorded as 7.016 g/L and 1.839, respectively.

5.1.3 Application of Aqueous Two-Phase Extraction on the temperature gradient process

Aqueous Two-Phase Extraction on the temperature gradient process can enhance purification efficiency around 27% of CPC obtained from this technique when compared with the conventional method (ATPE without TG). The results of the effect of TG on CPC concentration in the top phase at complete separation. The highest concentration was found TG25 (13.932 g/L), significantly higher than the conventional method. According to the results, the highest purity and yield values were 2.337 and 91.18, respectively.

5.1.4 Mass transfer studies of Aqueous Two-Phase Extraction on the temperature gradient process

Different temperatures have a significant effect on mass transfer coefficients it can observed that overall mass transfer coefficients (k_La) the isothermal diffusion coefficient (D_i) and the thermal diffusion coefficient (D_T) during Aqueous Two-Phase Extraction on the temperature gradient process is 0.0270 min^{-1} 2.281 x 10^{-12} m^2/s and 4.813 x 10^{-13} m^2/s. K (at TG25) which was significant more than the conventional method.

5.1.5 Mathematical model of Aqueous Two-Phase Extraction process

A mathematical model developed for simulating phase-equilibrium behavior in the Aqueous Two-Phase Extraction on the temperature gradient process and the CPC-Purification GUI was created by using the mathematical model of predicting the partition coefficient and purity, which can accurately predict. The error of less than 10%

5.1.6 Design the high purity CPC extractor and engineering economic analysis

The Aqueous Two-Phase Extraction on the temperature gradient prototype was presented, the cost of extractor was estimated as 1,200,000 THB. The economic analysis was analyzed as the powder CPC which was referred to as the product produced by Aqueous Two-Phase Extraction on the temperature gradient extractor. The results were found the attractive to state its commercial feasibility by the simple payback period was estimated at about 2 years.

5.2 Recommendation

5.2.1 Further studies should be undertaken into the step of purification. Because this study uses only a single-step purification process. There may be limitations to the saturation of the solvent. In which the multi-step purification may increase the purity of the extract even more.

5.2.2 Further studies should be backward extraction in order to be reused solvents. This will reduce the cost of the process and also study the suitability for zero waste management.

5.3 Novelty of this research

5.3.1 The modified correlation was established to predict the cell growth, CPC formation, and nitrogen consumption during the cultivation by using fed-batch with the NH_4HCO_3 as nitrogen source. This correlation provides the characteristic variable of cultivation namely nitrate concentration (C_{S1}) and ammonium concentration (C_{S2}). Not only cell growth rate estimation, but also the valve of nitrate and ammonium inhibit prediction were developed by the modified and ammonium inhibit prediction were developed by the modified correlation. The modified correlation was developed not only to estimate cell growth rate, CPC formation, and nitrogen consumption but also to predict the value of nitrate and ammonium inhibit. Lead to development into commercial-scale cultivation, the controlling is well relative to establish "Smart Farm" culture modeling, production controlling, and feed monitoring that is invariable underpinning by sensors and sensor networks. In a control system, a controller unit would continuously record such as the culture temperature, pH, and biomass growth by the sensor. The cultivation information was continuously transferred to the computer data logger where the data would be analyzed, displayed, and recorded.

5.3.2 Aqueous Two-Phase Extraction on the temperature gradient process is a new finding and is suitable for CPC purification that can enhance purification efficiency around 27% when compared with the conventional method (ATPE without TG). There are many advantage such as reduce the processing time, uncomplicated, and lower cost than other purification method (ion-exchange chromatography). It is a better alternative to existing methods, especially in terms of scaling up to an industrial scale. Which can increase the purity of CPC extracts from food grade to higher grades and increase the value of the extracts. The modified correlation of TLL and weight fraction on the temperature gradient process was established to predict the partition coefficient and purity. This correlation in the function of TG increased the accuracy of prediction. The modified correlation can be the new finding model for predicting the purification process

5.3.3 Aqueous Two-Phase Extraction on the temperature gradient process is the advanced knowledge of food engineering especially in the field of heat and mass transfer principles. The researchers successfully investigated the isothermal and thermo diffusion of the purification process by using ATPE (a binary aqueous solution of PEG4000 and potassium phosphate). The isothermal diffusion coefficient (D_i) significantly increased with increased TG. The Soret effect (S_T) and thermo diffusion coefficient (D_T) were obtained at a high TG, but this should not go beyond 25. It can be concluded that the Soret effect (S_T) and thermos diffusion coefficient (D_T) were good parameters for explaining CPC purification efficiency.

REFERENCES

Adams, M. 2005. **Superfoods for optimum health: chlorella and spirulina**. Truth Publishing International, Ltd.

Agasoster, T. 1998. Aqueous two-phase partitioning sample preparation prior to liquid chromatography of hydrophilic drugs in blood. **Journal of Chromatography B: Biomedical Sciences and Applications**, 716(1-2), 293-298.

Albertsson, P.-A. 1956. Chromatography and partition of cells and cell fragments. **Nature**, 177(4513), 771-774.

---. 1986. Aqueous polymer-phase systems. **Partition of Cell Particles and Macromolecules: Separation and Purification of Biomolecules, Cell Organelles, Membranes, and Cells in Aqueous Polymer Two-Phase Systems and Their Use in Biochemical Analysis and Biotechnology**.

Aldred, P. A., Tjerneld, F. & Modlin, R. F. 1993. Partitioning of ecdysteroids using temperature-induced phase separation. **Journal of Chromatography A**, 628(2), 205-214.

Alred, P. A., Kozlowski, A., Harris, J. M. & Tjerneld, F. 1994. Application of temperature-induced phase partitioning at ambient temperature for enzyme purification. **Journal of Chromatography A**, 659(2), 289-298.

Antelo, F. S., Anschau, A., Costa, J. A. & Kalil, S. J. 2010. Extraction and purification of C-phycocyanin from Spirulina platensis in conventional and integrated aqueous two-phase systems. **Journal of the Brazilian Chemical Society**, 21(5), 921-926.

Asenjo, J., Turner, R., Mistry, S. & Kaul, A. 1994. Separation and purification of recombinant proteins from Escherichia coli with aqueous two-phase systems. **Journal of Chromatography A**, 668(1), 129-137.

Asenjo, J. A. & Andrews, B. A. 1989. **Design and Use of Enzyme Systems for Selective Product Release from Microbial Cells**. Springer Berlin Heidelberg.

Badger, M. & Price, G. 2003. The Role of Carbonic Anhydrase in Photosynthesis. **Annu. Rev. Plant Biol**, 45(-), 369-392.

Bai, N. & Seshadri, C. V. 1980. On coiling and uncoiling of trichomes in the genus

Spirulina. **Algological Studies**, 26(-), 32-47.

Bao, Y., Wen, S., Cong, W., Wu, X. & Ning, Z. 2012. An Optical-Density-Based Feedback Feeding Method for Ammonium Concentration Control in Spirulina platensis Cultivation. **Journal of Microbiology and Biotechnology**, 22(7), 967-974.

Barbosa, M. J., Rocha, J. M. S., Tramper, J. & Wijffels, R. H. 2001. Acetate as a carbon source for hydrogen production by photosynthetic bacteria. **Journal of Biotechnology**, 85(1), 25-33.

Beijerinck, M. W. 1910. Ueber Emulsionsbildung bei der Vermischung wässeriger Lösungen gewisser gelatinierender Kolloide. **Zeitschrift für Chemie und Industrie der Kolloide**, 7(1), 16-20.

Belay, A. 2002. The potential application of Spirulina (Arthrospira) as a nutritional and therapeutic supplement in health management. **J Am Nutraceutical Assoc**, 5(27-48.

Ben-Amotz, A., Tornabene, T. G. & Thomas, W. H. 1985. Chemical profile of selected species of microalgae with emphasis on lipids. **Journal of Phycology**, 21(1), 72-81.

Benavides, J. & Rito-Palomares, M. 2008. Practical experiences from the development of aqueous two-phase processes for the recovery of high value biological products. **Journal of Chemical Technology & Biotechnology: International Research in Process, Environmental & Clean Technology**, 83(2), 133-142.

Benneman, J. 1988. Microalgal Biotechnology: Products, Process and Opportunities, vol. 1. **Washington: OMEC International Inc**.

Bennett, A. & Bogorad, L. 1973. Complementary chromatic adaptation in a filamentous blue-green alga. **The Journal of cell biology**, 58(2), 419-435.

Berggren, K., Johansson, H.-O. & Yjerneld, F. 1995. Effects of salts and the surface hydrophobicity of proteins on partitioning in aqueous two-phase systems containing thermoseparating ethylene oxide-propylene oxide copolymers. **Journal of Chromatography A**, 718(1), 67-79.

Berggren, K., Nilsson, A., Johansson, G., Bandmann, N., Nygren, P.-Å. & Tjerneld, F. 2000. Partitioning of peptides and recombinant protein–peptide fusions in

thermoseparating aqueous two-phase systems: effect of peptide primary structure. **Journal of Chromatography B: Biomedical Sciences and Applications**, 743(1-2), 295-306.

Bermejo, R., Talavera, E. M. & Orte, J. C. 1997. Chromatographic purification of biliproteins from Spirulina platensis high-performance liquid chromatographic separation of their α and β subunits. **Journal of Chromatography A**, 778(1-2), 441-450.

Blanco, B., Elman, H., Salazar, R. & Berberian, M. 2000. Dynamic simulation of the concentration profiles in a liquid-liquid extraction tower. **Revista de la Facultad de Ingenieria**, 15(2), 67-68.

Boublík, T. 1970. Hard-Sphere Equation of State. **The Journal of Chemical Physics**, 53(1), 471-472.

Boussiba, S. & Richmond, A. E. 1979. Isolation and characterization of phycocyanins from the blue-green alga Spirulina platensis. **Archives of Microbiology**, 120(2), 155-159.

Brain, C. M. 2017. **Bioprocessing in Microalgae.** Doctor. Newcastle University.

Cabezas, H. 1996. Theory of phase formation in aqueous two-phase systems. **Journal of Chromatography B: Biomedical Sciences and Applications**, 680(1), 3-30.

Carvalho, C. P., Coimbra, J. S. R., Costa, I. A. F., Minim, L. A., Silva, L. H. M. & Maffia, M. C. 2007. Equilibrium data for PEG 4000+ salt+ water systems from (278.15 to 318.15) K. **Journal of Chemical & Engineering Data**, 52(2), 351-356.

Chaiklahan, R., Chirasuwan, N., Loha, V., Tia, S. & Bunnag, B. 2011. Separation and purification of phycocyanin from Spirulina sp using a membrane process. **Bioresource technology**, 102(2011), 7159-7164.

Charpy, L., Langlade, M. J. & Alliod, R. 2008. La Spiruline peut-elle être un atout pour la santé et le développement en Afrique. **Rapport d'expertise pour le Ministère de l'Agriculture et de la Pêche**.

Chen, C. Y., Kao, P. C., Tsai, C. J., Lee, D. J. & Chang, J. S. 2013. Engineering strategies for simultaneous enhancement of C-phycocyanin production and CO_2 fixation with Spirulina platensis. **Bioresour Technol**, 145(2013

), 307-312.

Chethana, S., Nayak, C. A., Madhusudhan, M. C. & Raghavarao, K. S. 2015. Single step aqueous two-phase extraction for downstream processing of C-phycocyanin from Spirulina platensis. **J Food Sci Technol**, 52(4), 2415-2421.

Chew, K. W., Chia, S. R., Krishnamoorthy, R., Tao, Y., Chu, D.-T. & Show, P. L. 2019. Liquid biphasic flotation for the purification of C-phycocyanin from Spirulina platensis microalga. **Bioresource technology**, 288(121519.

Ciferri, O. 1983. Spirulina, the edible microorganism. **Microbiological reviews**, 47(4), 551-578.

Cole, K. 1991. Preparation of plasmid and high molecular weight DNA by the use of salt-polymer two-phase extraction. **Biotechniques**, 11(-), 18-24.

Colla, L. M., Reinehr, C. O., Reichert, C. & Costa, J. A. V. 2007. Production of biomass and nutraceutical compounds by Spirulina platensis under different temperature and nitrogen regimes. **Bioresource technology**, 98(7), 1489-1493.

Costa, M., Botta, A. & Cardille, J. 2003. Effects of large-scale changes in land cover on the discharge of the Tocantins River, Southeastern Amazonia. **Journal of Hydrology**, 283(206-217.

Costesèque, P., Pollak, T., Platten, J. & Marcoux, M. 2004. Transient-state method for coupled evaluation of Soret and Fick coefficients, and related tortuosity factors, using free and porous packed thermodiffusion cells: application to CuSO4 aqueous solution (0.25 M). **The European Physical Journal E**, 15(3), 249-253.

Dominguez, H. 2013. **Functional ingredients from algae for foods and nutraceuticals**. Elsevier.

Dreyer, S. E. 2008. **Aqueous two-phase extraction of proteins and enzymes using tetraalkylammonium-based ionic liquids.** Doctor degree. Universität Rostock.

Duangsee, R., Phoopat, N. & Ningsanond, S. 2009. Phycocyanin extraction from Spirulina platensis and extract stability under various pH and temperature. **Asian Journal of Food and Agro-Industry**, 2(4), 819-826.

Edmond, E. & Ogston, A. 1968. An Approach to Study of Phase Separation in Ternary Aqueous Systems. **The Biochemical journal**, 109(569-576.

Ekberg, B., Sellergren, B. & Albertsson, P.-Å. 1985. Direct chiral resolution in an

aqueous two-phase system using the counter-current distribution principle. **Journal of Chromatography A**, 333(211-214.

FDA. 1981 (June 23). FDA Talk Paper. 41, 160.

Flory, P. J. 1942. Thermodynamics of high polymer solutions. **The Journal of chemical physics**, 10(1), 51-61.

Franco, T., Andrews, A. & Asenjo, J. 1996. Use of chemically modified proteins to study the effect of a single protein property on partitioning in aqueous two-phase systems: effect of surface hydrophobicity. **Biotechnology and bioengineering**, 49(3), 300-308.

Gantt, E. 1981. Phycobilisomes. **Annual Review of Plant Physiology**, 32(1), 327-347.

Gautam, S. & Simon, L. 2006. Partitioning of β-glucosidase from Trichoderma reesei in poly (ethylene glycol) and potassium phosphate aqueous two-phase systems: Influence of pH and temperature. **Biochemical Engineering Journal**, 30(1), 104-108.

Gershwin, M. E. & Belay, A. 2007. **Spirulina in human nutrition and health**. CRC press.

Glazer, A. N. 1994. Phycobiliproteins—a family of valuable, widely used fluorophores. **Journal of Applied Phycology**, 6(2), 105-112.

Gündüz, U. 2000. Partitioning of bovine serum albumin in an aqueous two-phase system: optimization of partition coefficient. **Journal of Chromatography B: Biomedical Sciences and Applications**, 743(1-2), 259-262.

Guo, T., Su, D., Huang, Y., Wang, Y. & Li, Y.-H. 2015. Ultrasound-assisted aqueous two-phase system for extraction and enrichment of Zanthoxylum armatum lignans. **Molecules**, 20(8), 15273-15286.

Hachem, F., Andrews, B. A. & Asenjo, J. A. 1996. Hydrophobic partitioning of proteins in aqueous two-phase systems. **Enzyme and Microbial Technology**, 19(7), 507-517.

Hadiyanto, H. & Suttrisnorhadi, S. 2016. Response surface optimization of ultrasound assisted extraction (UAE) of phycocyanin from microalgae Spirulina platensis. **Emirates Journal of Food and Agriculture**, 227-234.

Harris, J. M. (1992). Introduction to biotechnical and biomedical applications of poly (ethylene glycol). In **Poly (ethylene glycol) Chemistry** (pp. 1-14): Springer.

Harris, P., Karlström, G. & Tjerneld, F. 1991. Enzyme purification using temperature-induced phase formation. **Bioseparation**, 2(4), 237-246.

Hart, R. A., Lester, P. M., Reifsnyder, D. H., Ogez, J. R. & Builder, S. E. 1994. Large scale, in situ isolation of periplasmic IGF–I from E. coli. **Bio/technology**, 12(11), 1113-1117.

Hemlata, G. P., Bano, F. & Fatma, T. 2011. Studies on Anabaena sp. nccu-9 with special reference to phycocyanin. **J Algal Biomass Utln**, 2(1), 30-51.

Henrikson, R. 1989. Earth food spirulina. **Laguna Beach, CA: Ronore Enterprises, Inc**, 187.

Hill, T. L. 1986. **An introduction to statistical thermodynamics**. Courier Corporation.

Hofmeister, F. 1888. The doctrine of the action of the salts. **Arch Exp Pathol Pharmakol**, 24(-), 247-260.

Huddleston, J., Veide, A., Köhler, K., Flanagan, J., Enfors, S.-O. & Lyddiatt, A. 1991. The molecular basis of partitioning in aqueous two-phase systems. **Trends in Biotechnology**, 9(1), 381-388.

Huddleston, J. G., Willauer, H. D., Boaz, K. R. & Rogers, R. D. 1998. Separation and recovery of food coloring dyes using aqueous biphasic extraction chromatographic resins. **Journal of Chromatography B: Biomedical Sciences and Applications**, 711(1-2), 237-244.

Huggins, M. L. 1942. Some properties of solutions of long-chain compounds. **The Journal of Physical Chemistry**, 46(1), 151-158.

Hustedt, H. 1986. Extractive enzyme recovery with simple recycling of phase forming chemicals. **Biotechnology letters**, 8(11), 791-796.

Igarashi, L., Kieckbusch, T. G. & Franco, T. T. 2004. Mass transfer in aqueous two-phases system packed column. **J Chromatogr B Analyt Technol Biomed Life Sci**, 807(1), 75-80.

Jaturonglumlert, S., Promya, J. & Varith, J. 2017. Modeling of Spirulina Growth Rate with LED Illumination and Applications. **Engng.J.CMU.**, 24(1), 142-151.

Jerley, A. A. & Prabu, D. M. 2015. Purification, characterization and antioxidant

properties of C-Phycocyanin from *Spirulina platensis*. **Scrutiny International Research Journal of Agriculture, Plant Biotechnology and Bio Products**, 2(1), 7-15.

Jiang, J. & Prausnitz, J. M. 2000. Molecular thermodynamics for partitioning of native and denatured proteins in aqueous two-phase systems. **The Journal of Physical Chemistry B**, 104(30), 7197-7205.

Johansson, G. (1994). Recovery of proteins and phase-forming chemicals. In **Methods in enzymology** (Vol. 228, pp. 569-573): Elsevier.

Johansson, H.-O., Karlström, G., Tjerneld, F. & Haynes, C. A. 1998. Driving forces for phase separation and partitioning in aqueous two-phase systems. **Journal of Chromatography B: Biomedical Sciences and Applications**, 711(1), 3-17.

Johansson, H.-O., Lundh, G., Karlström, G. & Tjerneld, F. 1996. Effects of ions on partitioning of serum albumin and lysozyme in aqueous two-phase systems containing ethylene oxide/propylene oxide co-polymers. **Biochimica et Biophysica Acta (BBA)-General Subjects**, 1290(3), 289-298.

Jordan, P. & Vilter, H. 1991. Extraction of proteins from material rich in anionic mucilages: partition and fractionation of vanadate-dependent bromoperoxidases from the brown algae Laminaria digitata and L. saccharina in aqueous polymer two-phase systems. **Biochimica et Biophysica Acta (BBA)-General Subjects**, 1073(1), 98-106.

Khan, H. U. 2012. The role of Ion Exchange Chromatography in purification and characterization of molecules. **Ion Exchange Technologies**, 331-342.

Koncsag, C. & Barbulescu, A. (2011). Liquid-Liquid Extraction with and without a Chemical Reaction. In (pp. 207-232): In Tech.

Kuboi, R., Umakoshi, H. & Komasawa, I. 1995. Extractive cultivation of Escherichia coli using poly (ethylene glycol)/phosphate aqueous two-phase systems to produce intracellular. beta.-galactosidase. **Biotechnology progress**, 11(2), 202-207.

Kula, M.-R. 1990. Trends and future prospects of aqueous two-phase extraction. **Bioseparation**, 1(181-189.

Kula, M.-R., Kroner, K. H. & Hustedt, H. (1982). Purification of enzymes by liquid-liquid extraction. In **reaction engineering** (pp. 73-118): Springer.

Kula, M. R. & Selber, K. 2009. Protein purification, aqueous liquid extraction. **Encyclopedia of Industrial Biotechnology: Bioprocess, Bioseparation, and Cell Technology**, 1-22.

Kumar, D., Dhar, D. W., Pabbi, S., Kumar, N. & Walia, S. 2014. Extraction and purification of C-phycocyanin from Spirulina platensis (CCC540). **Indian Journal of Plant Physiology**, 19(2), 184-188.

Kwon, G. S. & Okano, T. 1996. Polymeric micelles as new drug carriers. **Advanced Drug Delivery Reviews**, 21(2), 107-116.

Lamarca, C., Lenhoff, A. M. & Dhurjati, P. 1990. Partitioning of host and recombinant cells in aqueous two-phase polymer systems. **Biotechnology and bioengineering**, 36(5), 484-492.

Lantz, P.-G., Tjerneld, F., Hahn-Hägerdal, B. & Rådström, P. 1996. Use of aqueous two-phase systems in sample preparation for polymerase chain reaction-based detection of microorganisms. **Journal of Chromatography B: Biomedical Sciences and Applications**, 680(1-2), 165-170.

Lee, B. & Richards, F. M. 1971. The interpretation of protein structures: estimation of static accessibility. **Journal of molecular biology**, 55(3), 379-IN374.

Leema, J. M., Kirubagaran, R., Vinithkumar, N., Dheenan, P. & Karthikayulu, S. 2010. High value pigment production from Arthrospira (Spirulina) platensis cultured in seawater. **Bioresource Technology**, 101(23), 9221-9227.

Li, G., Dong, G., Li, B., Li, Q., Kronzucker, H. J. & Shi, W. 2012. Isolation and characterization of a novel ammonium overly sensitive mutant, amos2, in Arabidopsis thaliana. **Planta**, 235(2), 239-252.

Liao, X., Zhang, B., Wang, X., Yan, H. & Zhang, X. 2011. Purification of C-Phycocyanin from Spirulina platensis by Single-Step Ion-Exchange Chromatography. **Chromatographia**, 73(291-296.

Luedeking, R. & Piret, E. L. 1959. A kinetic study of the lactic acid fermentation. Batch process at controlled pH. **Biotechnology and Bioengineering**, 1(4), 393-412.

Lundberg, S. & Backman, L. (1994). Protein-protein and protein-ligand interactions. In **Methods in enzymology** (Vol. 228, pp. 241-254): Academic Press.

Luo, X., Smith, P., Raston, C. L. & Zhang, W. 2016. Vortex Fluidic Device-Intensified Aqueous Two Phase Extraction of C-Phycocyanin fromSpirulina maxima. **ACS Sustainable Chemistry & Engineering**, 4(7), 3905-3911.

Manirafasha, E., Murwanashyaka, T., Ndikubwimana, T., Ahmed, N. R., Liu, J., Lu, Y., Zeng, X., Ling, X. & Jing, K. 2018. Enhancement of cell growth and phycocyanin production in Arthrospira (Spirulina) platensis by metabolic stress and nitrate fed-batch. **Bioresource technology**, 255(293-301.

Mansoori, G., Carnahan, N. F., Starling, K. & Leland Jr, T. 1971. Equilibrium thermodynamic properties of the mixture of hard spheres. **The Journal of Chemical Physics**, 54(4), 1523-1525.

Mattiasson, B. 1986. Ultrafiltration Affinity Purification. A Process for Large-Scale Biospecific Separations. **Membrane Separations in Biotechnology**.

Mazzola, P. G., Lopes, A. M., Hasmann, F. A., Jozala, A. F., Penna, T. C., Magalhaes, P. O., Rangel-Yagui, C. O. & Pessoa Jr, A. 2008. Liquid–liquid extraction of biomolecules: an overview and update of the main techniques. **Journal of Chemical Technology & Biotechnology**, 83(2), 143-157.

McMillan, W. G. & Mayer, J. E. 1945. The Statistical Thermodynamics of Multicomponent Systems. **The Journal of Chemical Physics**, 13(7), 276-305.

Middaugh, C. R. & Lawson, E. Q. 1980. Analysis of protein association by partitioning in aqueous two-phase polymer systems: Applications to the tetramer-dimer dissociation of hemoglobin. **Analytical Biochemistry**, 105(1), 364-368.

Minuth, T., Gieren, H., Pape, U., Raths, H., Thömmes, J. & Kula, M. 1997. Pilot scale processing of detergent-based aqueous two-phase systems. **Biotechnology and bioengineering**, 55(2), 339-347.

Minuth, T., Thömmes, J. & Kula, M.-R. 1996. A closed concept for purification of the membrane-bound cholesterol oxidase from Nocardia rhodochrous by surfactant-based cloud-point extraction, organic-solvent extraction and anion-exchange chromatography. **Biotechnology and applied biochemistry**, 23(2), 107-116.

Monod, J. 1949. The growth of bacterial cultures. **Annual Reviews in Microbiology**,

3(1), 371-394.

Moorhead, K., Capelli, B. & Cysewski, G. R. 2011. **SPIRULINA : Nature's Superfood**.

Moraes, C. C. & Kalil, S. J. 2009. Strategy for a protein purification design using C-phycocyanin extract. **Bioresource technology**, 100(21), 5312-5317.

Moraine, R. & Rogovin, P. 1971. Xanthan biopolymer production at increase concentration by pH control. **Biotechnology and Bioengineering**, 13(3), 381-391.

Nagar, S., Sharma, N. & Kumar, S. 2018. C-phycocyanin extraction and purification from spirulina platensis. **Research Inventy: International Journal of Engineering Science**, 8(2), 60-63.

Nascimento, C. E., Gioielli, L. A., Converti, A., Oliveira Moraes, I., Sato, S. & Carvalho, J. C. M. 2014. Urea increases fed-batch growth and γ-linolenic acid production of nutritionally valuable Arthrospira (Spirulina) platensis cyanobacterium. **Engineering in Life Sciences**, 14(5), 530-537.

Nerli, B. B., Espariz, M. & Picó, G. A. 2001. Thermodynamic study of forces involved in bovine serum albumin and ovalbumin partitioning in aqueous two-phase systems. **Biotechnology and Bioengineering**, 72(4), 468-474.

Niu, J.-F., Wang, G.-C., Lin, X.-z. & Cheng, Z. 2007. Large-scale recovery of C-phycocyanin from Spirulina platensis using expanded bed adsorption chromatography. **Journal of chromatography. B, Analytical technologies in the biomedical and life sciences**, 850(267-276.

Oliveira, J. T. A., Silveira, S. B., Vasconcelos, I. M., Cavada, B. S. & Moreira, R. A. 1999. Compositional and nutritional attributes of seeds from the multiple purpose tree Moringa oleifera Lamarck. **Journal of the Science of Food and Agriculture**, 79(6), 815-820.

Ornstein, L. S. 1914. Accidental deviations of density and opalescence at the critical point of a single substance. **Proc. Akad. Sci.**, 17(793.

Pahlich, E., Kerres, R. & Jäger, H.-J. 1983. Influence of Water Stress on the Vacuole/Extravacuole Distribution of Proline in Protoplasts of <em>Nicotiana rustica</em&gt. **Plant Physiology**, 72(2), 590.

Pan-utai, W., Kahapana, W. & Iamtham, S. 2018. Extraction of C-phycocyanin from Arthrospira (Spirulina) and its thermal stability with citric acid. **Journal of Applied Phycology**, 30(1), 231-242.

Pandey, G., Zhang, B., Chang, A. N., Myers, C. L., Zhu, J., Kumar, V. & Schadt, E. E. 2010. An Integrative Multi-Network and Multi-Classifier Approach to Predict Genetic Interactions. **PLOS Computational Biology**, 6(9), e1000928.

Partanen, J. I., Mori, Y., Louhi-Kultanen, M. & Kallas, J. J. 2003. Activity coefficients of potassium dihydrogen phosphate in aqueous solutions at 25° C and in aqueous mixtures of urea and this electrolyte in the temperature range 20–35° C. **Zeitschrift für Physikalische Chemie**, 217(6), 723-738.

Patil, G., Chethana, S., Madhusudhan, M. & Raghavarao, K. 2008. Fractionation and purification of the phycobiliproteins from Spirulina platensis. **Bioresource technology**, 99(15), 7393-7396.

Patil, G. & Raghavarao, K. 2007. Aqueous two phase extraction for purification of C-phycocyanin. **Biochemical Engineering Journal**, 34(2), 156-164.

Platten, J. K. 2006. The Soret effect: a review of recent experimental results.

Raghavarao, K., Rastogi, N., Gowthaman, M. & Karanth, N. (1995). Aqueous two-phase extraction for downstream processing of enzymes/proteins. In **Advances in applied microbiology** (Vol. 41, pp. 97-171): Elsevier.

Ramelmeier, R., Terstappen, G. & Kula, M. 1991. The partitioning of cholesterol oxidase in Triton X-114-based aqueous two-phase systems. **Bioseparation**, 2(5), 315-324.

Rito-Palomares, M. 2004. Practical application of aqueous two-phase partition to process development for the recovery of biological products. **Journal of Chromatography B**, 807(1), 3-11.

Rito-Palomares, M., Negrete, A., Galindo, E. & Serrano-Carreon, L. 2000. Aroma compounds recovery from mycelial cultures in aqueous two-phase processes. **Journal of Chromatography B: Biomedical Sciences and Applications**, 743(1-2), 403-408.

Rito-Palomares, M. & Middelberg, A. P. J. 2002. Aqueous two-phase systems for the

recovery of a recombinant viral coat protein from Escherichia coli. **Journal of Chemical Technology & Biotechnology: International Research in Process, Environmental & Clean Technology**, 77(9), 1025-1029.

Rito-Palomares, M., Nunez, L. & Amador, D. 2001. Practical application of aqueous two-phase systems for the development of a prototype process for c-phycocyanin recovery from Spirulina maxima. **Journal of chemical technology and biotechnology**, 76(12), 1273-1280.

Rogers, R. D., Bond, A. H., Bauer, C. B., Zhang, J. & Griffin, S. T. 1996. Metal ion separations in polyethylene glycol-based aqueous biphasic systems: correlation of partitioning behavior with available thermodynamic hydration data. **Journal of Chromatography B: Biomedical Sciences and Applications**, 680(1-2), 221-229.

Rogers, R. D., Willauer, H. D., Griffin, S. T. & Huddleston, J. G. 1998. Partitioning of small organic molecules in aqueous biphasic systems. **Journal of Chromatography B: Biomedical Sciences and Applications**, 711(1-2), 255-263.

Roobol-Bóza, M., Dolby, V., Doverskog, M., Barrefelt, Å., Lindqvist, F., Oppermann, U. C., Van Alstine, K. K. & Tjerneld, F. 2004. Membrane protein isolation by in situ solubilization, partitioning and affinity adsorption in aqueous two-phase systems: Purification of the human type 1 11β-hydroxysteroid dehydrogenase. **Journal of Chromatography A**, 1043(2), 217-223.

Ruangyot, T., Jaturonglumlert, S., Nitatwichit, C. & Varith, J. 2016. Factors affecting phycocyanin extraction from Spirulina platensis by using freezing and thawing combined with ultrasonic method. **Journal of fisheries technoligy research**, 10(4), 78-87.

Sanchez-Ferrer, A., Bru, R. & Garcia-Carmona, F. 1989. Novel procedure for extraction of a latent grape polyphenoloxidase using temperature-induced phase separation in Triton X-114. **Plant Physiology**, 91(4), 1481-1487.

Sarada, R., Pillai, M. G. & Ravishankar, G. 1999. Phycocyanin from Spirulina sp: influence of processing of biomass on phycocyanin yield, analysis of efficacy of extraction methods and stability studies on phycocyanin. **Process**

biochemistry, 34(8), 795-801.

Sasakawa, S. & Walter, H. 1972. Partition behavior of native proteins in aqueous dextran-poly (ethylene glycol)-phase systems. **Biochemistry**, 11(15), 2760-2765.

Sassano, C., Gioielli, L., Almeida, K., Sato, S., Perego, P., Converti, A. & Carvalho, J. 2007. Cultivation of Spirulina platensis by continuous process using ammonium chloride as nitrogen source. **Biomass and Bioenergy**, 31(8), 593-598.

Schimpf, M. E. & Semenov, S. N. 2000. Mechanism of polymer thermophoresis in nonaqueous solvents. **The Journal of Physical Chemistry B**, 104(42), 9935-9942.

Scopes, R. (1994). **Protein Purification, Principles and Practice**: New York: Springer-Verlag.

Scott, R. L. 1949. The thermodynamics of high polymer solutions. V. Phase equilibria in the ternary system: polymer 1—polymer 2—solvent. **The Journal of chemical physics**, 17(3), 279-284.

Sé, R. & Aznar, M. 2002. Thermodynamic modelling of phase equilibrium for water+ poly (ethylene glycol)+ salt aqueous two-phase systems. **Brazilian Journal of Chemical Engineering**, 19(2), 255-266.

Shalaby, M. A., Zorba, H. Y. & Ziada, R. 2010. Reproductive toxicity of methomyl insecticide in male rats and protective effect of folic acid. **Food and chemical toxicology** 48(-), 3221-3226.

Shanbhag, V. P. & Axelsson, C. G. 1975. Hydrophobic Interaction Determined by Partition in Aqueous Two-Phase Systems: Partition of Proteins in Systems Containing Fatty-Acid Esters of Poly (ethylene glycol). **European journal of biochemistry**, 60(1), 17-22.

Sikdar, S. K., Cole, K. D., Stewart, R. M., Szlag, D. C., Todd, P. & Cabezas, H. 1991. Aqueous two-phase extraction in bioseparations: an assessment. **Bio/Technology**, 9(3), 252-256.

Silveira, S. T., Burkert, J. d. M., Costa, J. A. V., Burkert, C. A. V. & Kalil, S. J. 2007. Optimization of phycocyanin extraction from Spirulina platensis using factorial design. **Bioresource technology**, 98(8), 1629-1634.

Silveira, S. T., de Menezes Quines, L. K., Burkert, C. A. V. & Kalil, S. J. 2008. Separation of phycocyanin from Spirulina platensis using ion exchange chromatography. **Bioprocess and biosystems engineering**, 31(5), 477-482.

Soley biotechnology Institute. 2000. **C-Phycocyanin**. [Online]. Available http://www.soleybio.com/products/c-phycocyanin.html (20 March 2017).

Sonani, R. R., Rastogi, R. P., Patel, R. & Madamwar, D. 2016. Recent advances in production, purification and applications of phycobiliproteins. **World J Biol Chem**, 7(1), 100-109.

Strandberg, L., Köhler, K. & Enfors, S.-O. 1991. Large-scale fermentation and purification of a recombinant protein from Escherichia coli. **Process biochemistry**, 26(4), 225-234.

Su, C.-H., Liu, C.-S., Yang, P.-C., Syu, K.-S. & Chiuh, C.-C. 2014. Solid–liquid extraction of phycocyanin from Spirulina platensis: Kinetic modeling of influential factors. **Separation and Purification Technology**, 123(64–68.

Taboada, M. E., Graber, T. A., Asenjo, J. & Andrews, B. 2000. Drowning-out crystallisation of sodium sulphate using aqueous two-phase systems. **Journal of Chromatography B: Biomedical Sciences and Applications**, 743(1-2), 101-105.

Tavanandi, H. A., Mittal, R., Chandrasekhar, J. & Raghavarao, K. 2018. Simple and efficient method for extraction of C-Phycocyanin from dry biomass of Arthospira platensis. **Algal research**, 31(239-251.

Thaisamak, P., Jaturonglumlert, S., Varith, J., Saleena Taip, F. & Nitatwichit, C. 2019. Kinetic model of ultrasonic-assisted extraction with controlled temperature of c-phycocyanin from S. Platensis. **International Journal of GEOMATE**, 16(

Tietze, H. W. 2004. Spirulina micro food macro blessing. **Harald W, 4th edn. Tietz Publishing, Australia**.

Veide, A., Lindbäck, T. & Enfors, S.-O. 1989. Recovery of β-galactosidase from a poly (ethylene glycol) solution by diafiltration. **Enzyme and microbial technology**, 11(11), 744-751.

Veiga, N. 2016. **Recycling of the culture medium for pilot scale production of**

Arthrospira platensis (Spirulina). Thesis to obtain the Master of science degree in biological engineering/NFM ....

Vincent, W. F. & Silvester, W. B. 1979. Growth of blue-green algae in the Manukau (New Zealand) oxidation pond“ II. Experimental studies on algal interaction. **Water Research**, 13(8), 717-723.

Volkmann, H., Imianovsky, U., Oliveira, J. L. & Sant'Anna, E. S. 2008. Cultivation of Arthrospira (Spirulina) platensis in desalinator wastewater and salinated synthetic medium: protein content and amino-acid profile. **Brazilian Journal of Microbiology**, 39(1), 98-101.

Vonshak, A., Torzillo, G. & Tomaseli, L. 1994. Use of chlorophyll fluorescence to estimate the effect of photoinhibition in outdoor cultures ofSpirulina platensis. **Journal of applied phycology**, 6(1), 31-34.

Walker, S. G. & Lyddiatt, A. 1998. Aqueous two-phase systems as an alternative process route for the fractionation of small inclusion bodies. **Journal of Chromatography B: Biomedical Sciences and Applications**, 711(1-2), 185-194.

Walter, H. & Johansson, G. 1994. **Aqueous two-phase systems**. Elsevier.

Weinstein, O., Semiat, R. & Lewin, D. 1998. Modeling, simulation and control of liquid-liquid extraction columns. **Chemical Engineering Science**, 53(2), 325-339.

Xie, Y., Jin, Y., Zeng, X., Chen, J., Lu, Y. & Jing, K. 2015. Fed-batch strategy for enhancing cell growth and C-phycocyanin production of Arthrospira (Spirulina) platensis under phototrophic cultivation. **Bioresour Technol**, 180(281-287.

Yang, Z., Guo, R., Xu, X., Fan, X. & Luo, S. 2011. Hydrogen and methane production from lipid-extracted microalgal biomass residues. **International Journal of Hydrogen Energy**, 36(5), 3465-3470.

Zeng, A. P., Ross, A., Biebl, H., Tag, C., Günzel, B. & Deckwer, W. D. 1994. Multiple product inhibition and growth modeling of Clostridium butyricum and Klebsiella pneumoniae in glycerol fermentation. **Biotechnology and Bioengineering**, 44(8), 902-911.

Zhang, X., Zhang, F., Luo, G., Yang, S. & Wang, D. 2015. Extraction and separation of phycocyanin from Spirulina using aqueous two-phase systems of ionic liquid and salt. **Journal of Food and Nutrition Research**, 3(1), 15-19.

Zhang, Y. & Cremer, P. S. 2006. Interactions between macromolecules and ions: the Hofmeister series. **Current opinion in chemical biology**, 10(6), 658-663.

Zhao, H. 2006. Are ionic liquids kosmotropic or chaotropic? An evaluation of available thermodynamic parameters for quantifying the ion kosmotropicity of ionic liquids. **Journal of Chemical Technology & Biotechnology**, 81(877-891.

Zhao, L., Peng, Y.-l., Gao, J.-m. & Cai, W.-m. 2014. Bioprocess intensification: an aqueous two-phase process for the purification of C-phycocyanin from dry Spirulina platensis. **European Food Research and Technology**, 238(3), 451-457.

Zijlstra, G., De Gooijer, C., Van der Pol, L. & Tramper, J. 1996. Design of aqueous two-phase systems supporting animal cell growth: A first step toward extractive bioconversions. **Enzyme and microbial technology**, 19(1), 2-8.

APPENDIX

APPENDIX A

MATLAB script

A.1 Simulation of Phase Equilibrium Behavior

```
%The ATPETGA for CPC purification
%Water-PEG4000-Potassium phosphate System
%Simulation of Phase Equilibrium Behavior
function [phi_2,phi_3,phi_top_store,phi_bot_store,du_store,N]=...
    Phase_diagram_S(MW,X,v,r,w,A,b,Mwater,zA,zB,c,phi1);
%%%%%%%%%%%%%%%%%%%%%%%%%%%%%%%%%%%%%%%%%%%%%%%%%%%%%%%%%%%%%%%%%%%%%%
%%%%%%%%%%%%%
% this is an m-file that calculates the phase equilibrium in a
specified
% ATPE consisting of Water-PEG4000-Potassium phosphate System
% the volume fraction (phi) of each component in both top and bottom
phase
% is calculated by minimizing the difference in the chemical
potential
% of each component in each phase
%%%%%%%%%%%%%%%%%%%%%%%%%%%%%%%%%%%%%%%%%%%%%%%%%%%%%%%%%%%%%%%%%%%%%%
% solver options: specifying the tolerances and maximum function
evals

fopts=optimset('TolFun',1e-10,...
    'TolX',1e-10,...
    'MaxFunEvals',1e4,...
    'Display','on');
L=eps*100;
s1=cputime;

% starting the loop that varies phi2 and phi3 for top phase
N=0;
% setting for top phase
phi=0.005:0.005:(1-phi1);
for i=1:length(phi)
    disp(sprintf('i=%3d/%3d',i,length(phi)));
    % for each fixed value of phi2
    phi2=phi(i);
    for j=1:length(phi)
        % phi3 is varied
        phi4=phi(j);
        if (phi1+phi2+phi4==1.0)
            N=N+1;
            % assigning the vector of volume fraction for top phase
            phi_top=[phi1 phi2 phi4];

            % calculating the ionic strength in the top phase
            I_top=CalcI(phi_top(3),Mwater,W,zA,zB);

            % calculating the interaction parameter between water and
            % salt in
            % the top phase
            [g14_top,dg14d4_top]=Calcgd(c,phi_top(3));

            % calculating the chemical potential for the top phase
            u_top=CalcU_S(phi_top,I_top,g14_top,dg14d4_top,X,r,...
                Mwater,A,b,W,zA,zB);

            % storing variables obtained for top phase
```

```
            phi_top_store(N,:)=phi_top;
            u_top_store(N,:)=u_top;
            %%%%%%%%%%%%%%%%%%%%%%%%%%%%%%%%%%%%%%%%%%%%%%%%%%%%
            %the optimization routine
            %
            s_init=[phi_top(1)*1/2 phi_top(2)*1/2];
            % optimizing to obtain phi bot that gives (u_top -
            % u_bot)=0

[s_bot,fval,exitflag,output]=fminsearch('dU_S',s_init,fopts,u_top,phi
_top,X,r,Mwater,W,zA,zB,c,A,b);
            if(exitflag<0|exitflag==0)
                disp('unsolved');
            else
                % assigning the vector of volume fraction for top
                %phase
                phi_bot=[s_bot(1) s_bot(2) 1-s_bot(1)-s_bot(2)];
                % calculating the vector of chemical potential for
                % bottom phase
                I_bot=CalcI(phi_bot(3),Mwater,W,zA,zB);
                % calculating the interaction parameter between water
                % and salt in
                % the bottom phase
                [g14_bot,dg14d4_bot]=Calcgd(c,phi_bot(3));

% calculating the chemical potential for the bottom phase
u_bot=CalcU_S(phi_bot,I_bot,g14_bot,dg14d4_bot,X,r,Mwater,A,...
      b,W,zA,zB);

% calculating the difference in the chemical potential of the  phases
du=u_top-u_bot;

% storing variables obtained for bottom phase
i_store(N,:)=i;
phi_bot_store(N,:)=phi_bot;

u_bot_store(N,:)=CalcU_S(phi_bot,I_bot,g14_bot,dg14d4_bot,...
                 X,r,Mwater,A,b,W,zA,zB);
du_store(N,:)=du;

% displaying the results
disp...
 (sprintf('phi_top=[%5.4f %5.4f %5.4f], phi_bot=[%5.4f %5.4f…
%5.4f],du=[%5.4f %5.4f %5.4f],lag=%d',phi_top,phi_bot,du,exitflag));
% displaying output and exitflag
%output
%exit flag
            end
        end
    end
end
```

```
% analyzing the results
%%%%%%%%%%%%%%%%%%%%%%%%%%%%%%%%%%%%%%%%%%%%%%%%%%%%%%%%%%%%%%%%%%%
% STEP 1,
% analyzing the difference between phi_bot and phi top (dU)
% to rid of the trivial solution
% square of the difference between phi bot and phi_top
diff=(phi_bot_store-phi_top_store).^2;
% finding the index of data where dU for component 2
% that is less than le-7
index=find(diff(:,2)<=1e-7);
%loop to eliminate the rows with dU less than le-7
for i=1:length(index)
    % deleting the row of the trivial solution of phl bot
    phi_bot_store(index(i):N-1,:)=phi_bot_store(index(i)+1:N,:);
    phi_bot_store(N,:)=[];

    % deleting the row of the trivial solution of phi top
    phi_top_store(index(i):N-1,:)=phi_top_store(index(i)+1:N,:);
    phi_top_store(N,:)=[];

    % renaming the index
    N=N-1;
    index=index-1;
end

%%%%%%%%%%%%%%%%%%%%%%%%%%%%%%%%%%%%%%%%%%%%%%%%%%%%%%%%%%%%%%%%%%%%%
%STEP 2:
% analyzing the difference between phi_bot and phi_top (dU)
% to rid of the trivial solution
% square of the difference between phi_bot and phi top
diff=(phi_bot_store-phi_top_store).^2;
% finding the index of data where dU for component 3
% that is less than le-7
index=find(diff(:,3)<=1e-7);

% loop to eliminate the rows with dU less than le-7
for i=1:length(index)
    % deleting the row of the trivial solution of phi_bot
    phi_bot_store(index(i):N-1,:)=phi_bot_store(index(i)+1:N,:);
    phi_bot_store(N,:)=[];

    % deleting the row of the trivial solution of phi top
    phi_top_store(index(i):N-1,:)=phi_top_store(index(i)+1:N,:);
    phi_top_store(N,:)=[];

    % renaming the index
    N=N-1;
    index=index-1;
end
```

```
%%%%%%%%%%%%%%%%%%%%%%%%%%%%%%%%%%%%%%%%%%%%%%%%%%%%%%%%%%
% STEP 3:
% analyzing data phi_bot(2) to rid of the trivial solution
% finding the index of data where composition of component 2
% decreases
index=find(phi_bot_store(:,2)==max(phi_bot_store(:,2)))

% deleting trivial solutions
phi_bot_store(index+1:N,:)=[]
phi_top_store(index+1:N,:)=[]
du_store(index+1:N,:)=[]

N=length(phi_bot_store)

%%%%%%%%%%%%%%%%%%%%%%%%%%%%%%%%%%%%%%%%%%%%%%%%%%%%%%%%%%%%%%%%%%%
% plotting the binodal curves and the tie-lines
% to check on linearity of tie-lines
% rearranging data in terms of volume fraction for plotting
phi_2=[phi_bot_store(:,2) phi_top_store(:,2)];
phi_3=[phi_bot_store(:,3) phi_top_store(:,3)];

% plotting phi_2 vs phi_3
figure;
hold on;
for i=1:length(phi_top_store)
    plot(phi_3(i,:),phi_2(i,:));
end
title('phi2 vs phi3');
xlabel('phi3');
ylabel('phi2');
hold off;

%%%%%%%%%%%%%%%%%%%%%%%%%%%%%%%%%%%%%%%%%%%%%%%%%%%%%%%%%%%%%%%%%%%%5
% calculating operation time
s2=oputime;
disp(sprintf('cputime=%.4f',s2-s1))
```

Calculation of chemical potentials

```
function U=CalcU_S(phi,I,g14,dg14d4,X,r,Mwater,A,b,W,zA,zB);
%%%%%%%%%%%%%%%%%%%%%%%%%%%%%%%%%%%%%%%%%%%%%%%%%%%%%%%%%%%
% inputs for the function
% phi segment fraction of each component
% I : ionic strength of the solution
% g13 : FH binary interaction parameter (empirical function of
phi(3))
% dg13d4 ' differentiation of g12 with respect to phi(3)
% X Flory interaction parameter
% r : number of segments per polymer
% 1 water
% 2 PEG4000
% 3 salt
% calculating delta chemical potential for component 1 for bottom
phase
```

```
U(1)=(((2*A*(I.^(3/2)))./(1+b.*(I.^(1/2))).*(Mwater./100)))+log(phi(1
))+...
     (phi(2)*(1-r(1)/r(2)))+(phi(3)*(1-
r(1)/r(3)))+r(1)*((g14.*phi(3).*...
     (1-phi(1)))-(dg14d4.*phi(1).*phi(2).*phi(3))+(X(1,2).*phi(2).*(1-
phi(1)))-...
     (X(2,4).*phi(2).*phi(3)));

% calculating delta chemical potential for component 2 for bottom
phase
U(2)=(-A*zA*zB*((I.^(1/2)./(1+b.*(I.^(1/2)))+...
     (2/b).*log(1+b.*I^(1/2)))))+...
     log(phi(2))+...
     (phi(1)*(1-r(2)/r(1)))+...
     (phi(3)*(1-r(2)/r(3)))+...
     r(2)*((-g14.*phi(1).*phi(3))+...
     (dg14d4.*phi(1).*phi(3).*(1-phi(2)))+...
     (X(1,2).*phi(1).*(1-phi(2)))+...
     (X(2,4).*phi(3).*(1-phi(2))));
U(3)=(-
A*zA*zB*((I.^(1/2)./(1+b.*(I.^(1/2)))+(2/b).*log(1+b.*I^(1/2)))))+...
     log(phi(3))+...
     (phi(1)*(1-r(3)/r(1)))+...
     (phi(2)*(1-r(3)/r(2)))+...
     r(4)*((g14.*phi(1).*(1-phi(3)))-...
     (dg14d4.*phi(1).*phi(2).*phi(3))+...
     (X(1,2)*phi(1)*phi(2))+...
     (X(2,3)*phi(2)*(1-phi(3))));
```

Calculation of Interaction Parameter and its Derivative Form

```
function [g13,dg13d3]=Calcgd(c,phi3);
%%%%%%%%%%%%%%%%%%%%%%%%%%%%%%%%%%%%%%%%%%%%%%%%%%%%%%%%%%%%%%%%%%%%
% this function calculates g13 and dg13d3 using an empirical
% function of mixture composition phi3 (salt)

%%%%%%%%%%%%%%%%%%%%%%%%%%%%%%%%%%%%%%%%%%%%%%%%%%%%%%%%%%%
g13=zeros(size(phi3));
dg13d3=zeros(size(phi3));
for i=1:length(phi3)
    for j=1:length(c)
        g13(i)=g13(i)+(c(j)*phi3(i).^(j-1))
        dg13d3(i)=dg14d4(i)+((j-1)*c(j)*phi3(i).^(j-2))
    end
end
```

Calculation of Ionic Strength

```
function I=CalcI(phi_top3,Mwater,W,zA,zB);
%%%%%%%%%%%%%%%%%%%%%%%%%%%%%%%%%%%%%%%%%%%%%%%%%%%%%%%%%%%
% this function calculates the ionic strength of an aqueous system
%%%%%%%%%%%%%%%%%%%%%%%%%%%%%%%%%%%%%%%%%%%%%%%%%%%%%%%%%%%
% calculating ionic strength of a solution
I=(1/2)*(phi4.*(Mwater/W)).*zA.*zB./(1-phi4)
```

Objective Function

```
function F=dU_S(s,u_top,phi_top,X,r,Mwater,W,zA,zB,c,A,b);
%%%%%%%%%%%%%%%%%%%%%%%%%%%%%%%%%%%%%%%%%%%%%%%%%%%%%%%%%%%%%%%%
% this is a function that is being minimized
% we are giving the objective function, F a huge value when certain
% conditions are violated
%%%%%%%%%%%%%%%%%%%%%%%%%%%%%%%%%%%%%%%%%%%%%%%%%%%%%%%%%%%%%%%%
% Input arguments
 s(1) = phi_bot(1);
 s(2) = phi_bot(2);
 s = [s(1) s(2)];

% calculating the volume fraction for the third component from the
mass balance
phi5_bot=1-s(1)-s(2);
% assigning the vector of volume fraction for bottom phase
phi_bot=[s(1) s(2) phi5_bot];

if(min(phi_bot)<-eps|max(phi_bot)>1.0000| ~isreal(phi_bot))
    F=1e10*sum(phi_bot.^2);
else

    % condition that returns huge value when phi top lS equal to phi
bot
    if(sum(((1./r(1:3)).*abs(phi_top-
phi_bot)).^2,2)<=length(phi_bot)*1e-8)
        F=1e10*sum(phi_bot.^2);
    else

        %condition that returns huge value when phi_top(2) <
phi_bot(2) and
        %phi_bot(3) <phi_top(3)
        if((phi_top(2)-phi_bot(2)).^2<=eps&...
                (phi_bot(3)-phi_top(3)).^2<=eps)
            F=1e10*sum(phi_bot.^2);
        else

            % calculating the ionic strength in the bottom phase
            I_bot=CalcI(phi_bot(3),Mwater,W,zA,zB);
            % calculating the interaction parameter between water and
salt in
            % the bottom phase
            [g13_bot,dg13d4_bot]=Calcgd(c,phi_bot(3));

% calculating the chemical potential for the bottom phase
u_bot=...
CalcU_S(phi_bot,I_bot,g13_bot,dg13d3_bot,X,r,Mwater,A,b,W,zA,zB);

% the objective function that we are minimizing
F=sum((((1./r(1:3)).*(abs(u_top-u_bot)./abs(phi_top-...
  phi_bot))).^2),2);
        end
    end
end
```

A.2 Simulation of CPC partitioning behavior

```
function varargout = Doctor_of_Food_Engineering(varargin)
% Doctor_of_Food_Engineering MATLAB code for
Doctor_of_Food_Engineering.fig
gui_Singleton = 1;
gui_State = struct('gui_Name',       mfilename, ...
                   'gui_Singleton',  gui_Singleton, ...
                   'gui_OpeningFcn',
@Doctor_of_Food_Engineering_OpeningFcn, ...
                   'gui_OutputFcn',
@Doctor_of_Food_Engineering_OutputFcn, ...
                   'gui_LayoutFcn',  [] , ...
                   'gui_Callback',   []);
if nargin && ischar(varargin{1})
    gui_State.gui_Callback = str2func(varargin{1});
end

if nargout
    [varargout{1:nargout}] = gui_mainfcn(gui_State, varargin{:});
else
    gui_mainfcn(gui_State, varargin{:});
end

function Doctor_of_Food_Engineering_OpeningFcn(hObject, eventdata,
handles, varargin)
handles.output = hObject;
im=imread('Logofoodeng.png');
imshow(im);
axes(handles.axes4);
im1=imread('prototype.png');
imshow(im1);
axes(handles.axes2);
im2=imread('Logomju.png');
imshow(im2);
axes(handles.axes12);

guidata(hObject, handles);
%%%%%%%%%%%%%%%%%%%%%%%%%%%%%%%%%%%%%%%%%%%%%%%%%%%%%%%%%%%%%%%%%%%%%%
function K=Partition_S(phi_top,phi_bot,X,r,A,b,MW,W,zA,zB);
%Matlab function
function pushbutton1_Callback(hObject, eventdata, handles)
TG=str2num(get(handles.edit1,'String'));
Vi=str2num(get(handles.edit7,'String'));
t=0:5:120;
phib1=0.769-((2.16*10^(-3))*t)-((4.72*10^(-4))*TG);
phit1=0.797-((2.17*10^(-3))*t)+((8.98*10^(-3))*TG);
phit2=0.155+((3.01*10^(-3))*t)+((2.10*10^(-3))*TG);
phib2=0.083-((7.82*10^(-4))*t)+((1.09*10^(-4))*TG);
phit3=0.333-((9.57*10^(-5))*t)+((6.64*10^(-4))*TG);
phib3=0.148-((1.19*10^(-3))*t)-((3.05*10^(-4))*TG);
phi_top=[phit1 phit2 phit3];
phi_bot=[phib1 phib2 phib3];

%this function calculates the partition coefficient of
%target protein (component 4) in ATPE
%calculating the ionic strength in top and bottom phases
```

```
I_top=CalcI(phit3,MW(1),W,zA,zB);
I_bot=CalcI(phib3,MW(1),W,zA,zB);
% terms of the ionic strength effects
% f1 = term 1
% f2 = term 2
f1_top=sqrt(I_top) ./(1 + b .* sqrt(I_top) ) ;
f1_bot=sqrt(I_bot) ./(1 + b .* sqrt (I_bot) ) ;
f2_top=(2/b)* log(1+b*sqrt(I_top));
f2_bot=(2/b)* log(1+b*sqrt(I_bot));
% partition coefficient
format short
K=(exp((r(4)./MW(4)).*((-A*zA*zB*((f1_top-f1_bot)+...
    (f2_top-f2_bot)))+...
    (((phit2-phib2).*...
    ((1./r(2))-1+X(1,4)-X(2,4))))+...
    (((phit3-phib3).*...
    ((1./r(3))-1+X(1,4)-X(3,4)))))))+((-0.004*TG.^3)+(0.1868*TG.^2)-
(1.811*TG)-3.25);
set(handles.text12,'String',(K(25)))

format short
PE=(0.0337*K)+1.6858;
set(handles.text13,'String',PE(25))

Y=0.2*Vi;
set(handles.text15,'String',Y)
Nc=ceil(Vi/50);
set(handles.text23,'String',Nc)

function edit7_Callback(hObject, eventdata, handles)

function edit7_CreateFcn(hObject, eventdata, handles)

if ispc && isequal(get(hObject,'BackgroundColor'),
get(0,'defaultUicontrolBackgroundColor'))
    set(hObject,'BackgroundColor','white');
end

function uibuttongroup1_SelectionChangedFcn(hObject, eventdata,
handles)
function uibuttongroup1_SizeChangedFcn(hObject, eventdata, handles)
function edit1_Callback(hObject, eventdata, handles)
function edit1_CreateFcn(hObject, eventdata, handles)
if ispc && isequal(get(hObject,'BackgroundColor'),
get(0,'defaultUicontrolBackgroundColor'))
    set(hObject,'BackgroundColor','white');
end
function edit2_Callback(hObject, eventdata, handles)
function edit2_CreateFcn(hObject, eventdata, handles)
if ispc && isequal(get(hObject,'BackgroundColor'),
get(0,'defaultUicontrolBackgroundColor'))
    set(hObject,'BackgroundColor','white');
end
function edit3_Callback(hObject, eventdata, handles)
function edit3_CreateFcn(hObject, eventdata, handles)
if ispc && isequal(get(hObject,'BackgroundColor'),
get(0,'defaultUicontrolBackgroundColor'))
```

```
    set(hObject,'BackgroundColor','white');
end
function edit4_Callback(hObject, eventdata, handles)
function edit4_CreateFcn(hObject, eventdata, handles)
if ispc && isequal(get(hObject,'BackgroundColor'),
get(0,'defaultUicontrolBackgroundColor'))
    set(hObject,'BackgroundColor','white');
end
function edit5_Callback(hObject, eventdata, handles)
function edit5_CreateFcn(hObject, eventdata, handles)

if ispc && isequal(get(hObject,'BackgroundColor'),
get(0,'defaultUicontrolBackgroundColor'))
    set(hObject,'BackgroundColor','white');
end
function edit6_Callback(hObject, eventdata, handles)

function edit6_CreateFcn(hObject, eventdata, handles)
if ispc && isequal(get(hObject,'BackgroundColor'),
get(0,'defaultUicontrolBackgroundColor'))
    set(hObject,'BackgroundColor','white');
end
function varargout = Doctor_of_Food_Engineering_OutputFcn(hObject,
eventdata, handles)
varargout{1} = handles.output;
```

A.3 Fitting of bimodal curve

```
%Binodal fiting curve
clear
Wp=[0.04746 0.02364 0.01754 0.01398 0.01358 0.20502 0.20564 0.22460
0.24206 0.28624];
Ws=[0.30476 0.36526 0.39742 0.42658 0.46958 0.07800 0.05484 0.04340
0.03548 0.05378];
f1 = @(p,Ws) p(1)+((p(2)*(Ws.^0.5)))+(p(3)*Ws);
pguess = [0.1,0.1,0.1];
disp('Regupathi Equation')
mdl = NonLinearModel.fit(Ws,Wp,f1,pguess)
%%%%%%%%%%%%%%%%%%%%%%%%%%%%%%%%%%%%%%%%%%%%%%%%%%%%%%%%%%%%%%%%
f2 = @(p,Ws) p(1)+((p(2)*(Ws.^0.5)))+(p(3)*Ws)+(p(4)*(Ws.^2));
pguess = [0.1,0.1,0.1,0.1];
disp('-----------------------------------------------------')
disp('Hu Equation')
mdl = NonLinearModel.fit(Ws,Wp,f2,pguess)
%%%%%%%%%%%%%%%%%%%%%%%%%%%%%%%%%%%%%%%%%%%%%%%%%%%%%%%%%%%%%%%%
f3 = @(p,Ws) exp(p(1)+((p(2)*(Ws.^0.5)))+(p(3)*(Ws.^3)));
pguess = [0.1,0.1,0.1];
disp('-----------------------------------------------------')
disp('Maria Equation')
mdl = NonLinearModel.fit(Ws,Wp,f3,pguess)
%%%%%%%%%%%%%%%%%%%%%%%%%%%%%%%%%%%%%%%%%%%%%%%%%%%%%%%%%%%%%%%%
f4 = @(p,Wp) 1./(p(1)+(p(2)*(Wp.^0.5))+(p(3)*(Wp)));
pguess = [0.1,0.1,0.1];
disp('-----------------------------------------------------')
disp('Graber Equation')
mdl = NonLinearModel.fit(Wp,Ws,f4,pguess)
```

APPENDIX B

Research Publications I

International Journal of GEOMATE, Sept., 2019 Vol.17, Issue 61, pp. 187 - 194
ISSN: 2186-2982 (P), 2186-2990 (O), Japan, DOI: https://doi.org/10.21660/2019.61.89205
Special Issue on Science, Engineering & Environment

KINETIC MODELS FOR PHYCOCYANIN PRODUCTION BY FED-BATCH CULTIVATION OF THE *SPIRULINA PLATENSIS*

Sakawduan Kaewdam[1], Somkiat Jaturonglumlert[1,*], Jaturapatr Varith[1], Chanawat Nitatwichit[1] and Kanjana Narkprasom[1]

[1] Faculty of Engineering and Agro-Industry, Maejo University, Chiang Mai 50290, Thailand;

*Corresponding Author, Received: 19 Dec. 2018, Revised: 10 Jan. 2019, Accepted: 31 Jan. 2019

ABSTRACT: C-Phycocyanin (CPC) is high-value bioproduct, generated in blue-green algae *Spirulina platensis*. Its wide application in different industries, widely used in food pharmaceuticals and cosmetics. There are many factors that influence the yields of *Spirulina platensis* cultivation, such as temperature, light intensity, pH, nutrient etc. Nitrogen is one of the most important factors in cell growth and pigment productivity. The fed-batch process is a strategy to control the growth and enhance CPC accumulation. In this study, *Spirulina platensis* was cultured in batch and fed-batch modes to investigate the CPC production. Kinetic model of growth and production on nitrate concentration so as CPC accumulation. On batch, cultivation found that increasing nitrogen source concentration led to increased CPC accumulation. The best CPC concentration (2.258 $mg \cdot mL^{-1}$) occurred when $NaNO_3$ was 3.5 $g \cdot L^{-1}$. The fed-batch cultivation proved to be an effective strategy to further enhance the CPC production of Spirulina platensis. The results indicate that the maximum CPC production (4.354 $g \cdot L^{-1}$) and productivity (97.53 $mg \cdot L^{-1} \cdot d^{-1}$) was obtained when using fed-batch with the NH_4HCO_3 3.0 mM. A kinetic model to describe the *Spirulina platensis* culture system including cell growth, CPC formation, as well as nitrogen consumption was proposed. The data fitted the model well. This was in good agreement with the experimental results and could be employed to predict the production of biomass, phycocyanin and the consumption of nitrogen in culture.

Keywords: *Spirulina platensis*, Phycocyanin, Fed-batch cultivation, Kinetic models

1. INTRODUCTION

Spirulina platensis (*Arthospira platensis*) is one of the widely cultured commercial microalgae that can provide raw materials for food, pharmaceuticals, animal feed, bioenergy. The chemical composition of *Spirulina platensis* indicated that it has high nutritional value due to its content of a wide range of essential nutrients, such as provitamins, minerals, proteins and polyunsaturated fatty acids such as gamma-linolenic acid (GLA) [1]. It is known as a "super food". The United States Food and Drug Administration confirmed in 1981 that spirulina is a source of protein and contains various vitamins and minerals, moreover, it may be legally marketed as a food supplement. Many countries have set up food quality and safety standards for spirulina.

There are many factors that influence the yields of *Spirulina platensis* cultivation, such as temperature, light intensity, pH, nutrient etc. Nitrogen is one of the most important factors in cell growth and pigment productivity. Colla *et al.*, (2007) [2] reported nitrogen source important for growth and accumulation of nutrients in the cells of *Spirulina platensis*. Nitrogen is involved in the formation process of essential components such as amino acids, chlorophyll, nucleic acid amylase, especially protein with up to 60-70% of dry weight. Protein in Spirulina contains mainly two phycobiliproteins namely C-phycocyanin (CPC) and allophycocyanin (APC) approximately a ratio of 10:1 [3]. The supply of nitrogen source in the medium is a fundamental requisite to cultivate *Spirulina platensis* and ammonium salt is also shown to be particularly effective not only to produce biomass but also to exalt its CPC content.

Nutrient-rich medium is used to ensure high growth rate of the microalgae cells, by switching to a different composition to induce the nutrient stress. This can be achieved by the fed-batch techniques. The fed-batch process is an important strategy because it makes possible to control the growth and the CPC accumulation phased by modifying the feed throughout the cultivation process. The current study aimed to investigate the CPC production by comparing between culturing in batch and fed-batch and study kinetic model of growth and production on nitrate concentration as CPC accumulation was also established in this work.

2. MATERIALS AND METHODS

2.1 Operation of Batch Cultivation

The batch cultivation was conducted in 2 L of the bottle. The microalgae were pre-cultured and

International Journal of GEOMATE, Sept., 2019 Vol.17, Issue 61, pp. 187 - 194

inoculated in the bottle, the medium used for strain culture was adapted from Zarrouk medium consisting of (per liter): 16 g $NaHCO_3$, 2.5 g $NaNO_3$, 1 g NaCl , 0.5 g K_2HPO_4 , 0.2 g $MgSO_4$ and study difference four level of sodium nitrate (1.5 2.5 3.5 and 4.5 $g \cdot L^{-1}$). The initial biomass was maintained as 0.37 $g \cdot L^{-1}$. The culture was controlled at 28 - 30 °C, pH 9-10 (Algae Connect, Model ALS-SPARC-2A, USA), and LED illumination (BASTVA, Model GW-AQM55W, China) with the ratio of red and blue as 3:1 with lighting period of 16 hours per day at 350 $\mu mol \cdot m^{-2} \cdot s^{-1}$ [4]. During the cultivation, the CO_2 either pure from the tank was bubbled into the bottle to control the pH at 9.0-9.5 as the carbon source. (Fig 1). During cultivation liquid samples were collected at set time intervals to determine the cell concentration, CPC concentration and residual nitrogen source concentration.

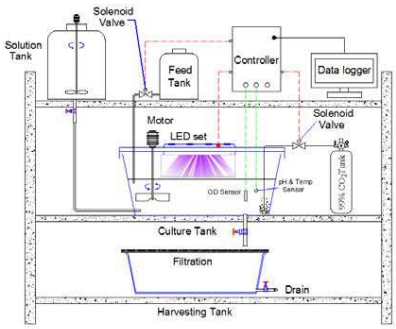

Fig 1. Operation of batch and fed-batch cultivation

2.2 Operation of Fed-batch Cultivation

Three type ammonium salts were selected for nitrogen sources in *Spirulina platensis* cultivation. Three levels in each salt are containing the range of high and low medium (1.0 2.0 and 3.0 mM). By mean of 1.0 mM is minimum concentration which *Spirulina platensis* use for living and 3.0 mM is the concentration at toxicity phenomena in cultivation [5]. All treatment was carried out in 2 L of the bottle which was controlled the medium of culture (per liter) that include: 16 g $NaHCO_3$, 2.5 g $NaNO_3$, 1 g NaCl , 0.5 g K_2HPO_4 , 0.2 g $MgSO_4$. The initial biomass was maintained as 0.37 $g \cdot L^{-1}$. The culture condition was controlled at 28 - 30 °C, pH 9-10 and LED illumination with the ratio of red and blue as 3:1 with lighting period of 16 hours per day at 350 $\mu mol \cdot m^{-2} \cdot s^{-1}$. For fed-batch cultivation, time regulator was set up for pulse-feeding nitrogen source during the experiment. Liquid samples were collected at set time intervals to determine the cell concentration, CPC concentration and residual nitrogen source concentration.

The nitrite concentration was measured by the chronotropic acid method [6]. The biomass concentration was determined by measuring the optical density of the sample at a wavelength of 680 nm (denoted as OD_{680}) using a UV/Vis spectrophotometer (Model SPECTROSC, USA). The OD_{680} values were converted to wet biomass concentration (the moisture content in the wet basis is 83.59 ±0.66 %) via appropriate calibration between OD_{680} and cell weight.

$$W=5.8667 \times OD_{680}-2.5563 \quad (1)$$

The specific growth rate of Spirulina culture was obtained by the following calculation.

$$\mu=\frac{\ln(W/W_0)}{t} \quad (2)$$

Where W and W_0 indicate the biomass concentration ($g \cdot L^{-1}$) at initial and cultivation time (days:d), respectively. The biomass productivity during the culture period was calculated from the Eq. (3).

$$P_w=\frac{\Delta W}{\Delta t} \quad (3)$$

2.3 Determination of C-phycocyanin Content

A fixed amount of the biomass (5 g) was mixed with 25 ml of 0.1 M sodium phosphate buffer (pH = 7.0), then keep in freezing condition (-10 °C) for overnight and thawing next in room temperature. After that, the ultrasound-assisted extractions based on research of Ruangyot *et al.* (2016) [7] was used as the extraction method. The cell debris was removed by centrifugation at 3500 rpm for 30 minutes, and the supernatant (blue color) was collected to CPC analysis. The supernatant (crude extract) was measured the absorbance by using UV/Vis spectrophotometer at the wavelengths of 620 nm and 652 nm for calculating the concentration of CPC ($g \cdot L^{-1}$) according to the following Eq. (4) [8]. The content of CPC (%) was calculated according to Boussiba and Richmond (1979) [9] following Eq. (5). The yield ($mg \cdot g^{-1}$) and productivity of CPC ($g \cdot L^{-1} \cdot d^{-1}$) according to the following Eq. (6) and (7)

$$C_{CPC}=\frac{A_{620}-0.474A_{652}}{5.34} \quad (4)$$

$$\%CPC=\frac{A_{620} \times V \times 100}{3.39 \times W \times \%DW} \quad (5)$$

$$Y_{CPC}=\frac{CPC \times V}{D} \quad (6)$$

$$P_{CPC}=\mu \times W \times \%CPC \quad (7)$$

2.4 Kinetic Model Development

Monod model and Haldane model are widely used for describing the effect of substrate concentration (C_s) on specific growth rate (μ), Eq. (8) and Eq. (9).

International Journal of GEOMATE, Sept., 2019 Vol.17, Issue 61, pp. 187 - 194

$$\mu=\mu_m\left(\frac{C_S}{C_N+C_S}\right) \quad (8)$$

$$\mu=\mu_m\left(\frac{C_S}{C_N+C_S+\frac{C_S^2}{C_I}}\right) \quad (9)$$

Where C_N and C_I are optimal substrate concentration and inhibit concentration at the maximum specific growth rate. In this study, the kinetic model is modified from the Monod model and the Haldane model for simulating the kinetic parameters of *Spirulina platensis* cultivation namely specific growth rate (μ) and CPC productivity (P_{CPC}). In these equations, the maximum growth rate constant (μ_m) and maximum CPC productivity constant ($P_{CPC,m}$) are assumed to be a function of nitrate concentration (C_{S1}) and ammonium concentration (C_{S2}) as shown in Eq. (10) and Eq. (11). Furthermore, in fed-batch cultivation, the kinetic model would be considered to account the substrate inhibition of growth at higher substrate concentrations as shown in Eq. (12) and Eq. (13).

$$\mu=\mu_m\left(\frac{C_{S1}}{C_{N1}+C_{S1}}\right)\left(\frac{C_{S2}}{C_{N2}+C_{S2}}\right) \quad (10)$$

$$P_{CPC}=P_{CPC,m}\left(\frac{C_{S1}}{C_{N1}+C_{S1}}\right)\left(\frac{C_{S2}}{C_{N2}+C_{S2}}\right) \quad (11)$$

$$\mu=\mu_m\left(\frac{C_{S1}}{C_{N1}+C_{S1}+\frac{C_{S1}^2}{C_{I1}}}\right)\left(\frac{C_{S2}}{C_{N2}+C_{S2}+\frac{C_{S2}^2}{C_{I2}}}\right) \quad (12)$$

$$\mu_{CPC}=P_{CPC,m}\left(\frac{C_{S1}}{C_{N1}+C_{S1}+\frac{C_{S1}^2}{C_{I1}}}\right)\left(\frac{C_{S2}}{C_{N2}+C_{S2}+\frac{C_{S2}^2}{C_{I2}}}\right) \quad (13)$$

3. RESULTS AND DISCUSSION

3.1 Effect of Sodium Nitrate on Cell Growth and CPC Production

Nitrogen source is an important factor that affects the viability and productivity of microalgae in batch cultivation. The final *Spirulina platensis* biomass in different sodium nitrate concentration was given in Fig. 2. The result shows that a rapid increase on biomass production was observed in medium containing 3.5 $g\cdot L^{-1}$ sodium nitrate that was presented the maximum biomass concentration (4.859 $g\cdot L^{-1}$). At 3.5 $g\cdot L^{-1}$ sodium nitrate was presented the maximum biomass concentration, both CPC productivity and significantly increased when the concentration of sodium nitrate was increased from 1.5-3.5 $g\cdot L^{-1}$ (Table 1). However, a sharp decrease was observed when the concentration of sodium nitrate reached 4.5 $g\cdot L^{-1}$, which is this level fall inhibition region. This could be directly supported by the observation of changing cells color from green to white during cultivation interval the first five days. The growth rate began to decline in the third day. Thus, 3.5 $g\cdot L^{-1}$ sodium nitrate seemed to be the optimal concentration of sodium nitrate for the growth and CPC accumulation of spirulina platensis, with the maximum biomass productivity of 0.314 $g\cdot L^{-1}\cdot d^{-1}$, the specific growth rate of 0.169 d^{-1}, CPC productivity of 44.59 $mg\cdot L^{-1}\cdot d^{-1}$ and 14.20% of yield.

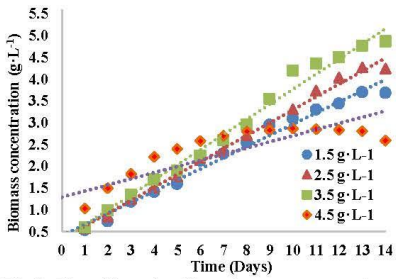

Fig 2. The effect of sodium nitrate concentration on cell growth

3.2 Time Course Performance on Cell Growth and CPC Production

The cellular component of microalgae usually varies with the cell growth phase. In this work, spirulina was cultivated in a batch culture around 14 days to investigate variation in CPC production (Fig 3). The CPC concentration increased simultaneously along with nitrogen consumption and the maximum values (2.840 $mg\cdot mL^{-1}$) was obtained at the beginning of nitrogen depletion. This trend is well in agreement with the report of Chen *et al.* (2013) [10]. It has been suggested that CPC belongs to a family of phycobiliproteins which have obtained a secondary role as intracellular nitrogen storage compounds and mobilized for other purposes in times of nitrogen shortage. Therefore, in order to attain the maximum CPC concentration, the beginning of nitrogen depletion period should be the optimal time for adding a nitrogen source to cultivate and enhance the cell growth rate and CPC concentration. Thus, it is necessary to develop an effective strategy that could enhance biomass production and achieve the high CPC concentration simultaneously.

International Journal of GEOMATE, Sept., 2019 Vol.17, Issue 61, pp. 187 - 194

Table 1. The effect of sodium nitrate concentration on kinetic parameters of *Spirulina platensis* cultivation.

Nitrate concentration ($g \cdot L^{-1}$)	W ($g \cdot L^{-1}$)	P_X ($g \cdot L^{-1} \cdot d^{-1}$)	μ (d^{-1})	P_{CPC} ($mg \cdot L^{-1} \cdot d^{-1}$)	% CPC
1.5	3.692	0.231	0.151	25.55	11.06
2.5	4.237	0.272	0.163	30.71	11.29
3.5	4.859	0.314	0.169	44.59	14.20
4.5	2.865	0.154	0.128	8.79	5.71

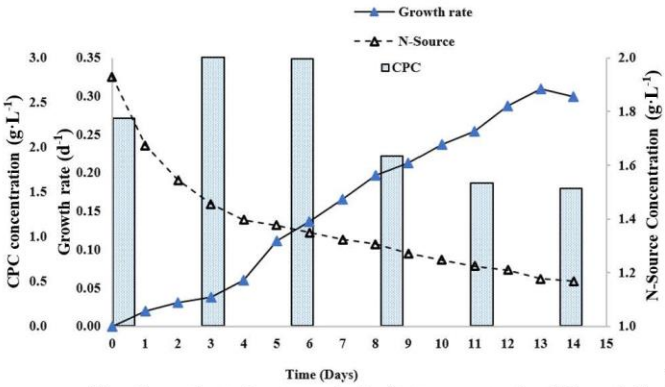

Fig.3 Time-course profiles of growth rate (empty symbol), nitrate concentration (full symbol) and CPC concentration (column) during the batch cultivation of *Spirulina platensis*.

3.3 Improvement of CPC Production of *Spirulina Platensis* by Using Fed-Batch Operation

On the basis of batch culture results, different pulse-feeding fed-batch protocols were investigated with the aim of increasing the total availability of the supplied nitrogen source (N-source) as well as avoiding the above inhibitory level. All experiment was carried out using $NaNO_3$ because it was particularly important as nitrogen source at the beginning of the cultivation. Then, the concentrated ammonium solution was used as N-source pulse-feeding every day to reach a concentration in the medium including 1, 2 and 3 mM. Ammonia is preferentially assimilating over nitrate because the above mention is described it is favorable nutrient of *Spirulina platensis* in term of the energy situation. The results of the fed-batch process were shown in Fig. 4 and Table 2.

Spirulina platensis responses were varied with different ammonium solution. The biomass production and productivity of *Spirulina platensis* were increased significantly when increasing the NH_4HCO_3 concentration. Since nitrogen was required for synthesis of the amino acid, which was used to making proteins up. Additionally, increasing of nitrogen concentration might because of an increase in protein biosynthesis. The maximum biomass concentration and growth rate were obtained in the culture of pulse-fed with 3 mM NH_4HCO_3, but a decrease in both was observed when increasing the NH_4Cl and $(NH_4)_2SO_4$ concentration (2 and 3 mM) indicating that the inhibition phenomena of growth were appeared by the high level of ammonium.

Moreover, to investigate the performance of the fed-batch operation, four strategies were defined for reducing times of feeding and increase the concentration of a solution. For the time-course profiles of growth rate, four strategies were defined namely: pulse-fed with 3 NH_4HCO_3 every day; 3 NH_4HCO_3 every two days; 6 mM NH_4HCO_3 every day and 6 mM NH_4HCO_3 every two days, respectively (Fig 5A-5D). While the growth rate in fed-batch with 3 mM NH_4HCO_3 every day (1.187 d^{-1}) was slightly higher than 6 mM NH_4HCO_3 every two days feeding (1.143 d^{-1}). However, the growth rate decreased in case of fed-batch with 6 mM NH_4HCO_3 every day indicating that this level is over toxicity limit.

International Journal of GEOMATE, Sept., 2019 Vol.17, Issue 61, pp. 187 - 194

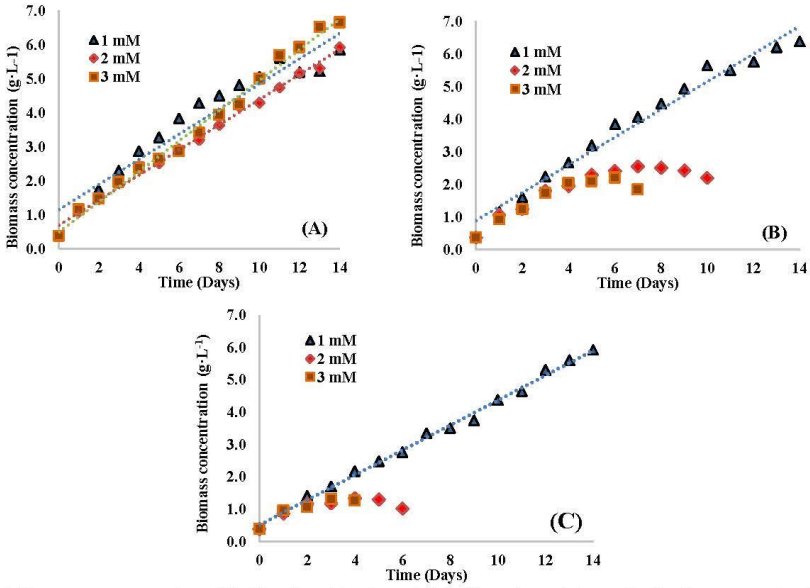

Fig.4 Biomass concentration of fed-batch cultivation of *Spirulina platensis* by pulse-feeding every day (A) Ammonium bicarbonate (NH_4HCO_3) (B) Ammonium Chloride (NH_4Cl) and (C) Ammonium sulfate $(NH_4)_2SO_4$

Table 2. The effect of ammonium concentration on kinetic parameters of fed-batch cultivation of *Spirulina platensis.*

Ammonia concentration (mM)		W ($g \cdot L^{-1}$)	P_X ($g \cdot L^{-1} \cdot d^{-1}$)	μ (d^{-1})	P_{CPC} ($mg \cdot L^{-1} \cdot d^{-1}$)	% CPC
NH_4HCO_3	1.0	5.857	0.391	0.196	176.7	17.67
	2.0	5.927	0.396	0.197	192.1	19.21
	3.0	6.649	0.448	0.205	217.7	21.77
NH_4Cl	1.0	6.385	0.429	0.202	150.6	15.06
	2.0	2.548	0.210	0.176	123.9	12.39
	3.0	2.207	0.182	0.168	n/a	n/a
$(NH_4)_2SO_4$	1.0	5.915	0.396	0.197	113.2	11.32
	2.0	1.327	0.219	0.164	n/a	n/a
	3.0	1.304	0.106	0.101	n/a	n/a

n/a is cannot found because of ammonium inhibition during culture.

International Journal of GEOMATE, Sept., 2019 Vol.17, Issue 61, pp. 187 - 194

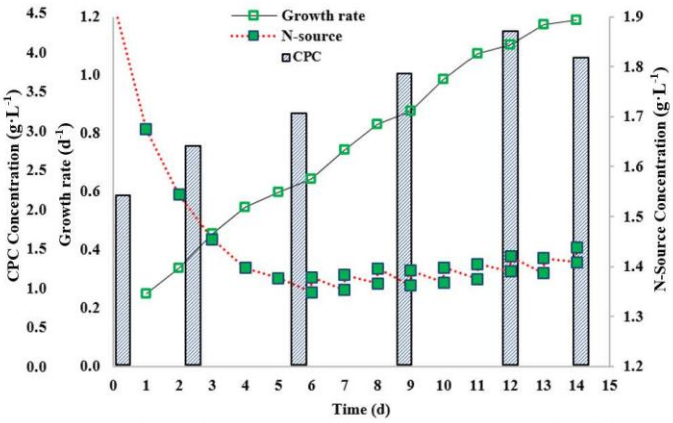

Fig.6 Time-course profiles of growth rate (empty symbol), N-source concentration (full symbol) and CPC concentration (column) during the fed-batch with 3 mM NH_4HCO_3.

Table 3. Comparison of kinetic parameters under fed-batch operation from this work with those reported in the literature.

Operation strategies	Biomass production ($g \cdot L^{-1}$)	Biomass productivity ($mg \cdot L^{-1} \cdot d^{-1}$)	CPC productivity ($mg \cdot L^{-1} \cdot d^{-1}$)	Reference	
Batch	0.770	92.4	67	Sassano *et al.*, 2007	[11]
Batch	2.250	740.0	125	Chen *et al.*, 2013	[10]
Batch	3.114	n/a	14	Leema *et al*, 2010	[12]
Fed-batch	1.759	113.9	n/a	Nascimento *et al.*, 2014	[1]
Fed-batch	6.780	588.2	94	Xie et al., 2015	[13]
Fed-batch	6.649	448.0	98	This study	

This result was an illustration of *Spirulina platensis* cultivation that refers about the nitrogen source was not only show an adverse impact on growth rate, the productivity of Spirulina platensis but also significantly in term of increasing the CPC formation. For nitrate inhibition on growth, the value of nitrate inhibit (C_{I1}) is 17,234.4 $g \cdot L^{-1}$, which means that when the nitrate concentration was lower than the result, it would not occur the inhibition on the growth rate and CPC growth rate. Moreover, the value of ammonium inhibition (C_{I2}) was 0.188 $g \cdot L^{-1}$, indicating that the amount of ammonium concentration should be lower than this value and it could use as the optimal inhibition ammonium concentration for fed-batch cultivation.

In commercial scale cultivation, the controlling is well relative for establishing "Smart Farm" culture modeling, production controlling and feed monitoring that is invariable underpinning by sensors and sensor networks. In a control system, a controller unit would record continuously such as the culture temperature, pH, and biomass growth by the sensor. This information of cultivating was continuously transferred to the computer data logger where the data would be analyzed, displayed and recorded.

$$\frac{d(C_{NN})}{dt} = (0.615 - 2.030\ P_{CPC})\, C_{S1} C_{S2} \quad r^2 = 0.902 \quad (18)$$

The kinetic model in fed-batch cultivation Eq. (16) was used for estimated nitrogen consumption (C_{NN}) according to the relationship between the CPC growth rate and N-source concentration as shown in Eq. (18). When the nitrogen consumption exceeded the pre-set value, the nutrients feeding system was activated for a predefined period, so that the nitrogen source feeding solution could be fed into the culture. This system was verified by comparison with the constant feeding method. When the constant feeding was used, owing to the amount of ammonium fed being larger than of the cell growth demanded, the ammonium in the medium accumulated to a certain concentration to inhibit cell growth.

International Journal of GEOMATE, Sept., 2019 Vol.17, Issue 61, pp. 187 - 194

4. CONCLUSIONS

The cultivation of microalgae *Spirulina platensis* was feasible using ammonium salt such as ammonium bicarbonate (NH_4HCO_3) ammonium chloride (NH_4Cl) and ammonium sulphate ($(NH_4)_2SO_4$). The application of ammonium salt as nitrogen source presented several advantages. Besides being a cheaper source compared to the traditional ones (nitrates), it was readily assimilated by the microorganism, without any expenditure of energy. Ammonia toxicity could be circumvented by the application of the fed-batch process with exponentially-increasing feeding rates. The fed-batch cultivation with ammonium bicarbonate feeding was proved to be an effective method to further enhance the CPC production, giving the maximum biomass production (6.649 $g \cdot L^{-1}$) and productivity (0.448 $g \cdot L^{-1} \cdot d^{-1}$). Further studies on the extraction and purification method by using high technology such as ultrasonic microbubble temperature differential etc.

5. ACKNOWLEDGMENTS

Authors are grateful to Division of Food Engineering at Engineering and Agro-Industry, Maejo University, Chiang Mai, Thailand for facilities. This research was also received funding from the Thailand Research Fund (TRF).

6. REFERENCES

[1] Nascimento, C. E., Gioielli, L. A., Converti, A., Oliveira Moraes, I., Sato, S., and Carvalho, J. C. M., Urea increases fed-batch growth and γ-linolenic acid production of nutritionally valuable *Arthrospira (Spirulina) platensis* cyanobacterium, Engineering in Life Sciences, Vol. 14, Issue 5, 2014, pp.530-537.

[2] Colla, L. M., Reinehr, C. O., Reichert, C., and Costa, J. A. V., Production of biomass and nutraceutical compounds by *Spirulina platensis* under different temperature and nitrogen regime, Bioresource Technology, Vol. 98, Issue 7, 2007, pp.1489-1493.

[3] Bermejo, R., Talavera, E. M., Alvarez-Pez, and J. M., Orte, J. C., Chromatographic purification of biliproteins from *Spirulina platensis* high-performance liquid chromatographic separation of their α and β subunits, Journal of Chromatography A, Vol. 778, Issue 1, 1997, pp.441-450.

[4] Jaturongloumlart, S., Promya, J., Varith, J. (2017). Modeling of Spirulina Growth Rate with LED Illumination and Applications. Engineering Journal Chiang Mai University, 24(1), 142-151.

[5] Li, G., Dong, G., Li, B., Li, Q., Kronzucker, H. J., and Shi, W., Isolation and characterization of a novel ammonium overly sensitive mutant, amos2, in Arabidopsis thaliana, Planta, Vol. 235, Issue 2, 2012, pp. 239-252.

[6] APHA, Standard Methods for the Examination of Water and Wastewater APHA: Washington, DC, 2005.

[7] Ruangyot, T., Jaturonglumlert, S., Nitatwichit, C., Varith, J. (2016). Factors affecting phycocyanin extraction from Spirulina platensis by using freezing and thawing combined with the ultrasonic method. Journal of fisheries technology research, 10(2), 78-87.

[8] Bennett, A., and Bogorad, L., Complementary chromatic adaptation in a filamentous blue-green alga, The Journal of cell biology, Vol.58, Issue 2, 1973, pp.419-435.

[9] Boussiba, S., and Richmond, A. E., Isolation and characterization of phycocyanins from the blue-green alga *Spirulina platensis*, Archives of Microbiology, Vol.120, 1979, pp..159-155

[10] Chen, C. Y., Kao, P. C., Tsai, C. J., Lee, D. J., and Chang, J. S., Engineering strategies for simultaneous enhancement of C-phycocyanin production and CO_2 fixation with *Spirulina platensis*. Bioresour Technol, 145, 2013, pp.307-312.

[11] Sassano, C., Gioielli, L., Almeida, K., Sato, S., Perego, P., Converti, A., and Carvalho, J., Cultivation of *Spirulina platensis* by a continuous process using ammonium chloride as a nitrogen source, Biomass and Bioenergy, Vol.31, Issue 8, 2007, pp.593-598.

[12] Leema, J. T. M., Kirubagaran, R., Vinithkumar, N. V., Dheenan, P. S., and Karthikayulu, S., High-value pigment production from *Arthrospira (Spirulina) platensis* cultured in seawater. Bioresource Technology, Vol.101, Issue 23, 2010, pp.9221-9227.

[13] Xie, Y., Jin, Y., Zeng, X., Chen, J., Lu, Y., and Jing, K., Fed-batch strategy for enhancing cell growth and C-phycocyanin production of *Arthrospira (Spirulina) platensis* under phototrophic cultivation, Bioresour Technol, Vol 180, 2015, pp.281-287.

Copyright © Int. J. of GEOMATE. All rights reserved, including the making of copies unless permission is obtained from the copyright proprietors.

APPENDIX C

Research Publications II

International Food Research Journal 27(2): 280 - 286 (April 2020)

Journal homepage: http://www.ifrj.upm.edu.my

Effect of isothermal and thermal diffusion on aqueous two-phase extraction for the purification of C-phycocyanin from *Spirulina platensis*

Kaewdam, S., *Jaturonglumlert, S., Varith, J., Nitatwichit, C. and Narkprasom, K.

Graduate Program in Food Engineering, Faculty of Engineering and Agro-Industry, Maejo University, Chiang Mai 50290, Thailand

Article history

Received: 12 December 2019
Received in revised form: 20 March 2020
Accepted: 25 March 2020

Keywords

purification, aqueous two-phase extraction, C-phycocyanin, Spirulina platensis, diffusion coefficient

Abstract

Aqueous two-phase extraction (ATPE) is effective for the purification of C-phycocyanin (CPC) from *Spirulina platensis*. Polyethylene glycol and potassium phosphate was used to purify the CPC. The influence of various different temperatures (dT) of process on purity (EP) partitioning and diffusion coefficient was evaluated. The optimal conditions for CPC purification was found at dT 25°C. CPC purity increased to 2.337 from an initial purity of 1.106. The concentration and recovery yield were found to be the highest at dT 25°C (13.932 g/L and 91.18, respectively), which was significantly higher than the conventional process. The dT affected the fluid viscosity variable, potentially due to a phenomenon which decreases the viscosity of the mixture and enhances the solvent solubility and diffusion capacity. The present work presented the diffusion coefficient in ATPE at various dT of the process. The isothermal diffusion coefficient (D_i) significantly increased to dT. The Soret effect (S_T) and thermal diffusion coefficient (D_T) were obtained at a high dT, but it should not be greater than 25°C. Hydrophobicity plays an important role in the thermal diffusion behaviour. A high diffusion coefficient is expected to result in the purification process due to high purity and efficiency.

© All Rights Reserved

Introduction

Phycobiliproteins are the major photosynthetic pigments in cyanobacteria. C-phycocyanin (CPC) is the major component of the phycobiliprotein family. CPC is a type of blue-coloured protein with great commercial and industrial significance, and is formed by two subunits of α and β. In addition to being widely used in the food and cosmetics industries (Moraes *et al.,* 2011), CPC has also been used as a fluorescent marker in biomedical research and as a therapeutic agent in oxidative stress-induced diseases. CPC purity is recognised as a good indicator of preparation purity, especially where other protein contaminants may be involved in the preparation processes. CPC purities of 0.7 is considered to be food grade, 1.5 as cosmetics grade, 2.5 as drug and food supplement, 3.9 as reactive grade, and greater than 4.0 as analytical grade (Rito-Palomares *et al.,* 2001).

Several methods have been developed to extract and purify CPC, such as precipitation, ion-exchange chromatography, and gel-filtration chromatography, but these are tedious and time-consuming (Niu *et al.,* 2007; Liao *et al.,* 2011; Chaiklahan *et al.,* 2011). The major drawback of almost all such methods is the large number of steps involved, high cost, low loading quantities, low recovery rates, and complexities and difficulties in up-scaling. Aqueous two-phase extraction (ATPE) is an effective purification technique for downstream processing. It is a better alternative to existing methods, especially in the early processing stages, in terms of scaling up to an industrial scale. Most ATPE-related researches on CPC purification focuses on process optimisation involving a varying type of salt, volume ratio, and molecular weight of polyethylene glycol, PEG (Patil *et al.,* 2008; Chethana *et al.,* 2015). The most common methods for phase separation are gravity and centrifugation. The small different densities between the two phases is an obstacle to the application of ATPE. Majority of CPC is gathered in the PEG phase. The viscosity of the PEG was increased by increasing the mass fraction of PEG. Therefore, it is important to use low viscosity and low density in the purification processes. Temperature variations can cause viscosity and density changes through natural convection. If the density is variable for a general fluid, a buoyancy force will arise, thus decreasing the mass transfer resistance, and improving the extraction efficiency. Therefore, the present work aimed to increase the efficiency of the process by experimenting in systems with different temperatures that affect the diffusion coefficient.

*Corresponding author.
Email: yaidragon@mju.ac.th

Materials and methods

Preparation of crude CPC extracts

All the experiments involved the utilisation of *Spirulina platensis* which was cultivated by a smart control (Jaturonglumlert *et al.,* 2017; Kaewdam *et al.,* 2019). Cells were harvested and washed twice with distilled water. Then, 5 g of biomass was mixed with 25 mL of 0.1 M sodium phosphate buffer (pH = 7.0), and frozen at -10°C overnight, before being thawed at room temperature for about 30 min. Ultrasound-assisted extraction (Thaisamak *et al.,* 2019) was performed. Next, the samples underwent centrifugation at 3,500 rpm for 30 min to remove cell debris, then the supernatant (blue colour) was collected, and the CPC concentration (g/L) of the crude extract was calculated by absorbance with UV/Vis spectrophotometer at wavelengths of 620 and 652 nm, using Eq. 1 (Ruangyot *et al.,* 2016):

$$CPC = \frac{A_{620} - 0.474A_{652}}{5.34} \quad \text{(Eq. 1)}$$

Aqueous two-phase extraction

Polyethylene glycol 4000 MW (PEG 4000) and potassium phosphates (K_2HPO_4:KH_2PO_4 = 1.82:1 to obtain the required pH 7.0) are the type of phase system of ATPE (Patil *et al.,* 2006). PEG 4000 (6%, w/v) and potassium phosphate (15%, w/v) was mixed with distilled water and later mixed with the crude extract. The mixture was stirred for about 30 min to equilibrate and allow for phase separation. The cylinder was set up in the equipment as shown in Figure 1A for 2 h, allowing phase separation to occur at the specified temperatures (dT = 0 [control], 15, 25, and 35°C), in which dT was the different temperature between top (T_1) and bottom (T_2). Pure CPC extracts after separation are shown in Figure 1B. The CPC and total protein concentrations in each phase were analysed to estimate the purity (EP), purification factor (PF), and partition coefficient (K) of the process, using Eqs. 2, 3 and 4, respectively.

$$EP = \frac{A_{620}}{A_{280}} \quad \text{(Eq. 2)}$$

where, A_{620} and A_{280} = absorbance of the sample at 620 and 280 nm, respectively. This relationship is indicative of the CPC extract purity with respect to most forms of contaminating proteins (Chethana *et al.,* 2015). Absorbance at 620 nm indicates the CPC concentration, while absorbance at 280 nm indicates the total protein concentration in the solution.

$$PF = \frac{EP_p}{EP_c} \quad \text{(Eq. 3)}$$

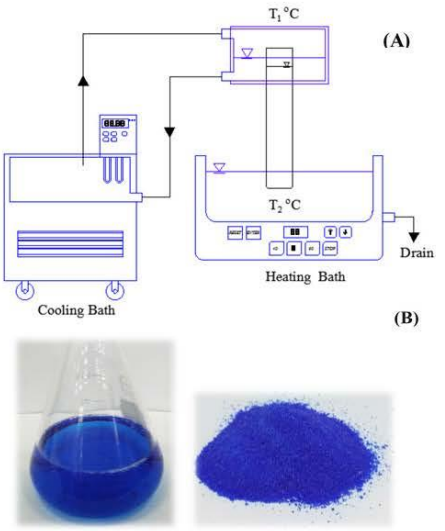

Figure 1. (A) the experimental setup, and (B) pure CPC after aqueous two-phase extraction.

where, PF = purification factor, EP_c = crude extract purity, and EP_p = extract purity after the purification process.

$$K = \frac{CPC_T}{CPC_B} \quad \text{(Eq. 4)}$$

where, K = partition coefficient, CPC_T and CPC_B = CPC concentration in the top phase and bottom phase, respectively.

The recovery yield (RC, %) of the CPC from the sample was calculated using Eq. (5) (Chew *et al.,* 2019), where, V_r = volume ratio, and in Eq. 6, V_T and V_B = volumes in the top and bottom phase, respectively:

$$RC = \frac{K \times V_r}{1 + K \times V_r} \times 100 \quad \text{(Eq. 5)}$$

$$V_r = \frac{V_T}{V_B} \quad \text{(Eq. 6)}$$

Polyacrylamide gel electrophoresis

Sodium dodecyl sulphate-polyacrylamide gel electrophoresis (SDS-PAGE) is an electrophoresis method that allows protein separation by mass. The method of Deutscher (1990) was followed using a 1 mm thick, and 15% polyacrylamide slab gel (5% stacking gel). Electrophoresis was run at room temperature at 150 V for approximately 90 min. The distances of buffer and bands were measured from the beginning

of the separation gel. The bands were visualised with Coomassie brilliant blue R250. The size of the phycocyanin subunit bands were determined using a Thermo Scientific Page Ruler Pre-stained Protein Ladder, a molecular weight with a broad range of 16 - 127 kDa (AccuProtein marker Chroma-I from Enzmart Biotech Co., LTD).

Phase partitioning

Pure PEG 4000 and potassium phosphate salt were used to prepare the biphasic systems in a 100 mL cylinder. The mixture was allowed to settle for 2 h at different temperatures (dT = 0 [control], 15, 25, 35°C) to obtain clear phase separation and reach equilibrium. A thermostatic water bath was used to control the temperature with a precision of ± 0.01 K (UC-150, Sturdy Industrial, Taiwan). Each resultant phase was collected with a volumetric pipette, and salt concentration was determined by a conductivity meter. The salt calibration curve was prepared with a known concentration of salt with suitable dilutions.

Determination of PEG concentration was performed by measuring the refractive index using a hand refractometer (N-1α ATAGO Co. Ltd, Japan). Calibration curves were prepared with a known concentration of PEG in the homogeneous regions of the binodal diagram of the individual ATPE (Nagaraja and Iyyaswami, 2015).

Prediction of diffusion coefficients

Estimation of the isothermal diffusion coefficient (Di) for CPC in both phases of ATPE utilised the correlation for protein diffusion coefficients proposed by Novak *et al.* (2015), which is based on the solute's molecular weight (M) and radius of gyration (R_G) as shown in Eq. 7:

$$D_i = \frac{6.85 \times 10^{-15} \times T}{\eta \cdot \sqrt{M^{1/3} R_G}} \qquad \text{(Eq. 7)}$$

where, η = dynamic viscosity of the solvent in Pa.s (dependent on operating temperature), and T = temperature in K. Meanwhile for CPC, M and R_G were 18500 Da and 54.1 Å, respectively (Thaisamak *et al.*,2020)

In 1879, the Swiss scientist, Charles Soret, discovered that a salt solution contained in a tube with the two ends at different temperatures generated a salt flux and temperature gradient, resulting in steady-state conditions in a concentration gradient. Although German scientist, Ludwig, described the same phenomenon several years before in a one-page report, the name "Soret effect" is usually attributed to the mass separation induced by temperature gradients (Platten, 2006). The Soret coefficient (S_T) in binary systems is defined as shown in Eq. 8:

$$S_T = \frac{D_T}{D_i} \qquad \text{(Eq. 8)}$$

where, D_T = thermal diffusion coefficient.

$$J_x(\mathrm{x,t}) = -\rho \mathrm{D}_i \frac{\partial c}{\partial x} - \rho D_T c(1-c)\frac{\Delta T}{a} \qquad \text{(Eq. 9)}$$

Using this approximation, if the concentration difference remains small, the thermal diffusive contribution is ruled out of Eq. 9 (Costesèque *et al.,* 2004), but is reintroduced via the boundary conditions that also uses the same approximation. Then, Eq. 9 becomes Eq. 10:

$$\frac{\partial c}{\partial t} = \mathrm{D}_i \frac{\partial^2 c}{\partial x^2} \qquad \text{(Eq. 10)}$$

The particular solutions of the diffusion equation, besides the stationary one is written as $c_\infty = c(x, t=\infty)$ are typically of the form:

$$c(x,y) = (A_n \cos \lambda_n x + B_n \sin \lambda_n x)\mathrm{e}^{-\lambda_n^2 D_i} \qquad \text{(Eq. 11)}$$

Finally, the general solution, which is the sum of all the particular solutions, is:

$$c(x,y) = c_\infty(x) + \sum_{n=1}^{\infty} A_n \cos\left(\frac{n\pi x}{a}\right)\exp\left(-n^2 \frac{t}{\tau_D}\right) \qquad \text{(Eq. 12)}$$

with:

$$c_\infty(x) = c_0 + \frac{D_T}{D_i} c_0(1-c_0)\frac{\Delta T}{h}\left(\frac{h}{2} - x\right) \qquad \text{(Eq. 13)}$$

and:

$$A_n = -\frac{4}{n^2\pi^2}\frac{D_T}{D_i} c_0(1-c_0)\Delta T \quad \text{(with n odd)} \qquad \text{(Eq. 14)}$$

Knowing $c(x,y)$, the concentration difference between the bottom and the top $c(o,t)$ - $c(h,t)$ within the cell is:

$$\frac{\Delta c(t)}{\Delta T} = \frac{D_T}{D_i} c_0(1-c_0)\left[1 - \frac{8}{\pi^2}\sum_{n\ odd}\frac{e^{-n^2\frac{t}{\tau_D}}}{n^2}\right] \qquad \text{(Eq. 15)}$$

with:

$$\tau_D = \frac{(V/A)^2}{\pi^2 D_i} \qquad \text{(Eq. 16)}$$

Therefore, it is necessary to collect experimental variations of concentration from initial to separation completely. The measured values are then divided by the corresponding ΔT and the experimental curve is drawn. Next, a curve fitting procedure using statistical

software is used to set two parameters, the Soret coefficient (S_T) and mass diffusion time (τ_D) of Eq. (15), and adjusted until Eq. (15) fits the experimental curve. So, the S_T and τ_D values are evaluated using the mathematical fitting procedure.

The enhancement factor (EF) was used to quantify the thermal diffusion effect. EF is defined by the ratio of the diffusion coefficient of the conventional process (D_0) and the diffusion coefficient of aqueous two-phase extraction coupled with different temperatures (D_{dT}) (summation of isothermal and thermal diffusion coefficient). The equation is defined as:

$$EF = \frac{D_{dT}}{D_0} \quad \text{(Eq. 10)}$$

Results and discussion

Effect of different temperature (dT) on ATPE process

Experiments were performed at three levels of dT (15, 25, and 35°C), while the other parameters were kept constant (PEG 4000 with saturation 6% [w/v], potassium phosphates 15% [w/v], pH 7.0, total volume 100 mL, and separation time of 2 h). Figure 2A shows the results of the effect of dT on CPC concentration in the top phase at complete separation. The highest concentration was found at dT 25°C (13.932 g/L), significantly higher than the conventional method. According to the result in Figure 2B, the highest purity and yield values were 2.337 and 91.18, respectively, which were obtained under the condition of dT at 25°C (Table 1).

The reason for this is a potential phenomenon which decreases the viscosity of the mixture and enhances the solvent solubility and diffusion capacity (Zhang *et al.*, 2015). Meanwhile, when the dT was greater than 35°C, the purity of CPC extracted in ATPE of PEG 4000 and potassium phosphates decreased sharply due to an observed significant reduction in the absorption strength at 620 nm, due to the characteristic absorption band of the CPC protein. Conversely, this means that the hydrogen bonding which interacted between the surface water of protein was destroyed at high temperatures.

SDS-PAGE analysis was used to confirm the purity of CPC and is shown in Figure 2C. Lane 1 indicates the molecular marker, while Lane 2 shows the pure CPC which is clearly visible in a band. This might be that during ATPE, the majority of the contaminant protein present in the crude extract was partitioned at the bottom phase, resulting in increased CPC purity. The molecular weights of CPC show two bands, α and β, with approximate sizes of 18 and 19 kDa, respectively. These results are similar to those obtained by Patil *et al.* (2006) and Chethana *et al.* (2015) who presented the molecular weight of CPC from *S. platensis* by SDS-PAGE.

Effect of different temperature (dT) on phase partitioning in the ATPE process

The partition coefficient (K) of purification increased monotonically with different temperatures, as shown in Table 1. To fully understand this behaviour, it is important to investigate the effect of the different temperatures on the CPC concentrations. Then, the concentration of salt and PEG in both phases can be determined using a conductivity meter and a refractometer, respectively. A set of experiments were subsequently conducted to generate binodal curves at different temperatures varying from 15 to 35°C. Binodal curves obtained by plotting the concentrations of PEG and phosphate salt in the top and bottom phases are shown in Figure 3, in which the binodal moved away from the origin when the temperature increased, causing the tie line length (TLL) to decrease. This can result in a faster and more complete separation due to preferential binding of the water molecules to the polar salt surface instead of the PEG at a higher temperature difference. These results have also been observed by several authors such as Sé and Aznar (2002), Gautam and Simon (2006), and Carvalho *et al.* (2007).

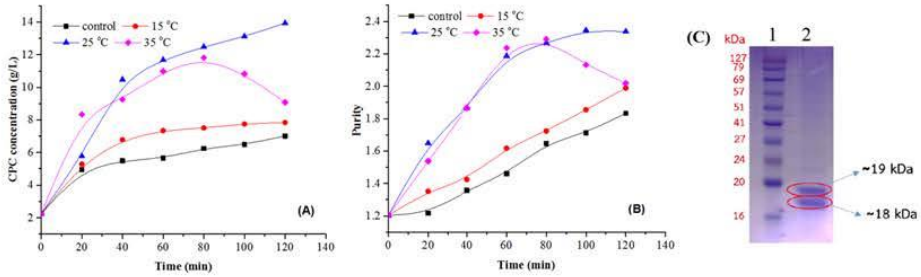

Figure 2. (A) Concentration profiles of CPC in top phase, and (B) purity of CPC in top phase, and (C) SDS PAGE of CPC. Lanes 1 and 2 were molecular marker and pure CPC, respectively.

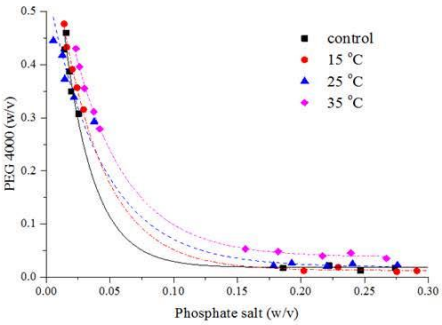

Figure 3. Phase diagram of PEG4000 and potassium phosphates in aqueous two-phase extraction.

Differential temperature on diffusion coefficients

Table 2 shows the experiments to determine the isothermal diffusion (from Eq. 7) thermal diffusion and Soret coefficients (from Eq. 15) of aqueous two-phase extraction, the corresponding Soret coefficients, mass diffusion times, and deduced isothermal diffusion and thermal diffusion coefficients.

Different temperatures had a significant effect on diffusion coefficient, as observed in Table 2, which shows that the isothermal diffusion coefficient (D_i) at dT of 25°C and the conventional method were 2.281×10^{-12} and 2.104×10^{-12} m^2/s, respectively. The Soret coefficient and thermal diffusion were found to be highest at dT of 25°C. This is why the ATPE coupled with different temperature technique is an effective driving force for the mass transfer of the CPC concentration. It might be relative importance of the diffusion coefficient due to

Table 1. Effect of different temperature on concentration and purity in ATPE.

dT	Control	15°C	25°C	35°C
CPC Concentration (g/L)				
Top phase	7.012 ± 0.29	7.840 ± 0.54	13.932 ± 1.25	9.069 ± 0.84
Bottom phase	1.975 ± 0.23	1.112 ± 0.25	0.758 ± 0.14	1.028 ± 0.36
Partition coefficient (K)	3.550	7.050	18.380	8.822
EP of CPC				
Top phase	1.839 ± 0.04	1.889 ± 0.29	2.337 ± 0.20	1.918 ± 0.33
Bottom phase	0.812 ± 0.05	0.856 ± 0.18	0.569 ± 0.13	0.746 ± 0.17
Purification factor (PF)	1.663	1.708	2.113	1.734
V_r and RC				
Volume of top phase (V_T, mL)	48 ± 2	39 ± 3	36 ± 3	43 ± 4
Volume of bottom phase (V_B, mL)	52 ± 3	61 ± 2	64 ± 3	57 ± 3
Volume ratio (V_r)	0.92	0.64	0.56	0.75
Recovery yield (RC, %)	76.62	81.84	91.18	86.94

Table 2. The mass diffusion times, Soret coefficient, the isothermal diffusion coefficient, and the thermal diffusion coefficient of ATPE.

dT	τ_D (min)	S_T (1/K)	D_i (m^2/s) × 10^{-12}	D_T ($m^2/s \cdot K$) × 10^{-13}	EF
control			2.104		-
15°C	23.325	0.162	2.210	3.580	1.220
25°C	52.797	0.211	2.281	4.813	1.313
35°C	16.753	0.192	2.351	2.398	1.231

temperature variations. Schimpf and Semenov (2000) extended the relations between the thermal diffusion coefficient and viscosity, in which reducing the viscosity, and resulted in the thermal diffusion coefficient increase. Therefore, the ATPE coupled with different temperatures affects viscosity and buoyancy forces, thereby resulting in improved mass transfer efficiency between the processes.

The value of isothermal diffusion and thermal diffusion coefficients were different in each experiment. From their values, it is possible to deduce that the enhancement factor (EF) is the factor that characterises the efficiency of a process compared with the conventional method, as shown in Table 2. The different temperature at 25°C was enhanced around 30% from the conventional method. This result indicates that different temperature not only affects efficiency of the ATPE process, but also enhances the efficiency of the transport phenomena during the process. This finding is similar to Chan *et al.* (2003) who concluded that the Soret coefficient and isothermal diffusion coefficient are driven by temperature gradients and concentration gradients.

Conclusion

Aqueous two-phase extraction (ATPE) with combined different temperatures (dT) is a new finding and is suitable for C-phycocyanin purification. The optimal different temperatures of the process were achieved by ATPE conducted at dT of 25°C. Furthermore, the present work successfully investigated the isothermal and thermal diffusion of the purification process using ATPE. The isothermal diffusion coefficient (D_i) significantly increased with increased dT. The Soret effect (S_T) and thermal diffusion coefficient (D_T) were obtained at a high dT, but this should not go beyond 25°C. It can thus be concluded that the Soret effect (S_T) and thermal diffusion coefficient (D_T) were good parameters for explaining C-phycocyanin purification efficiency. Further studies should be undertaken into the steps of purification, backward purification, or using continuous process to further increase purity.

Acknowledgement

Kaewdam, S., are grateful to the Division of Food Engineering at the Department of Engineering and Agro-Industry, Maejo University, Chiang Mai, Thailand for providing the facilities for the present work. The present work received funding from the Thailand Research Fund (TRF).

References

Carvalho, C. P., Coimbra, J. S. R., Costa, I. A. F., Minim, L. A., Silva, L. H. M. and Maffia, M. C. 2007. Equilibrium data for PEG 4000 + salt + water systems from (278.15 to 318.15) K. Journal of Chemical and Engineering Data 52(2): 351-356.

Chaiklahan, R., Chirasuwan, N., Loha, V., Tia, S. and Bunnag, B. 2011. Separation and purification of phycocyanin from *Spirulina* sp. using a membrane process. Bioresource Technology 102(14): 7159-7164.

Chan, J., Popov, J. J., Kolisnek-Kehl, S. and Leaist, D. G. 2003. Soret coefficients for aqueous polyethylene glycol solutions and some tests of the segmental model of polymer thermal diffusion. Journal of Solution Chemistry 32(3): 197-214.

Chethana, S., Nayak, C. A., Madhusudhan, M. C. and Raghavarao, K. S. M. S. 2015. Single step aqueous two-phase extraction for downstream processing of C-phycocyanin from *Spirulina platensis*. Journal of Food Science and Technology 52(4): 2415-2421.

Chew, K. W., Chia, S. R., Krishnamoorthy, R., Tao, Y., Chu, D.-T. and Show, P. L. 2019. Liquid biphasic flotation for the purification of C-phycocyanin from *Spirulina platensis* microalga. Bioresource Technology 288: article ID 121519.

Costesèque, P., Pollak, T., Platten, J. K. and Marcoux, M. 2004. Transient-state method for coupled evaluation of Soret and Fick coefficients, and related tortuosity factors, using free and porous packed thermodiffusion cells: application to $CuSO^4$ aqueous solution (0.25 M). The European Physical Journal E 15(3): 249-253.

Deutscher, M. P. 1990. Methods in enzymology volume 182 - guide to protein purification. 1st ed. United States: Academic Press.

Gautam, S. and Simon, L. 2006. Partitioning of β-glucosidase from *Trichoderma reesei* in poly(ethylene glycol) and potassium phosphate aqueous two-phase systems: influence of pH and temperature. Biochemical Engineering Journal 30(1): 104-108.

Jaturonglumlert, S., Promya, J. and Varith, J. 2017. Modeling of *Spirulina* growth rate with LED illumination and applications. Engineering Journal Chiang Mai University 24(1): 142-151.

Kaewdam, S., Jaturonglumlert, S., Varith, J., Nitatwichit, C. and Narkprasom, K. 2019. Kinetic models for phycocyanin production by fed-batch cultivation of the *Spirulina platensis*. International Journal of GEOMATE 17(61): 187-194.

Liao, X., Zhang, B., Wang, X., Yan, H. and Zhang, X. 2011. Purification of C-phycocyanin from *Spirulina platensis* by single-step ion-exchange chromatography. Chromatographia 73(3): 291-296.

Moraes, C. C., Sala, L., Cerveira, G. P. and Kalil, S. J. 2011. C-phycocyanin extraction from *Spirulina platensis* wet biomass. Brazilian Journal of Chemical Engineering 28(1): 45-49.

Nagaraja, V. H. and Iyyaswami, R. 2015. Aqueous two phase partitioning of fish proteins: partitioning studies and ATPS evaluation. Journal of Food Science and Technology 52(6): 3539-3548.

Niu, J.-F., Wang, G.-C., Lin, X.-Z. and Zhou, B.-C. 2007. Large-scale recovery of C-phycocyanin from *Spirulina platensis* using expanded bed adsorption chromatography. Journal of Chromatography B 850(1-2): 267-276.

Novak, U., Lakner, M., Plazl, I. and Žnidaršič-Plazl, P. 2015. Experimental studies and modeling of α-amylase aqueous two-phase extraction within a microfluidic device. Microfluidics and Nanofluidics 19(1): 75-83.

Patil, G., Chethana, S., Madhusudhan, M. C. and Raghavarao, K. S. 2008. Fractionation and purification of the phycobiliproteins from *Spirulina platensis*. Bioresource Technology 99(15): 7393-7396.

Patil, G., Chethana, S., Sridevi, A. S. and Raghavarao, K. S. M. S. 2006. Method to obtain C-phycocyanin of high purity. Journal of Chromatography A 1127(1-2): 76-81.

Platten, J. K. 2006. The Soret effect: a review of recent experimental results. Journal of Applied Mechanics 73(1): 5-15.

Rito-Palomares, M., Nuñez, L. and Amador, D. 2001. Practical application of aqueous two-phase systems for the development of a prototype process for c-phycocyanin recovery from *Spirulina maxima*. Journal of Chemical Technology and Biotechnology 76(12): 1273-1280.

Ruangyot, T., Jaturonglumlert, S., Nitatwichit, C. and Varith, J. 2016. Factors affecting phycocyanin extraction from *Spirulina platensis* by using freezing and thawing combined with ultrasonic method. Journal of Fisheries Technology Research 10(2): 78-87.

Schimpf, M. E. and Semenov, S. N. 2000. Mechanism of polymer thermophoresis in nonaqueous solvents. The Journal of Physical Chemistry B 104(42): 9935-9942.

Sé, R. A. G. and Aznar, M. 2002. Thermodynamic modelling of phase equilibrium for water + poly(ethylene glycol) + salt aqueous two-phase systems. Brazilian Journal of Chemical Engineering 19(2): 255-266.

Thaisamak, P., Jaturonglumlert, S., Varith, J., Narkprasom, K. and Nitatwichit, C. 2020. Effect of combined between microbubble and ultrasonic of C-phycocyanin extraction from *S. platensis*. International Journal of GEOMATE 18(65): 124-131.

Thaisamak, P., Jaturonglumlert, S., Varith, J., Taip, F. S. and Nitatwichit, C. 2019. Kinetic model of ultrasonic-assisted extraction with controlled temperature of C-phycocyanin from *S. platensis*. International Journal of GEOMATE 16(55): 176-183.

Zhang, X., Zhang, F., Luo, G., Yang, S. and Wang, D. 2015. Extraction and separation of phycocyanin from *Spirulina* using aqueous two-phase systems of ionic liquid and salt. Journal of Food and Nutrition Research 3(1): 15-19.

CURRICULUM VITAE

NAME	MS. SAKAWDUAN KAEWDAM
DATE OF BIRTH	21 December 1987
EDUCATION	2016-Present : Doctor of Engineering Program in Food Engineering, Faculty of Engineering and Agro-industry, Maejo University. 2011-2014 : Master of Engineering Program in Food Engineering, Faculty of Engineering and Agro-industry, Maejo University. 2006-2010: Bachelors of Engineering Program in Food Engineering, Faculty of Engineering and Agro-industry, Maejo University. 2005 : M.6 Certificate, Longwitthaya School, Phrae.